ort No. FHWA-RD-79-133

FATIGUE OF CURVED STEEL BRIDGE ELEMENTS

Fatigue Tests of Curved Plate Girder Assemblies

April 1980
Interim Report

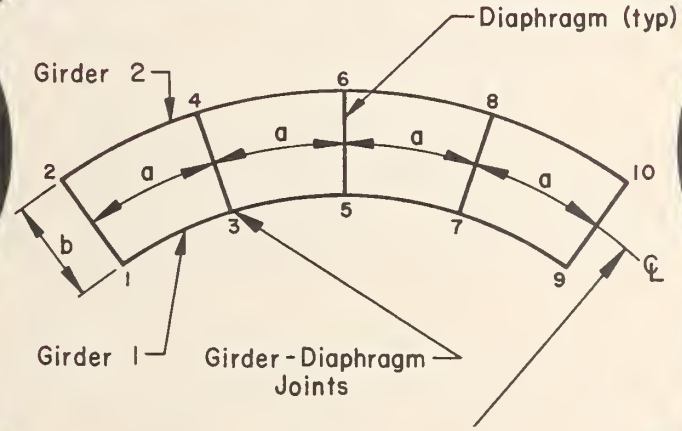

Document is available to the public through the National Technical Information Service, Springfield, Virginia 22161

Prepared for
FEDERAL HIGHWAY ADMINISTRATION
Offices of Research & Development
Structures & Applied Mechanics Division
Washington, D.C. 20590

FOREWORD

Horizontally curved steel plate and box girders are being used more frequently for highway structures, sometimes because of increased economy, and because of their esthetic appearance. The design of curved girders differs from that of straight girders in that torsional effects, including nonuniform torsion, must be considered. The resulting use of lateral bracing between curved plate girders and internal bracing and stiffening of curved box girders gives rise to complicated states of stress and to details which can be sensitive to repetitive loads. This situation prompted the FHWA to sponsor this research, the primary objective of which is to establish fatigue design guidelines for curved girder highway bridges in the form of simplified equations or charts.

This report is one in a series of eight on the results of the research and is being distributed to the Washington and field offices of the Federal Highway Administration, State highway agencies, and interested researchers.

Charles F. Scheffey
Director, Office of Research
Federal Highway Administration

Technical Report Documentation Page

1. Report No.	2. Government Accession No.	3. Recipient's Catalog No.
FHWA-RD-79-133,		

4. Title and Subtitle	5. Report Date
FATIGUE OF CURVED STEEL BRIDGE ELEMENTS - Fatigue Tests of Curved Plate Girder Assemblies	April 1980
	6. Performing Organization Code
7. Author(s) J. Hartley Daniels and W. C. Herbein	8. Performing Orgonization Report No. Fritz Engineering Lab Report No. 398.3
9. Performing Orgonization Name and Address Fritz Engineering Laboratory, Bldg. #13 Lehigh University Bethlehem, Pa. 18015	10. Work Unit No. (TRAIS) 35F2-052
	11. Contract or Grant No. DOT-FH-11-8198
12. Sponsoring Agency Name and Address U.S. Department of Transportation Federal Highway Administration, Washington, D. C. 20590	13. Type of Report and Period Covered Interim February 1976 - May 1977
	14. Sponsoring Agency Code S0970
15. Supplementory Notes FHWA Contract Manager Jerar Nishanian, HRS-11	

16. Abstract

Research on the fatigue behavior of horizontally curved, steel bridge elements was conducted at Lehigh University under the sponsorship of the Federal Highway Administration (FHWA) of the U.S. Department of Transportation. The investigation is centered on the effect of welded details on curved girder fatigue strength. Fatigue tests of five full-scale curved plate girder assemblies are a part of the investigation.

The fatigue behavior of five types of welded details from AASHTO Categories C and E is monitored while undergoing two million constant amplitude load cycles on the assemblies. Primary fatigue cracking due to in-plane bending and torsion was observed as well as secondary fatigue cracking due to out-of-plane bending of the web. The web performance under fatigue loading was also observed.

The observation of primary fatigue cracking at the welded details indicates that their fatigue behavior, on curved plate girders, is adequately described by the present AASHTO Category C and Category E design guidelines for straight girders. Groove-welded lateral attachments with circular transitions and secondary fatigue cracking of details at diaphragm locations are problem areas. The web performance demonstrated that allowable stress provisions for web slenderness ratios and transverse stiffener spacing are adequate in the AASHTO specifications and overly stringent in CURT guidelines.

17. Key Words	18. Distribution Statement
Bridges (structures), fatigue, girder bridges, structural engineering, testing, torsion, welding	Document is available to the public through the National Technical Information Service, Springfield, VA 22161

19. Security Classif. (of this report)	20. Security Classif. (of this page)	21. No. of Pages	22. Price
Unclassified	Unclassified	150	

Form DOT F 1700.7 (8-72)

ACKNOWLEDGMENTS

The investigation reported herein was conducted at Fritz Engineering Laboratory, Lehigh University, Bethlehem, Pennsylvania. Dr. Lynn S. Beedle is the Director of Fritz Laboratory and Dr. David A. VanHorn is the Chairman of the Department of Civil Engineering.

The work was a part of Fritz Laboratory Research Project 398, "Fatigue of Curved Steel Bridge Elements" sponsored by the Federal Highway Administration (FHWA) of the United States Department of Transportation. The FHWA Project Manager is Mr. Jerar Nishanian. The Advisory Panel members are Mr. A. P. Cole, Dr. Charles G. Culver, Mr. Richard S. Fountain, Mr. Gerald Fox, Dr. Theodore V. Galambos, Mr. Andrew Lally, Mr. Frank D. Sears, and Dr. Ivan M. Viest.

The following members of the faculty and staff of Lehigh University made major contributions in the conduct of this work: Dr. John W. Fisher, Dr. B. T. Yen, Dr. R. G. Slutter, Dr. N. Zettlemoyer, and R. P. Batcheler.

Mr. Kenneth Harpel and Mr. Robert Dales assisted in executing the test program. Mrs. Mary Snyder and Ms. Shirley Matlock typed the manuscript. The figures were prepared by Mr. John Gera and his staff. Mr. R. N. Sopko provided the photographs.

TABLE OF CONTENTS

		Page
1.	INTRODUCTION	1
	1.1 Background	1
	1.2 Objectives and Scope	2
2.	DESIGN AND FABRICATION OF ASSEMBLIES	4
	2.1 Analysis and Design of Assemblies	4
	2.2 Design of Welded Details	7
	2.3 Fabrication of Assemblies	12
3.	ERECTION AND INSTRUMENTATION OF ASSEMBLIES	16
	3.1 Erection	16
	3.2 Instrumentation	27
4.	INITIAL STATIC AND CYCLIC LOAD TESTS	49
	4.1 Initial Static Tests	49
	4.2 Initial Cyclic Tests	50
	4.3 Group 2 Welded Detail Locations	73
	4.4 Diaphragm and Lateral Bracing Members	74
5.	FATIGUE TESTING	77
	5.1 General Procedure	77
	5.2 Crack Detection and Repair	77
6.	RESULTS OF FATIGUE TESTS	81
	6.1 Primary Fatigue Cracks	81
	6.2 Secondary Fatigue Cracks	95
	6.3 Web Performance	103
7.	DISCUSSION OF TEST RESULTS	104
	7.1 Detail Type I_o	104
	7.2 Detail Type II_o	117
	7.3 Detail Types III_{oa} and III_{ob}	118
	7.4 Detail Type IV_o	120
	7.4.1 Fatigue Life Prediction	121
	7.4.2 Actual Flaws	125
	7.4.3 Summary - Type IV_o Detail	126
	7.5 Detail Type V_{oa}	126
	7.6 Detail Type V_{ob}	129
	7.7 Web Fatigue Strength	130

8. SUMMARY AND CONCLUSIONS 132

9. RECOMMENDATIONS FOR FURTHER WORK 134

10. REFERENCES 135

APPENDIX A: STATEMENT OF WORK 138
APPENDIX B: LIST OF REPORTS PRODUCED UNDER DOT-FH-11-8198 142
APPENDIX C: MATERIAL PROPERTIES 143

LIST OF ABBREVIATIONS AND SYMBOLS

a = crack shape semi-minor axis

b = crack shape semi-major axis

b_f = flange width

d = transverse stiffener spacing

r = radius of circular transition at end of groove-welded gusset plate

t_f = flange thickness

t_w = web thickness

D_w = web depth

L = span length measured at centerline of the test assembly

L_1 = span length measured at centerline of Girder 1 of the test assembly

L_2 = span length measured at centerline of Girder 2 of the test assembly

N = number of load cycles

R = horizontal radius of curvature of test assembly

S_r = stress range

I_o, II_o, III_{oa}, etc. = welded detail types/subtypes for open section (plate girder) test assemblies

δ = lateral web deflection

σ_y = yield stress

σ_u = ultimate stress

U.S. Customary-SI Conversion Factors

To convert	To	Multiply by
inches (in)	millimeters (mm)	25.40
inches (in)	centimeters (cm)	2.540
inches (in)	meters (m)	0.0254
feet (ft)	meters (m)	0.305
miles (miles)	kilometers (km)	1.61
yards (yd)	meters (m)	0.91
square inches (sq in)	square centimeters (cm^2)	6.45
square feet (sq ft)	square meters (m^2)	0.093
square yards (sq yd)	square meters (m^2)	0.836
acres (acre)	square meters (m^2)	4047
square miles (sq miles)	square kilometers (km^2)	2.59
cubic inches (cu in)	cubic centimeters (cm^2)	16.4
cubic feet (cu ft)	cubic meters (m^3)	0.028
cubic yards (cu yd)	cubic meters (m^3)	0.765
pounds (lb)	kilograms (kg)	0.453
tons (ton)	kilograms (kg)	907.2
one pound force (lbf)	newtons (N)	4.45
one kilogram force (kgf)	newtons (N)	9.81
pounds per square foot (psf)	newtons per square meter (N/m^2)	47.9
pounds per square inch (psi)	kilonewtons per square meter (kN/m^2)	6.9
gallons (gal)	cubic meters (m^3)	0.0038
acre-feet (acre-ft)	cubic meters (m^3)	1233
gallons per minute (gal/min)	cubic meters per minute (m^3/min)	0.0038
newtons per square meter (N/m^2)	pascals (Pa)	1.00

1. INTRODUCTION

1.1 Background

The increased utilization of horizontally curved girders in highway bridges has prompted the initiation of several research projects on curved girder bridges[1,2,3,4,5,6]. The research has been aimed at producing expanded design guidelines or specifications for curved girders.

In 1969 the Federal Highway Administration (FHWA) of the U.S. Department of Transportation (U.S. DOT), with the sponsorship of 25 participating state highway departments, commenced a large research project on curved girder bridges[7]. The project involved four universities (Carnegie-Mellon, Pennsylvania, Rhode Island, and Syracuse) and was commonly referred to as the CURT (Consortium of University Research Teams) Project. All of the work was directed towards the development of specific curved steel girder design guidelines for inclusion in the AASHTO (American Association of State Highway and Transportation Officials) bridge design specifications. The curved girders studied included both open (plate girder) and closed (box girder) cross sections.

The CURT program did not include a study of the fatigue behavior of horizontally curved steel bridges.

The research reported herein is part of a multiphase investigation of curved girder fatigue at Lehigh University entitled "Fatigue of Curved Steel Bridge Elements", and is sponsored by the FHWA.

It has long been recognized that fatigue problems in steel bridges are most probable at details associated with bolted and welded connections in tensile stress regions. Straight girder research has shown that welded details are more fatigue sensitive than bolted details. Modern bridge structures rely heavily on welded connections in the construction of main members and for securing attachments such as stiffeners and gusset plates. Therefore, the investigation is centered on the effect of welded details on curved girder fatigue strength.

The multiphase investigation is broken down into five tasks as shown in Appendix A. In Task 1 the analysis and design of large scale horizontally curved plate and box girder test assemblies are performed, including bridge classification and selection of welded details for study. Task 2 concerns special studies on stress range gradients, heat curving residual stresses, web slenderness ratios, and diaphragm spacing as related to fatigue performance. Fatigue tests of large scale plate and box girder test assemblies are performed in Task 3. Ultimate strength tests of the modified test assemblies are performed in Task 4. Design recommendations for fatigue are prepared in Task 5, based on the work of Tasks 1, 2 and 3. References 8 and 23 contain results from Tasks 1 and 2. Appendix B lists all the reports produced under this project.

1.2 Objectives and Scope

This report presents the results of fatigue tests of the curved plate girder test assemblies carried out in Task 3.

The objectives of the testing program are: (1) to establish the fatigue behavior of welded details on horizontally curved steel plate girder highway bridges, and (2) to compare the fatigue behavior of curved plate girders with straight girder performance to determine if revisions to the AASHTO bridge specification are required.

Five types of welded details are selected for placement on the webs and flanges of full-scale curved plate girder assemblies. Five assemblies are fabricated to accommodate the number of welded details. Each assembly consists of two curved girders joined by X-type diaphragms. An assembly is subjected to approximately two million constant amplitude load cycles under one of two different load conditions: (1) loads positioned directly over the web of one girder at the quarter points, or (2) loads positioned midway between the girders at the quarter points.

Two causes of fatigue cracking are anticipated: (1) primary cracking due to in-plane bending and torsion, (2) secondary cracking due to out-of-plane bending of the web. Each assembly is inspected periodically during the fatigue testing. Records of visible and through-thickness cracks are maintained.

2. DESIGN AND FABRICATION OF ASSEMBLIES

2.1 Analysis and Design of Assemblies

A thorough description of the analysis and design of the curved plate girder test assemblies is provided in Ref. 8. A brief summary is given here.

Since the research effort is centered on fatigue crack propagation at welded details, the type and number of details to be investigated has an influence on the design of the assemblies. In view of the number of details to be tested and the desired replication, five horizontally curved plate girder assemblies were designed to provide stress and deflection conditions typical of actual bridges at the details to be tested. The design of all assemblies is in accordance with the AASHTO design specifications except where modified by the CURT tentative design recommendations[7,9,10].

Figure 1 shows a schematic plan view of a typical curved plate girder assembly. Each assembly consists of two curved plate girders joined together by five X-type diaphragms at 3.0 m (10 ft.) intervals. Girder and girder-diaphragm joint numbering shown in the figure are the same for all five assemblies. Assemblies 4 and 5 also have horizontal X-type lateral bracing near the bottom flanges in the middle two bays of each assembly. Table 1 summarizes the cross-section dimentions of both curved girders for each assembly.

Preliminary designs of the plate girder assemblies were obtained using the Syracuse computer program[11]. The Berkeley computer

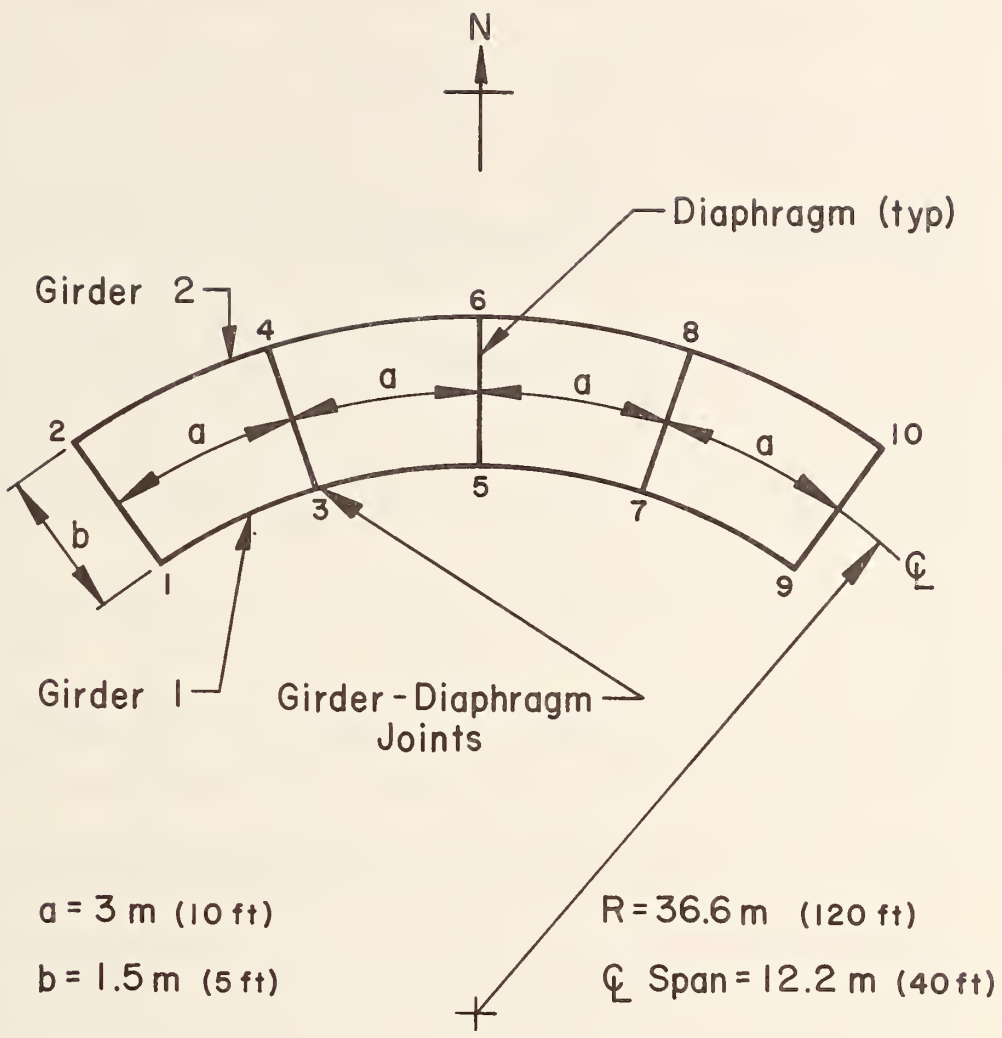

Fig. 1 Schematic Plan View of Typical Curved Plate Girder Assembly (From Ref. 8)

Table 1 Summary of Cross-Section Dimensions (From Ref. 8)

Assembly	Girder	Flange Width b_F mm (in)	Flange Thickness t_F mm (in)	Web Depth D_w mm (in)	Web Thickness t_w mm (in)	D_w/t_w
1	1	304.8 (12)	25.4 (1)	1371.6 (54)	9.5 (3/8)	144
	2	304.8 (12)	25.4 (1)	1371.6 (54)	7.1 (9/32)	192
2	1	203.2 (8)	12.7 (1/2)	1473.2 (58)	9.5 (3/8)	155
	2	254 (10)	19 (3/4)	1473.2 (58)	7.9 (5/16)	186
3	1	203.2 (8)	12.7 (1/2)	1473.2 (58)	9.5 (3/8)	155
	2	254 (10)	19.1 (3/4)	1473.2 (58)	9.5 (3/8)	155
4	1	203.2 (8)	12.7 (1/2)	1320.8 (52)	9.5 (3/8)	139
	2	304.8 (12)	25.4 (1)	1320.8 (52)	9.5 (3/8)	139
5	1	203.2 (8)	12.7 (1/2)	1320.8 (52)	9.5 (3/8)	139
	2	304.8 (12)	25.4 (1)	1320.8 (52)	9.5 (3/8)	139

program, CURVBRG was used for the final designs of all five assemblies [12].

2.2 Design of Welded Details

Table 2 summarizes the welded details selected for investigation[8]. There are five basic types (I_o to V_o) with subtypes for III_o and V_o. The detail type is shown by the Roman numeral in the upper left-hand corner of each drawing. The first subscript, o, refers to open section. A second subscript a or b is given when there are subtypes. The corresponding straight girder category, relating to the 1977 AASHTO specifications, Table 1.7.2A1 is shown by the capital letter in the upper right-hand corner of each drawing in Table 2 [10]. All details of interest are either Category C or Category E.

In all drawings in Table 2 a solid dot defines the location of the predicted fatigue crack. Often two or more such locations are possible depending on the stress distribution and/or initial flaw size. Only the welds relating to the details studied are shown. Groove welds are specifically identified. All welds shown without marking symbol are of the fillet type. Other welds such as those connecting webs to flanges are not shown for clarity. For any weld not shown in the drawings it can be assumed that the associated flaws and stress concentrations are not critical relative to those of the welds shown. Therefore fatigue crack growth in these welds, although likely present, is not expected to limit the detail life.

All major design work focused on the welded details located at diaphragm and bottom lateral bracing connections in the tensile stress

region of the assemblies. Because no room for error exists once fabrication is complete, the stress conditions at these locations must be known as accurately as possible prior to fabrication and testing. Because the individual plate girders are readily accessible after fabrication, additional details can be added between the diaphragms after initial static and cyclic load tests have determined the actual stress conditions in the girders. The welded details shown in Table 2 therefore fall into two basic groups depending on their positions along an assembly and whether they were placed during fabrication or in Fritz Laboratory.

Group 1 details consist of welded details at connections for diaphragms or bottom lateral bracing which are placed during fabrication of an assembly. Group 1 details are shown in Fig. 2.

Group 2 details consist of the additional details welded to an assembly in the laboratory after the initial static and cyclic load tests of that assembly are complete but prior to fatigue testing that assembly. Some of the welded details in Group 2 provide replication of Group 1 details thus increasing the benefit-cost ratio for each assembly. Group 2 details are discussed further in Art. 4.3.

All details on a given test assembly are designed to fail by fatigue cracking at about the same cycle life in order to reduce testing time and to reduce problems associated with crack repair. A life of two million cycles was chosen which represents a desired life expectancy for many bridges and can be considered a bench mark figure for fatigue testing. Allowable stress ranges of 55.2 MPa (8 ksi) and

Table 2 Summary of Welded Details

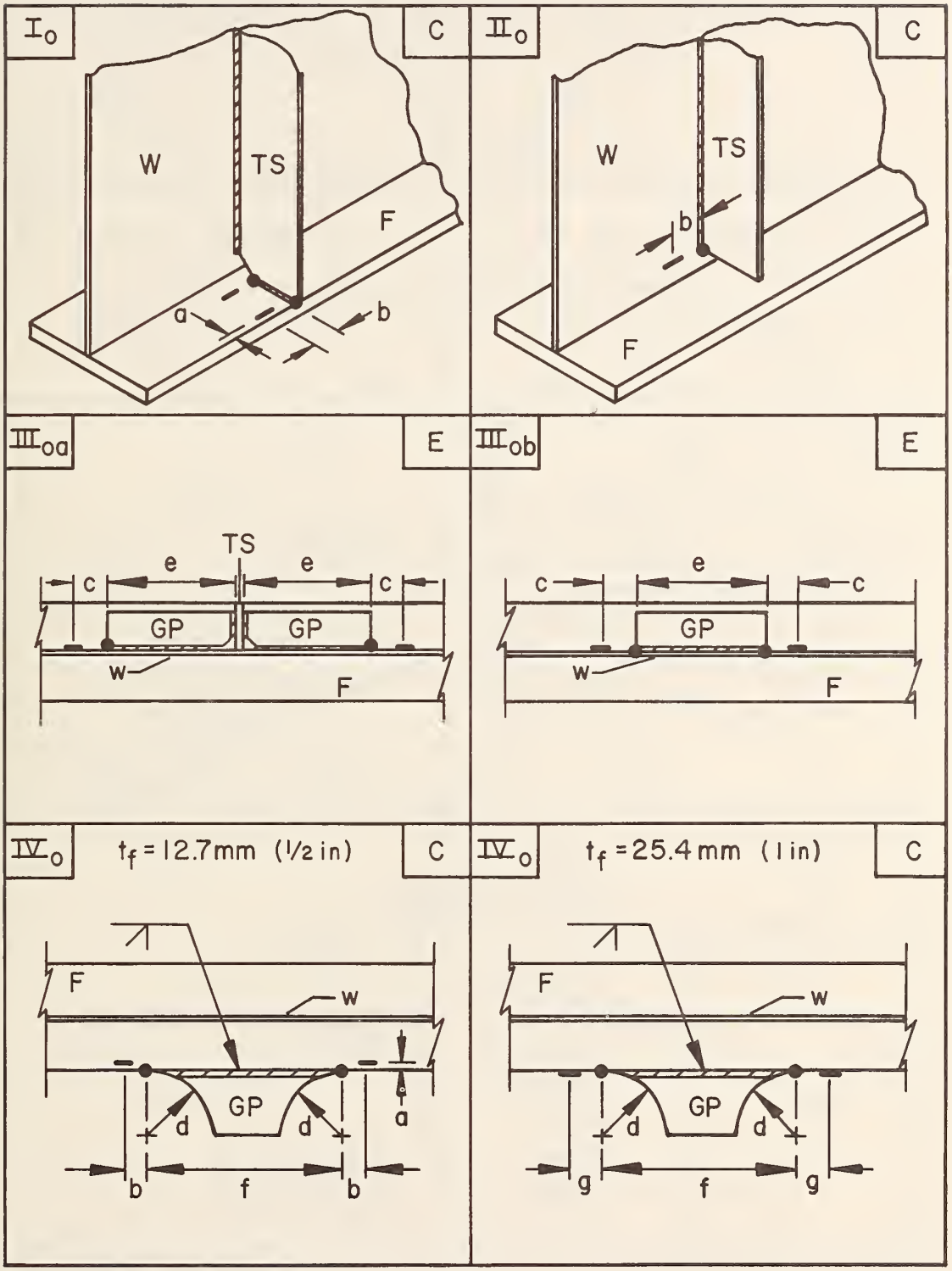

Table 2 (Continued)

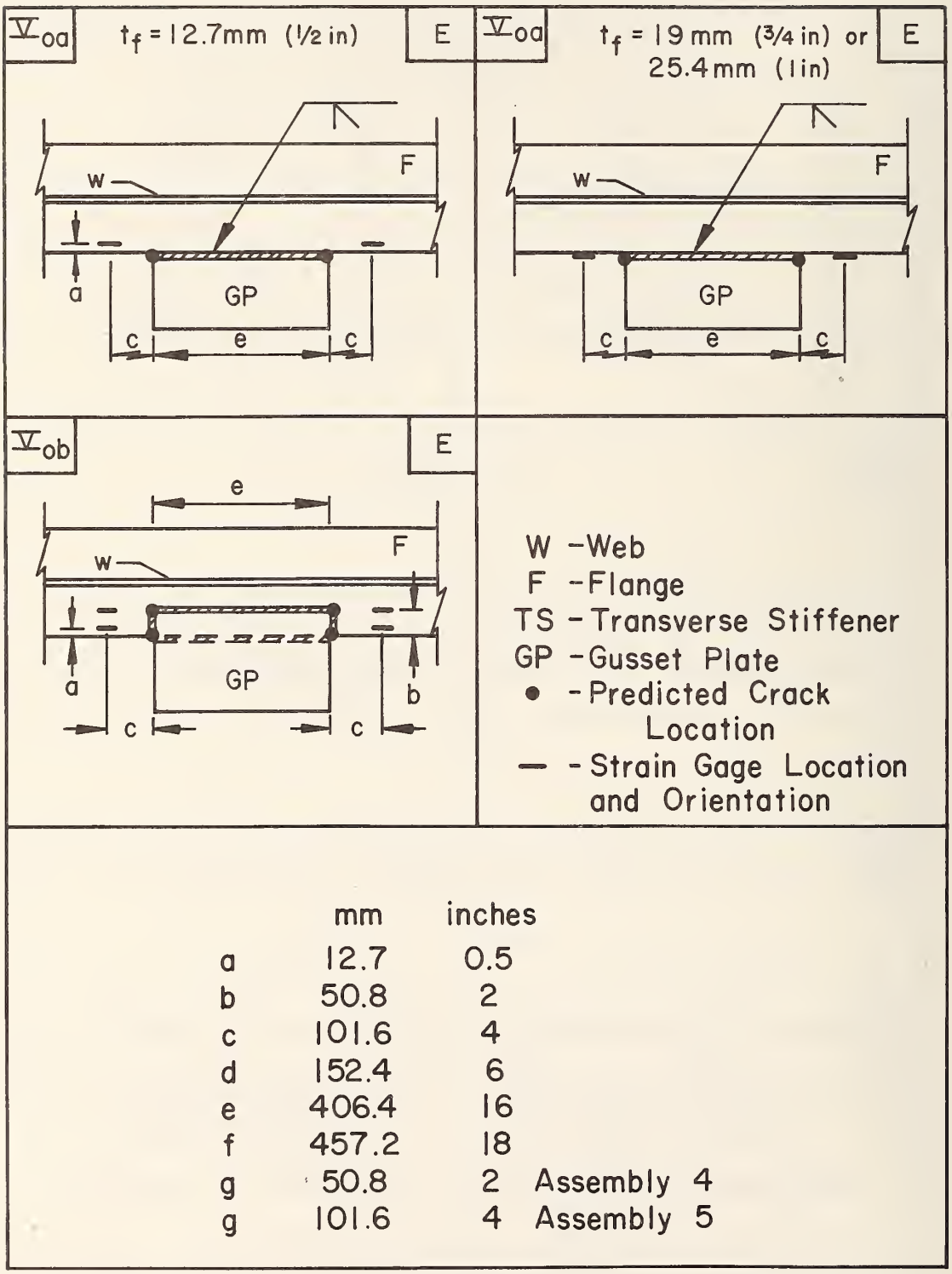

	mm	inches	
a	12.7	0.5	
b	50.8	2	
c	101.6	4	
d	152.4	6	
e	406.4	16	
f	457.2	18	
g	50.8	2	Assembly 4
g	101.6	4	Assembly 5

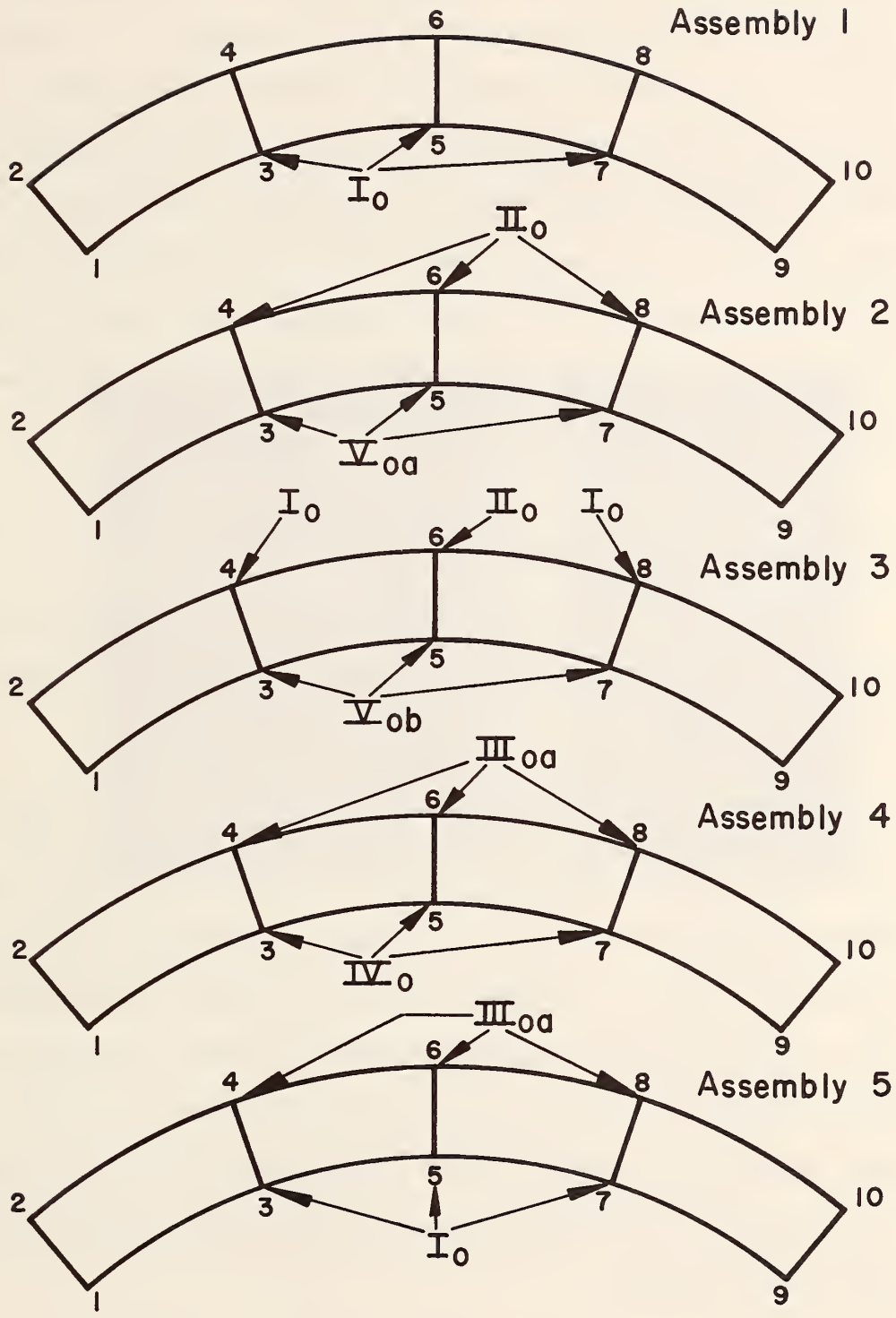

Fig. 2 Group 1 Details (Refer to Table 2)

89.6 MPa (13 ksi) for Category E and Category C details respectively represent the 95% confidence limit for 95% survival at two million cycles[10]. To ensure the formation of visible fatigue cracks at about two million cycles and to allow for a margin of error between calculated and measured stress ranges it is necessary to use design stress ranges in the tests somewhat higher than those recommended in AASHTO. For this reason a 69.0 MPa (10 ksi) design stress range was selected for all Category E details. A 103.4 MPa (15 ksi) design stress range was selected for all Category C details[8].

2.3 Fabrication of Assemblies

The five curved plate girder assemblies were fabricated and assembled by Bethlehem Fabricators, Inc., and delivered to Fritz Engineering Laboratory with the Group 2 details unattached.

All steel is ASTM A36 grade. A325 bolts, 22.2 mm (7/8 in.) in diameter are used in the diaphragm and bottom lateral bracing connections. All welding conforms to the American Welding Society bridge standards. Manual and automatic welding performed by the fabricator is by the submerged-arc process. Welding of Group 2 details in the laboratory is done manually using the covered electrode process. Nominal weld sizes of 6.4 mm (1/4 in.) and 7.9 mm (5/16 in.) are used throughout the assemblies with all welding performed with 482.6 MPa (70 ksi) electrodes.

Figures 3 and 4 show Assembly 1 during several stages of fabrication. Each flange was flame cut to the required radius prior to

Fig. 3 Curved Flanges Tack-Welded to Web - Assembly 1

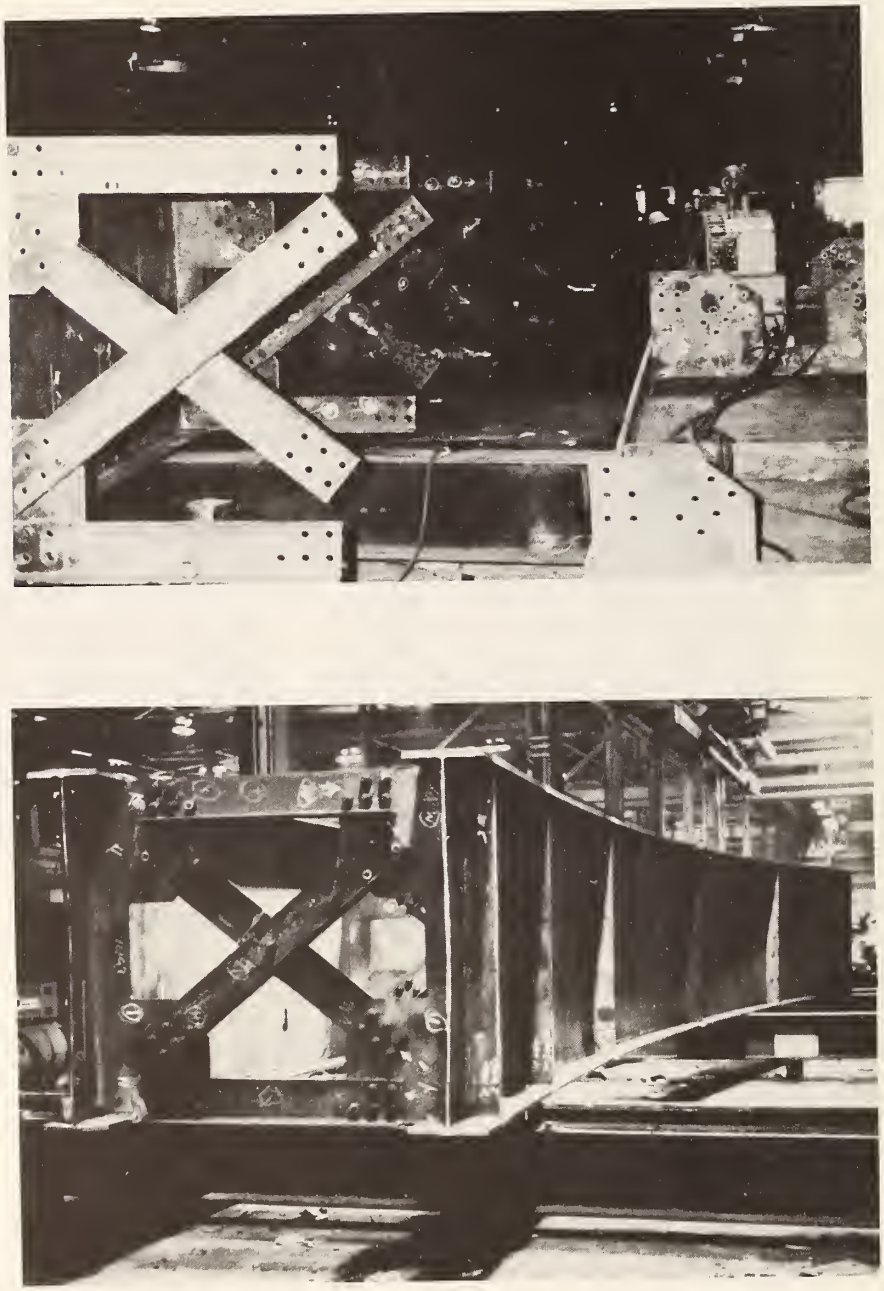

Fig. 4 Diaphragms Connecting Girders of Assembly 1

connection to the web. The web was then curved while being attached to the flange. The X-type diaphragm members were all bolted to one girder before positioning the second girder and bolting it to the diaphragms.

Girder 1 of each assembly (Fig. 1) has a radius of 35.8 m (117.5 ft.). Girder 2 has a radius of 37.3 m (122.5 ft.). Thus the centerline radius of each assembly is 36.6 m (120 ft.) when the girders are spaced 1.5 m (5 ft.) apart. Each girder was required to be fabricated to a tolerance of $\pm$152 mm (6 in.) of the required radius. In addition the deviation of the arc measured from the centerline of any 3 m (10 ft.) chord was not to vary by more than $\pm$6.4 mm (1/4 in.). The symmetry of curvature about midspan of each girder was checked in the laboratory by measuring distances from the web to a chord stretched between the end joints, 1 and 9 or 2 and 10 (Fig. 1). The measured distances for points equidistant from midspan are always within 12.7 mm (1/2 in.) of each other, and within $\pm$25.4 mm (1 in.) of the calculated distance based on the theoretical radius.

3. ERECTION AND INSTRUMENTATION OF ASSEMBLIES

3.1 Erection

Each of the plate girder assemblies was tested in fatigue on the dynamic test bed located in Fritz Engineering Laboratory, Lehigh University. Figures 5 and 6 are schematic views of an assembly on the dynamic test bed. Each assembly is supported at the ends of the two girders and loaded at the quarter points by hydraulic jacks. The two loading conditions and the horizontal restraint conditions are shown in Fig. 7.

Figures 8 and 9 provide views of Assemblies 1 and 3 with jacks in positions 1 and 2, respectively. The two heavy portal frames bolted to the dynamic test bed served as loading frames. The portal frames are braced to the test bed by diagonals in the longitudinal direction of the assemblies. All bolts anchoring the frame columns to the test bed are prestressed to minimize sway and uplifting of the frames.

For both static and cyclic loading, a 489.5 kN (110 kip) capacity Amsler hydraulic jack is centered on each of the two portal frames (Figs. 6, 8, and 9). The maximum jack strokes are 127 mm (5 in.) and 11.4 mm (0.45 in.) for static and cyclic loading, respectively. The jacks are located in position 1 for Assembly 1 and in position 2 for the other four assemblies (Fig. 7). Two Amsler pulsators generate the necessary hydraulic pressure for the jacks during the static and cyclic loading conditions. Synchronized mechanically, electrically, and hydraulically, these pulsators run at a constant speed of about

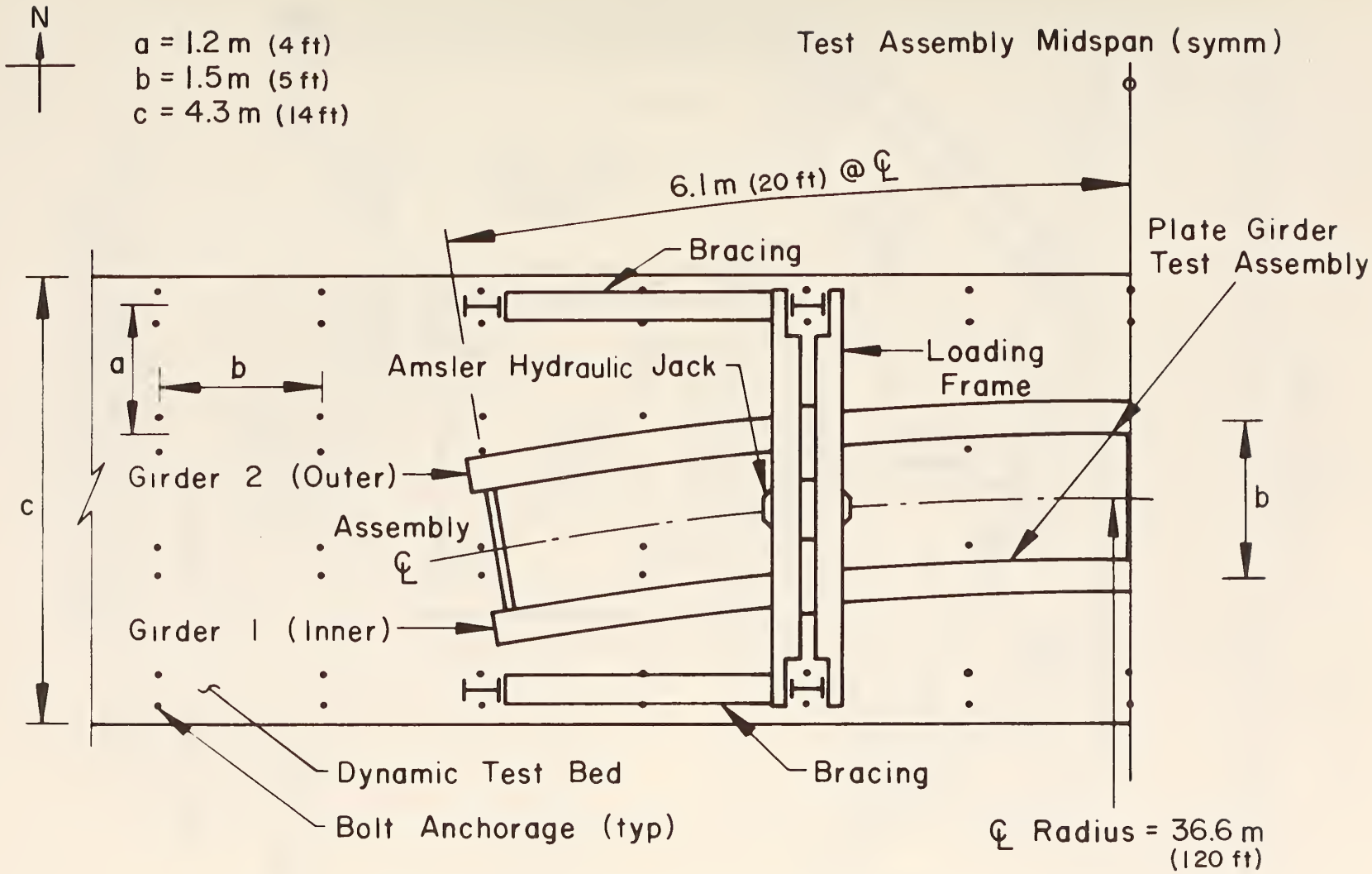

Fig. 5 Typical Assembly on Dynamic Test Bed - Schematic Plan View

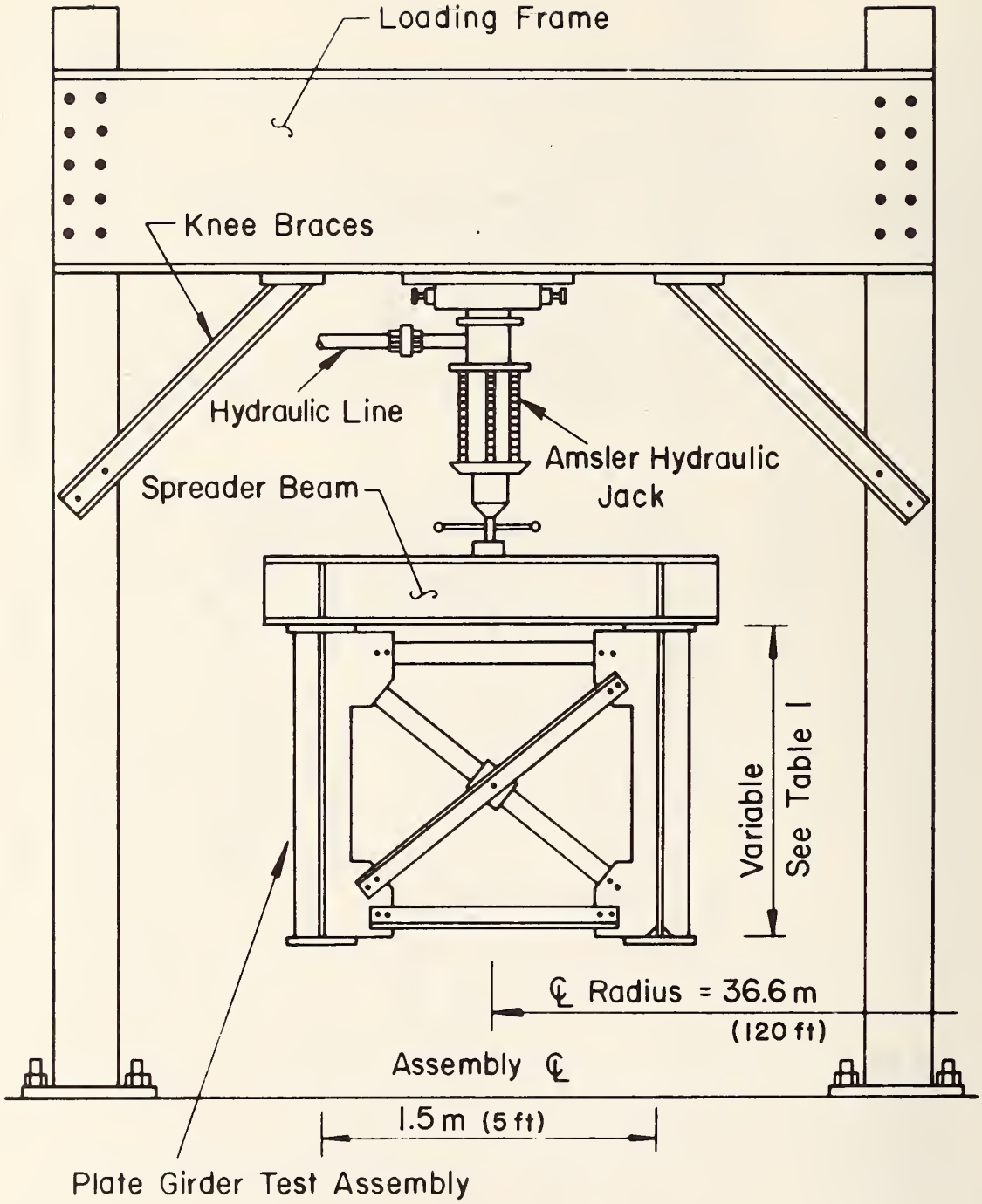

Fig. 6 Typical Assembly on Dynamic Test Bed - Schematic Section at Loading Frame

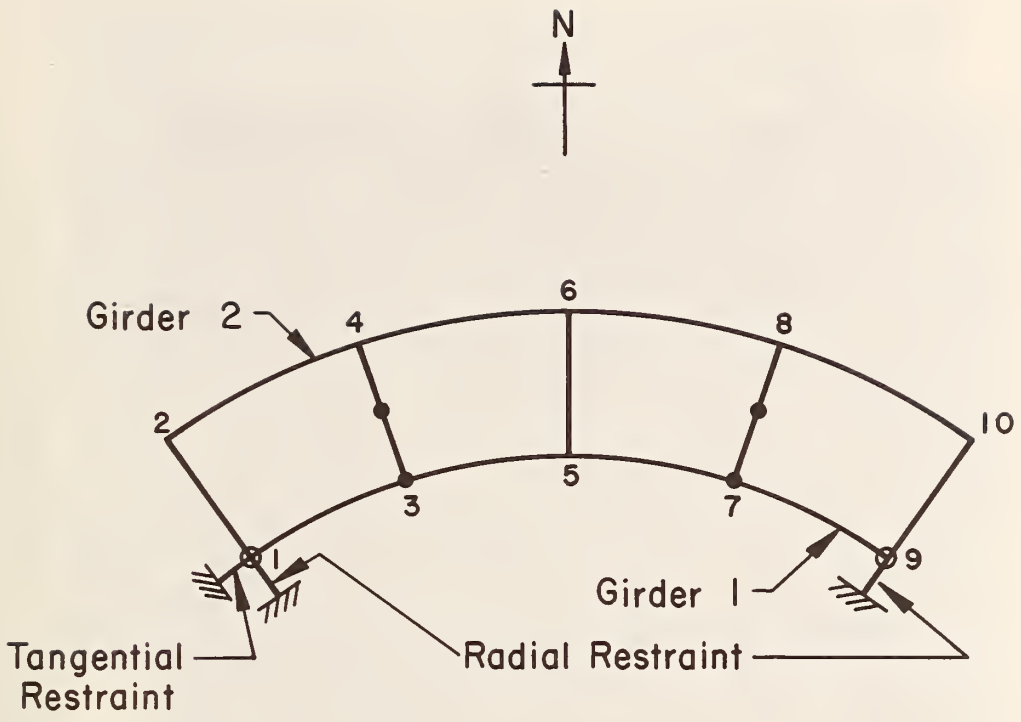

Loading Conditions

Position 1 - Over Joints 3 & 7

Position 2 - Midway Between Joints 3 & 4

Midway Between Joints 7 & 8

Fig. 7 Plan View of Typical Assembly Showing the Two Loading Conditions and the Horizontal Restraint Conditions

Fig. 8 Assembly 1 on Dynamic Test Bed - Jack Position 1

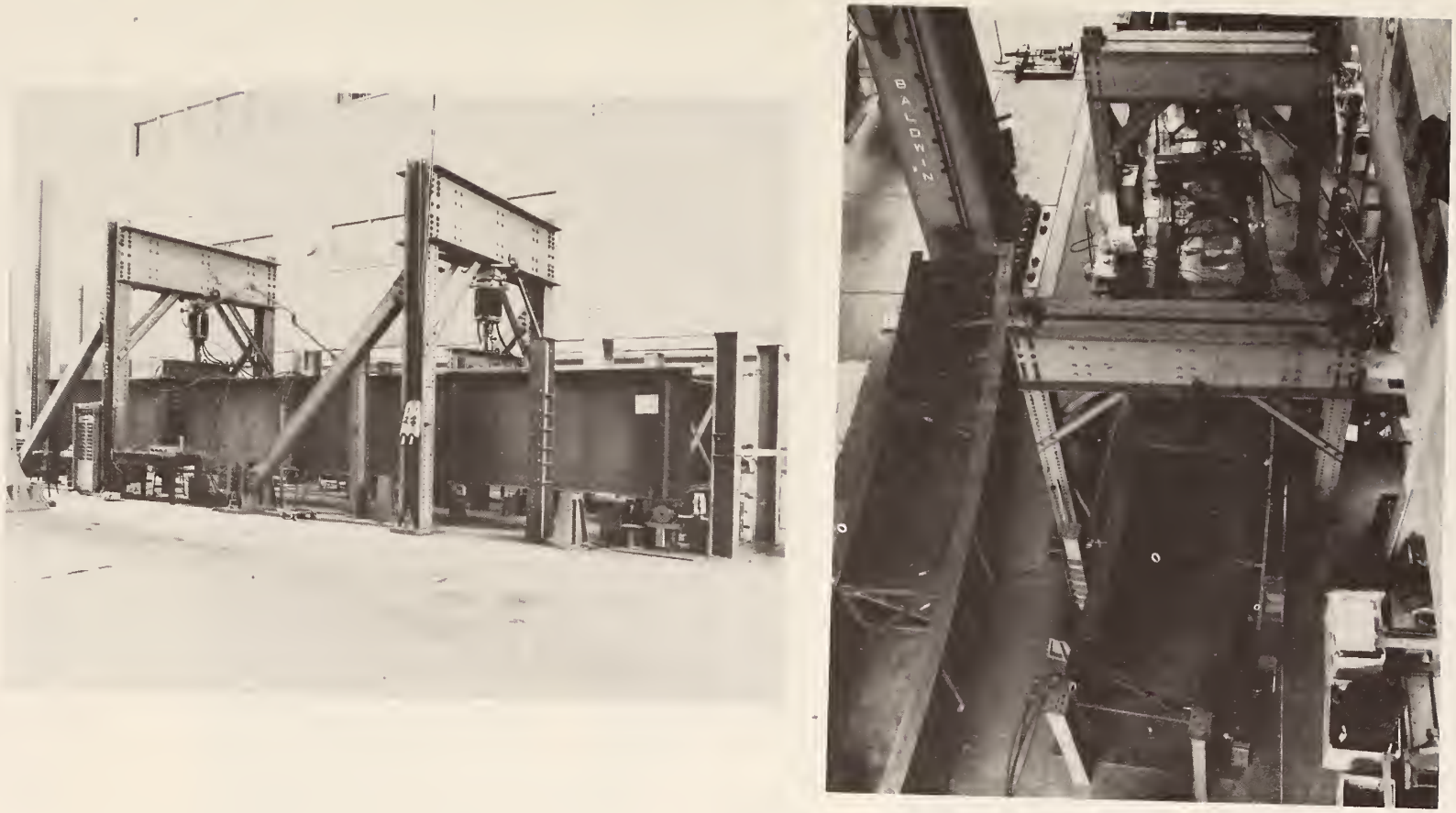

Fig. 9 Assembly 3 on Dynamic Test Bed - Jack Position 2

250 cycles per minute during fatigue testing. The approximate load magnitude is read off pressure gages which are directly connected to the hydraulic jacks. The fatigue tests were controlled by strains measured at many locations on the assemblies, not by the load indicated by the pressure gages. Reference 13 gives a more detailed description of the construction of the test bed and the associated testing equipment.

Loads are transmitted from the jacks to the assembly through a 297.4 mm (11 in.) deep load beam spanning the 1.5 m (5 ft.) distance between the girders. The locations of the jacks on the load beam for the two loading conditions are shown in Fig. 10. The ends of the load beam are supported by 3.2 mm (1/8 in.) shims 304.8 mm (12 in.) long and 25.4 mm (1 in.) wide placed longitudinally with respect to the girder directly over the webs at the loaded joints. The load beams are attached to the top flanges of an assembly by C clamps.

The end supports consist of two rollers at right angles to each other as shown in Fig. 11. Two 203.2 mm (8 in.) diameter steel rollers are sandwiched between three 50.8 mm (2 in.) thick plates. The axis of the upper roller is in line with the girder radius. The bottom roller is at right angles to the upper roller. The rollers are 228.6 mm (9 in.) in length and the top and bottom plates are 228.6 mm x 304.8 mm (9 in. x 12 in.). The middle plate is 304.8 mm (12 in.) square. To prevent rigid body movement of an assembly three degrees of freedom are fixed (Fig. 7). Radial displacement is prevented at joints 1 and 9 and tangential displacement is prevented at joint 1.

(a)

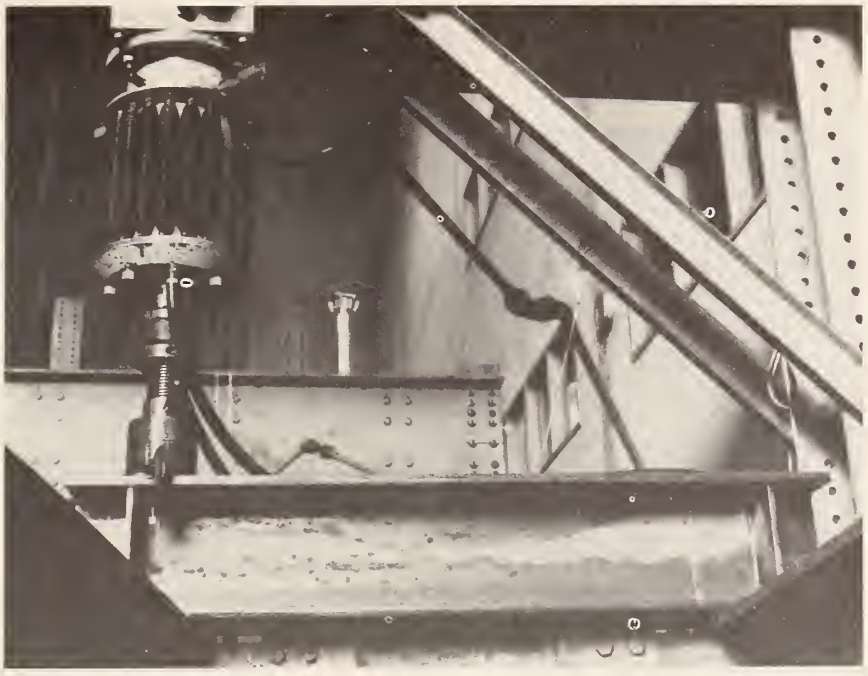

(b)

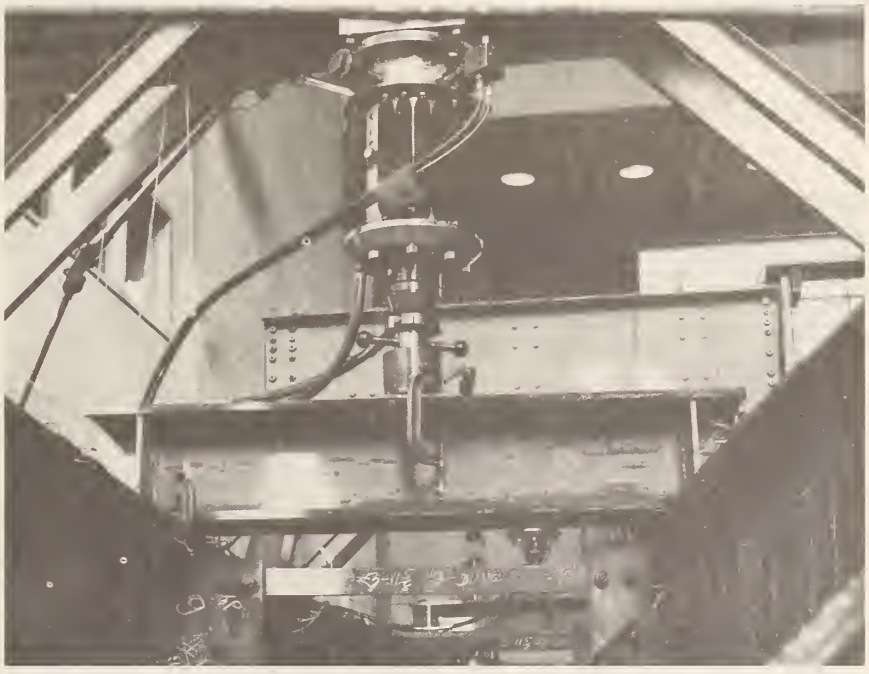

Fig. 10 Location of Hydraulic Jacks on Load Beam
(a) Position 1 (b) Position 2

(a) Support at Joint 1, Showing High Blocks Which Prevent Radial and Tangential Motion

(b) Support at Joint 2, Showing Short Blocks Which Allow Both Rollers to Move Freely

Fig. 11 Views of Rollers Used to Support Girders at Joints 1, 2, 9 and 10

Rolling motion of both rollers at joint 1 is prevented by the tightly fitted blocks mounted on the plates as shown in Fig. 11a. The rolling motion of the bottom roller is prevented at joint 9. The rollers at joints 2 and 10 are allowed to move freely as shown in Fig. 11b. The short blocks shown in the figure are for safety reasons. The top plate at each support is firmly clamped to the bottom flange of the girder, as shown in Fig. 11. The proper alignment of the rollers and plates is maintained by two tapered pins inserted into oversized holes at each interface of roller and plate. The alignment pins and holes are shown in Fig. 12.

The hold-down bolt pattern of the dynamic test bed requires that the portal frames be spaced 6.1 m (20 ft.) apart in the east-west direction (Fig. 5). For jack position 2, the jacks were positioned 6.09 m (19.98 ft.) apart, as required.

For jack position 1 on Assembly 1, the distance between joints 3 and 7 is 5.96 m (19.56 ft.). The jacks were spaced 6.09 m (19.98 ft.) apart to conform to the portal frame spacing which placed them 63.5 mm (2.5 in.) east and west of these joints. In addition, Assembly 1 was moved 711.2 mm (28 in.) north on the test bed so that the jacks would be close to joints 3 and 7. The actual position of the jacks was 44.4 mm (1.75 in.) north of joints 3 and 7. No attempt was made to place the jacks exactly over joints 3 and 7 because of the eccentric loading which would result on the portal frames.

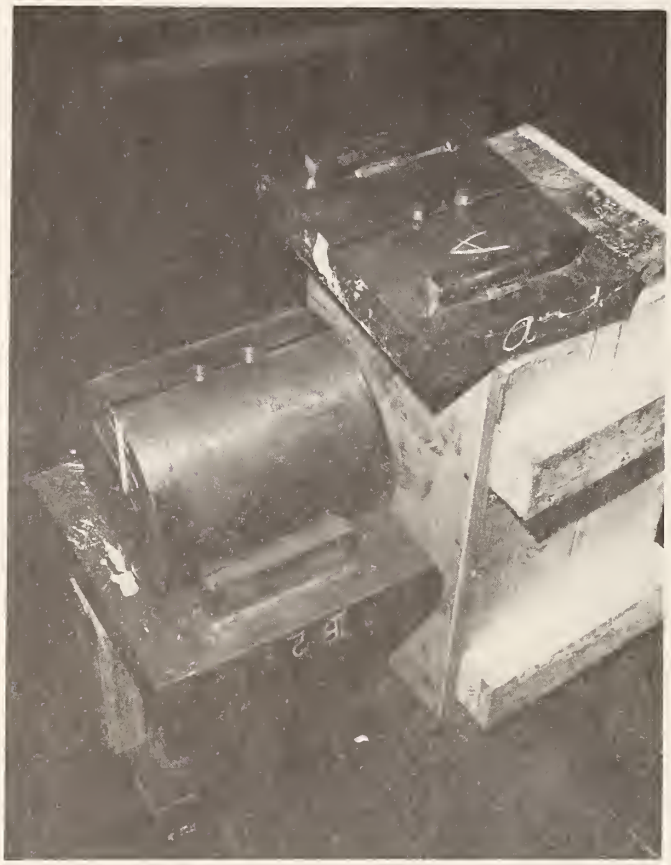

Fig. 12 Alignment Pins and Holes at Interface of Rollers and Plates

3.2 Instrumentation

Several sets of instrumentation were employed to monitor assembly behavior during the static and fatigue testing. Static tests were made to align each assembly and obtain the correlation between the actual and predicted stresses (Ref. 8). During all fatigue testing the main objective was to measure the stress range in the vicinity of each potential crack location.

During static alignment tests, three types of instrument observations were made. Strains in the assemblies were recorded by electrical resistance strain gages bonded to the flanges, webs, diaphragms, and bottom lateral bracing as shown in Figs. 13 through 23. These gages had a nominal gage length of 6.4 mm (1/4 in.).

Vertical and horizontal deflections under static loads were measured by Ames dial gages at locations shown in Figs. 24 and 25 during alignment tests. The dial gages had a least scale division of 25.4 μm (0.001 in.) and a stroke of 25.4 mm (1 in.).

Lateral web deflections relative to the flange-web intersections were measured at selected locations using a dial gage rig specially designed for this purpose as shown in Fig. 26. The Ames dial gages attached to the rig were identical to those described in the previous paragraph. The number of dial gages varied with the web depth. Calibration of the rig was accomplished on a machined surface before deflections were measured on an assembly.

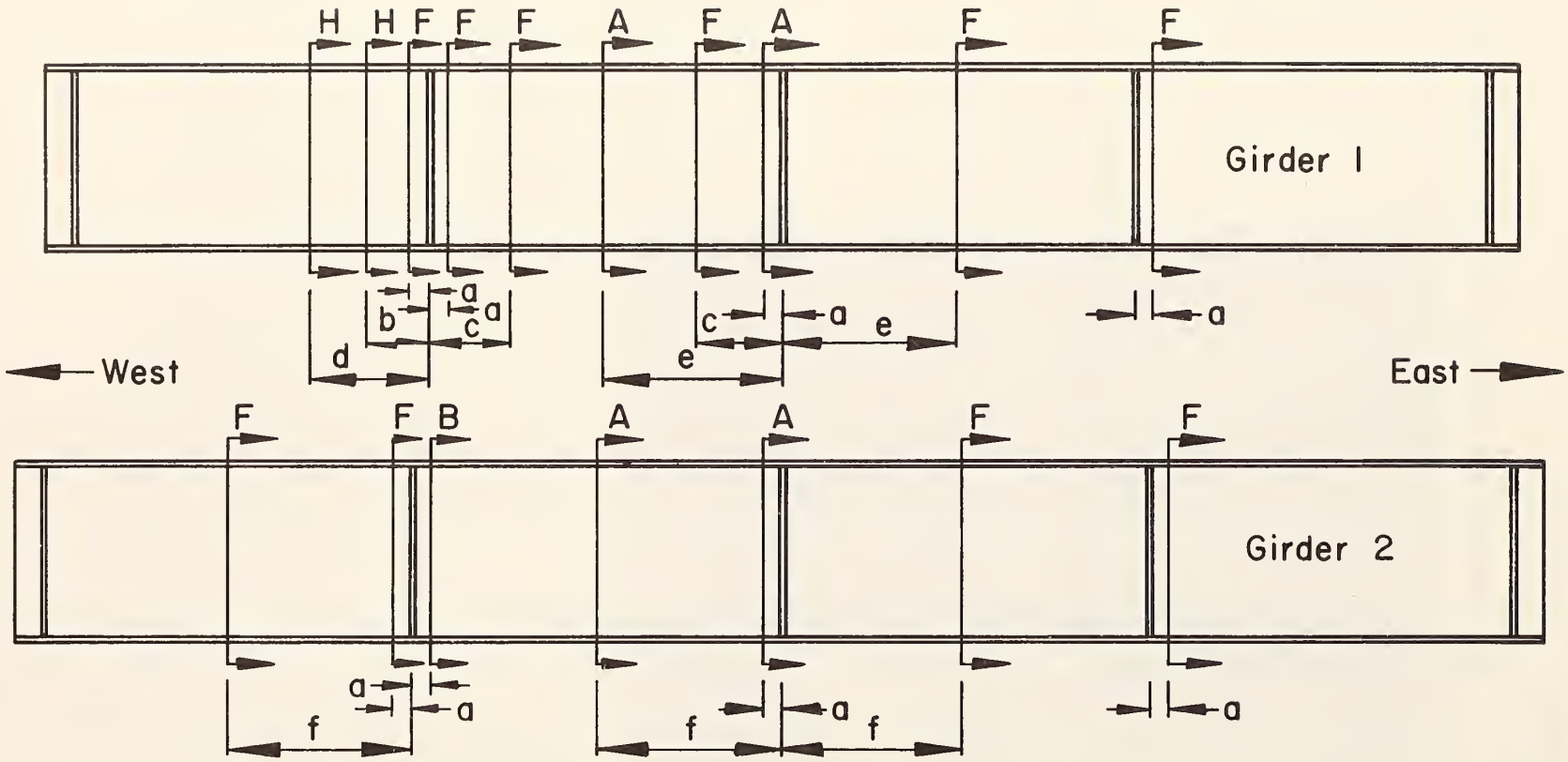

Dimensions mm (in)

a = 127 (5)
b = 508 (20)
c = 749 (29 1/2)
d = 1016 (40)
e = 1499 (59)
f = 1549 (61)

Section views on Fig. 18.

Fig. 13 Assembly 1 Cross Sections With Strain Gages

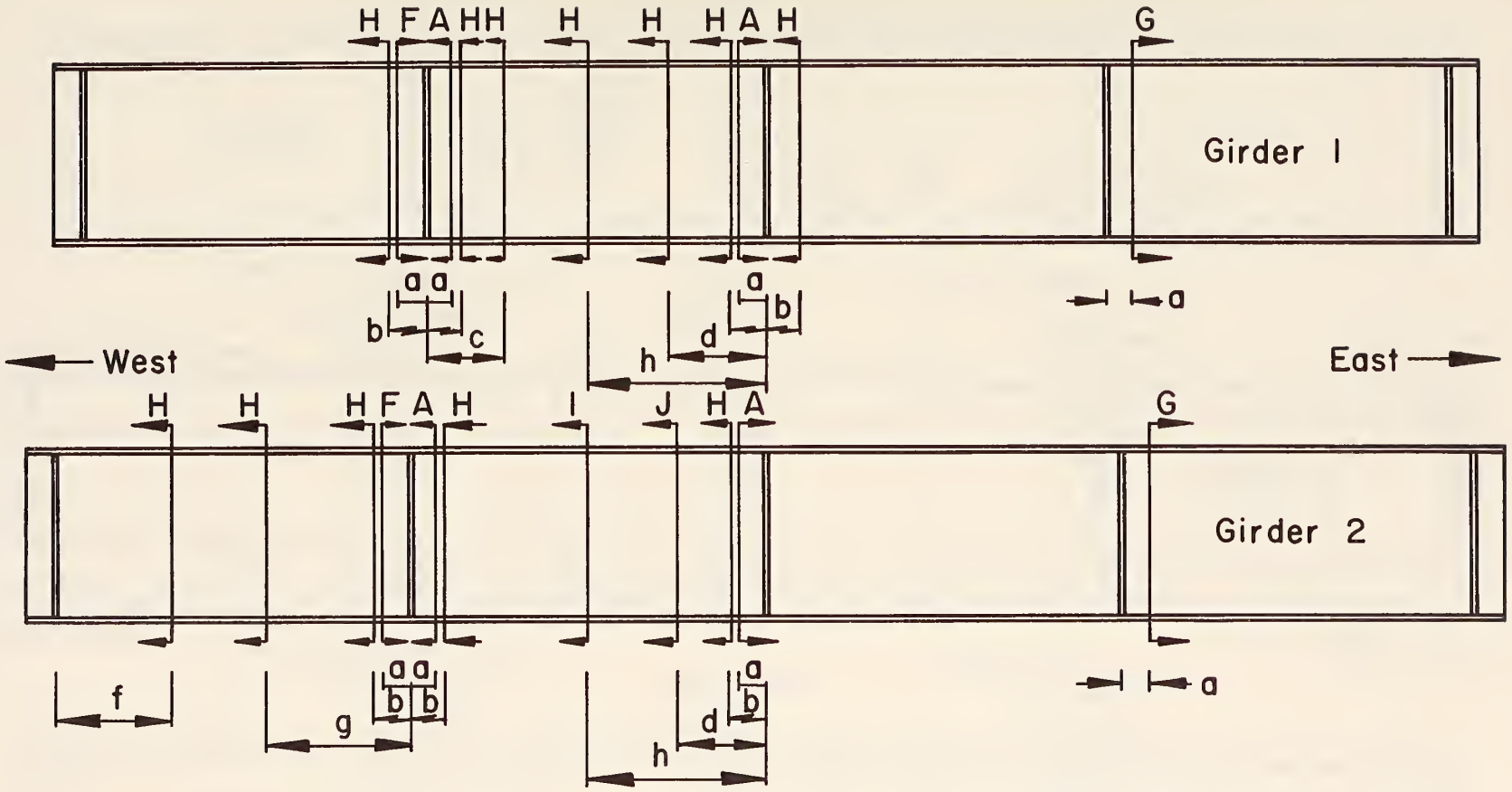

Fig. 14 Assembly 2 Cross Sections With Strain Gages

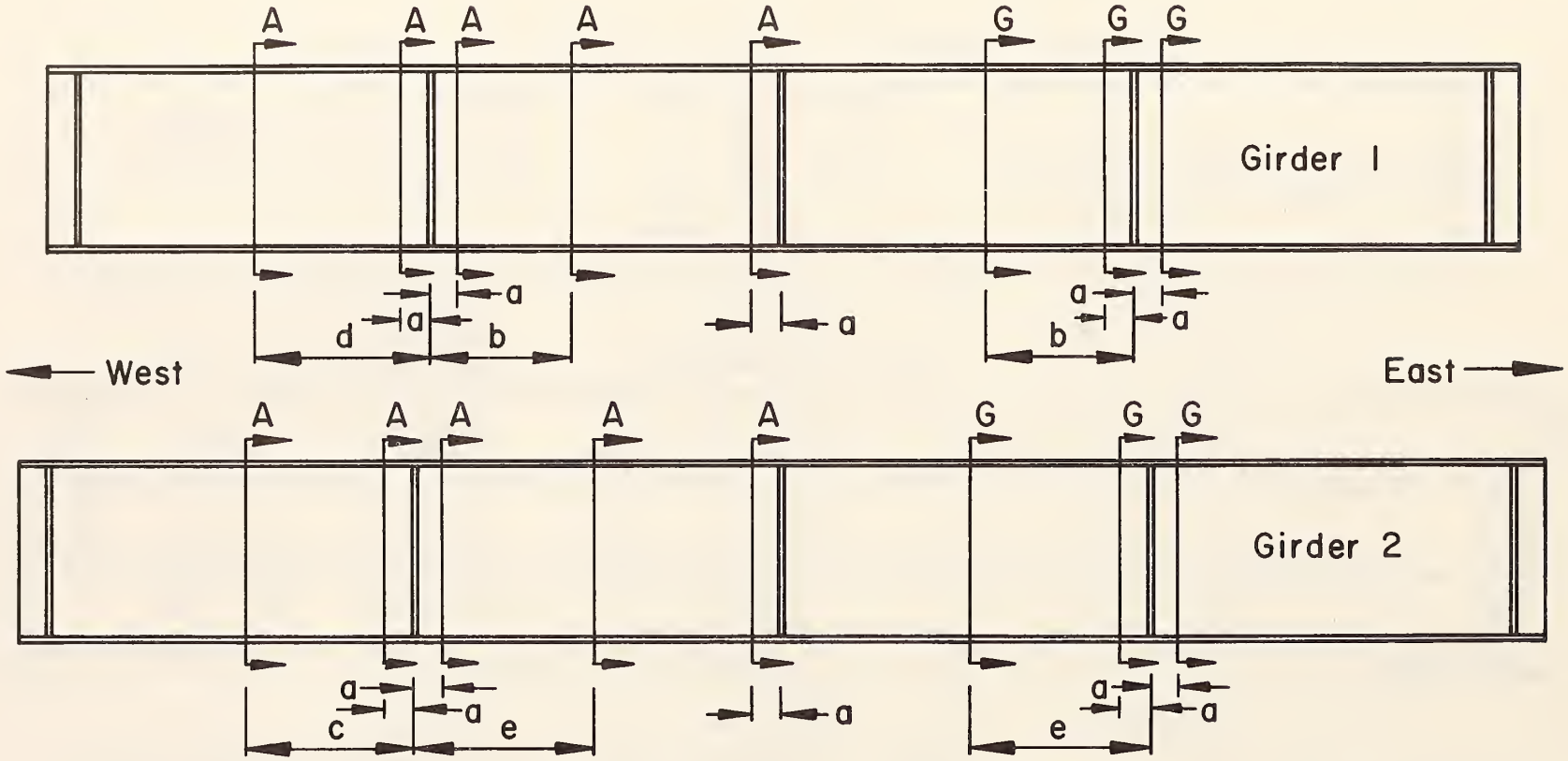

Dimensions mm (in)

a = 254 (10)
b = 1245 (49)
c = 1435 (56 1/2)
d = 1499 (59)
e = 1511 (59 1/2)

Section views on Fig. 18.

Fig. 15 Assembly 3 Cross Sections With Strain Gages

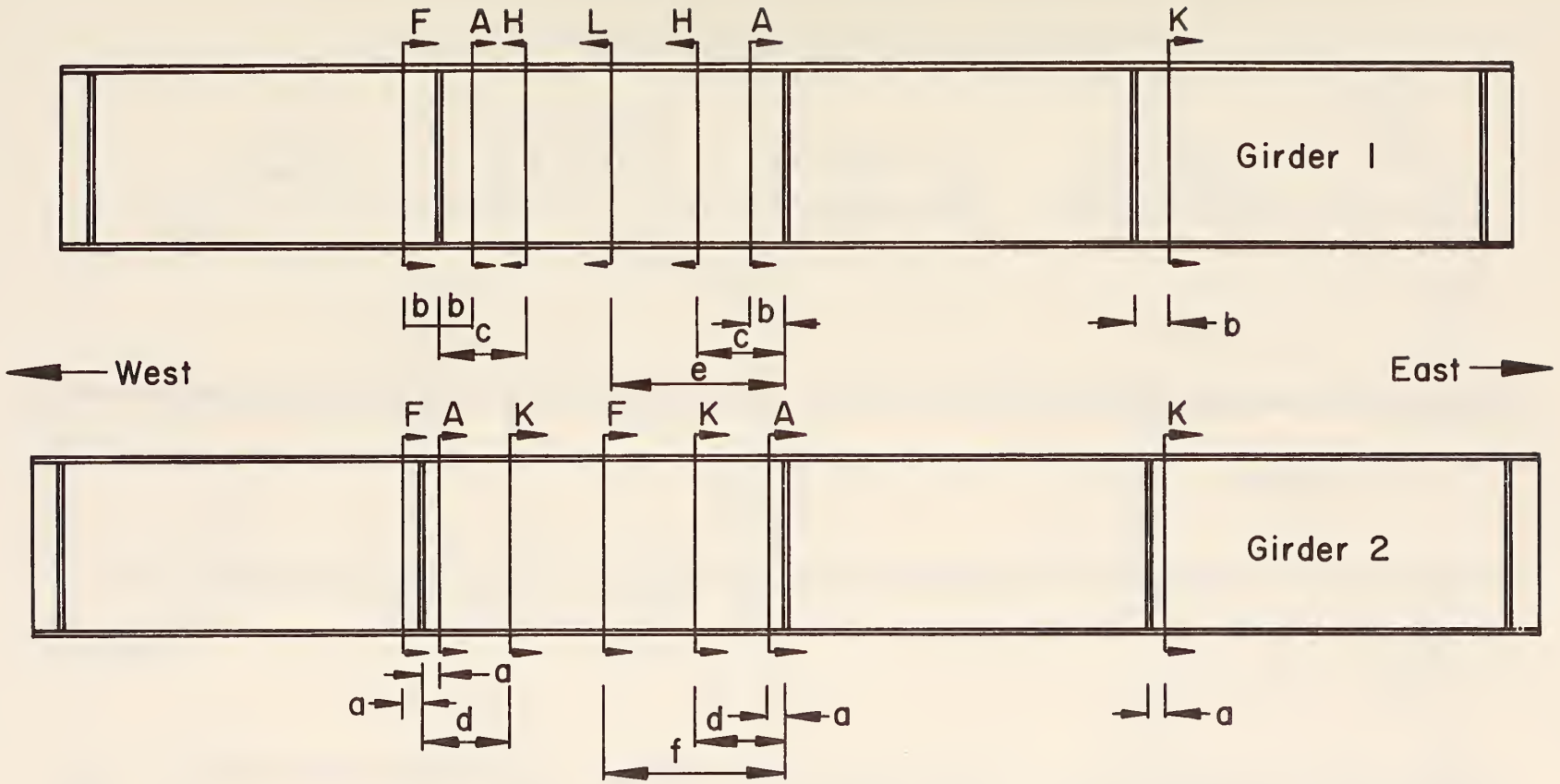

Fig. 16 Assembly 4 Cross Sections With Strain Gages

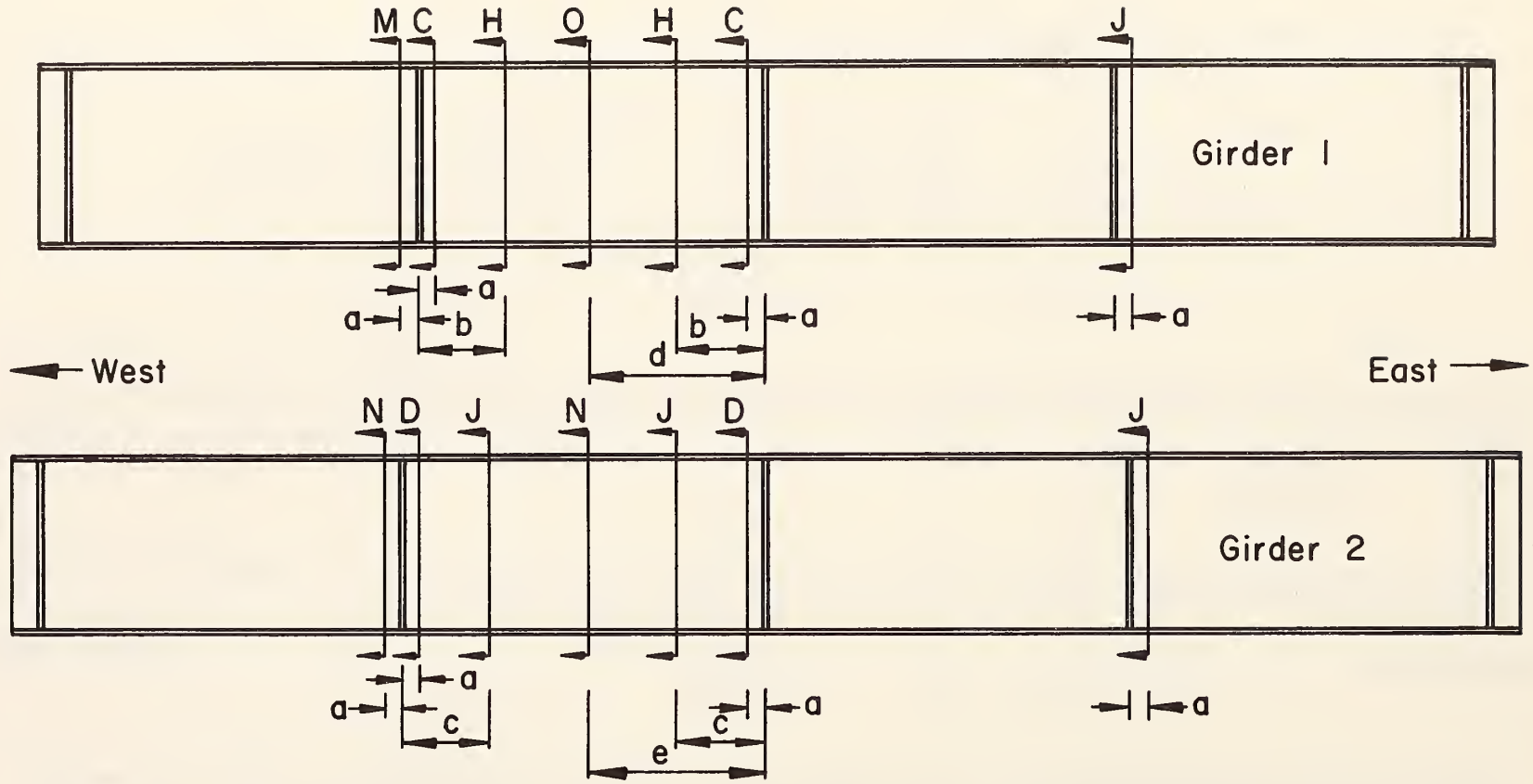

Fig. 17 Assembly 5 Cross Sections With Strain Gages

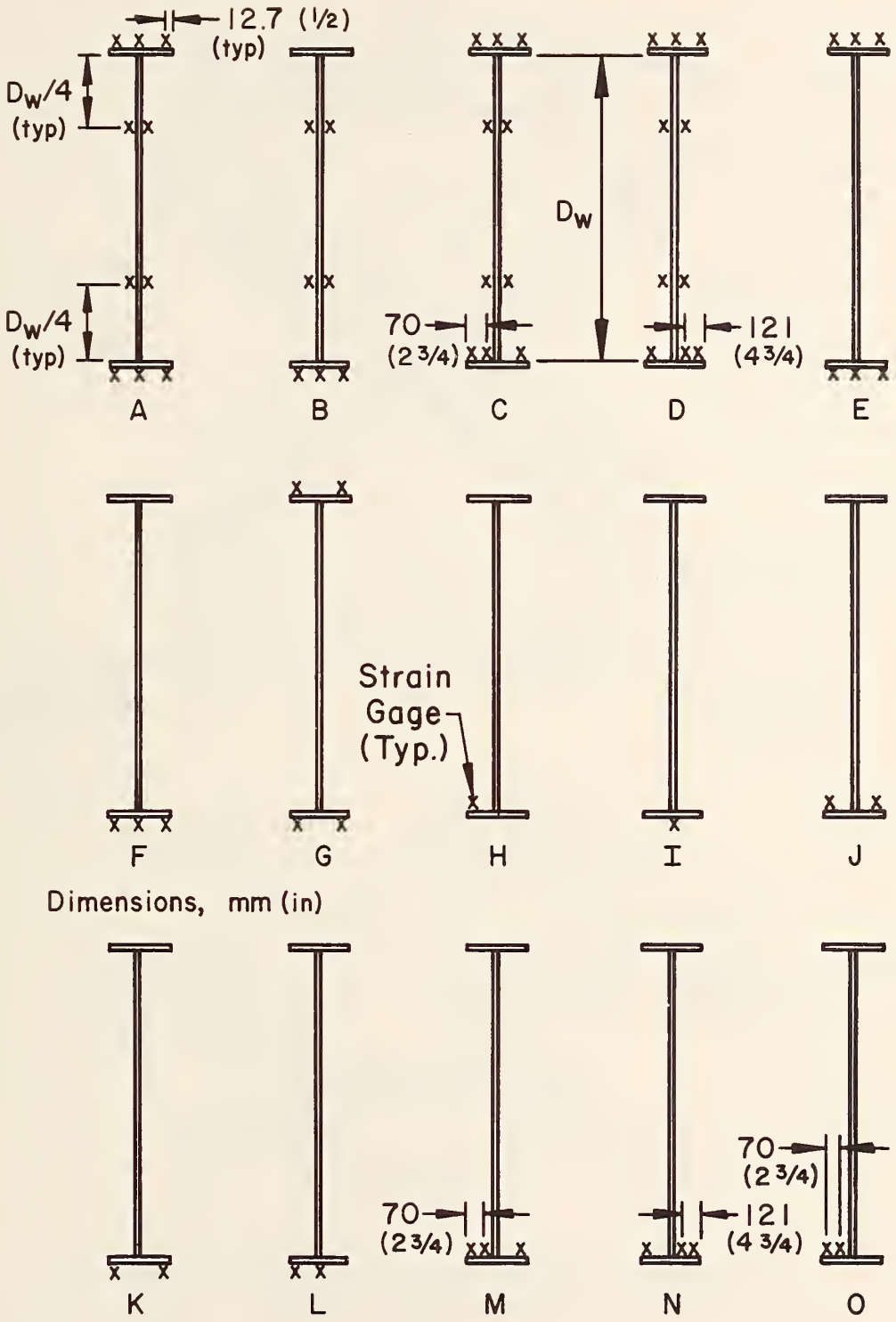

Fig. 18 Cross-Section Strain Gage Locations

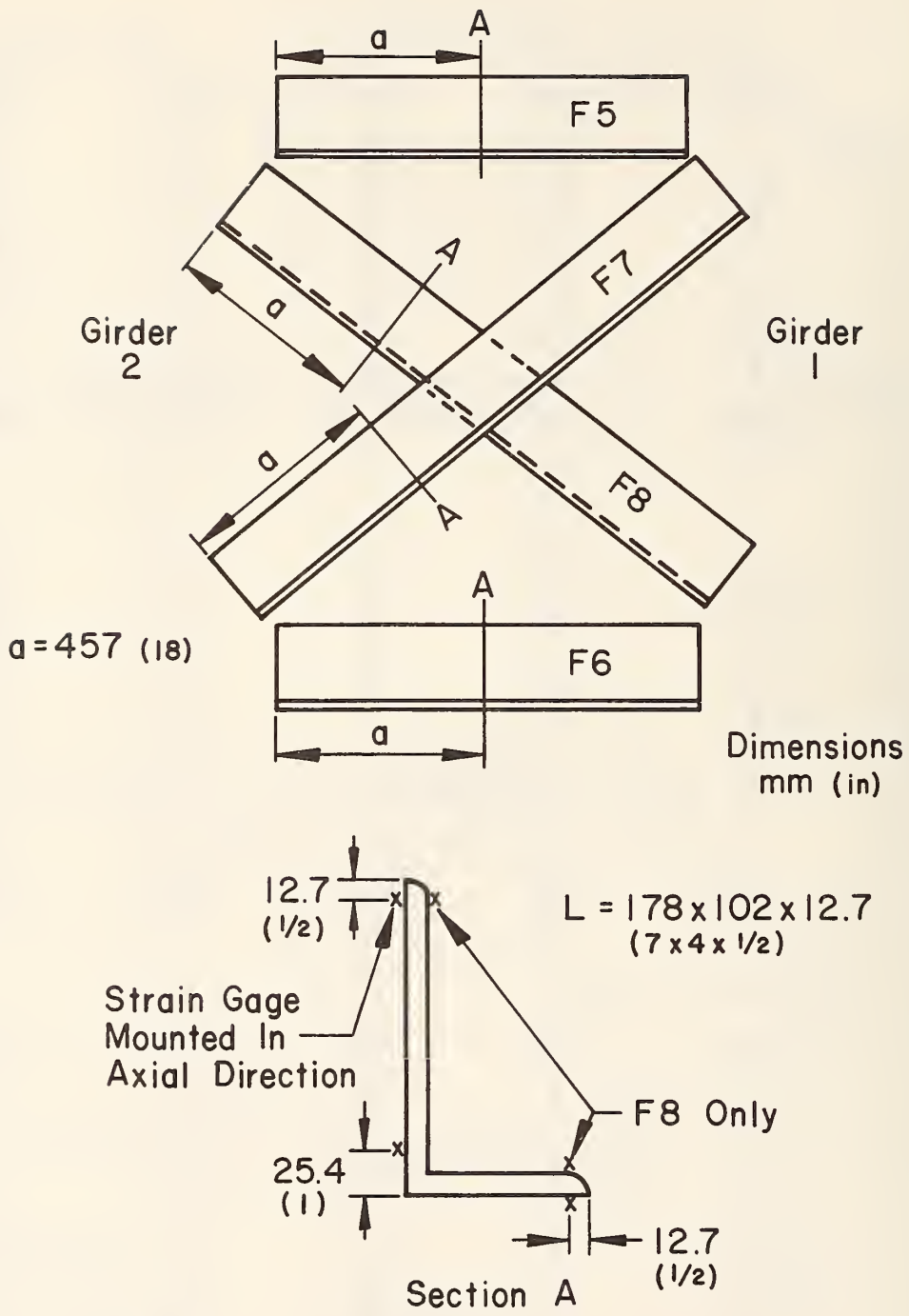

Fig. 19 Strain Gages on Assembly 1 Diaphragm Between Joints 3 and 4

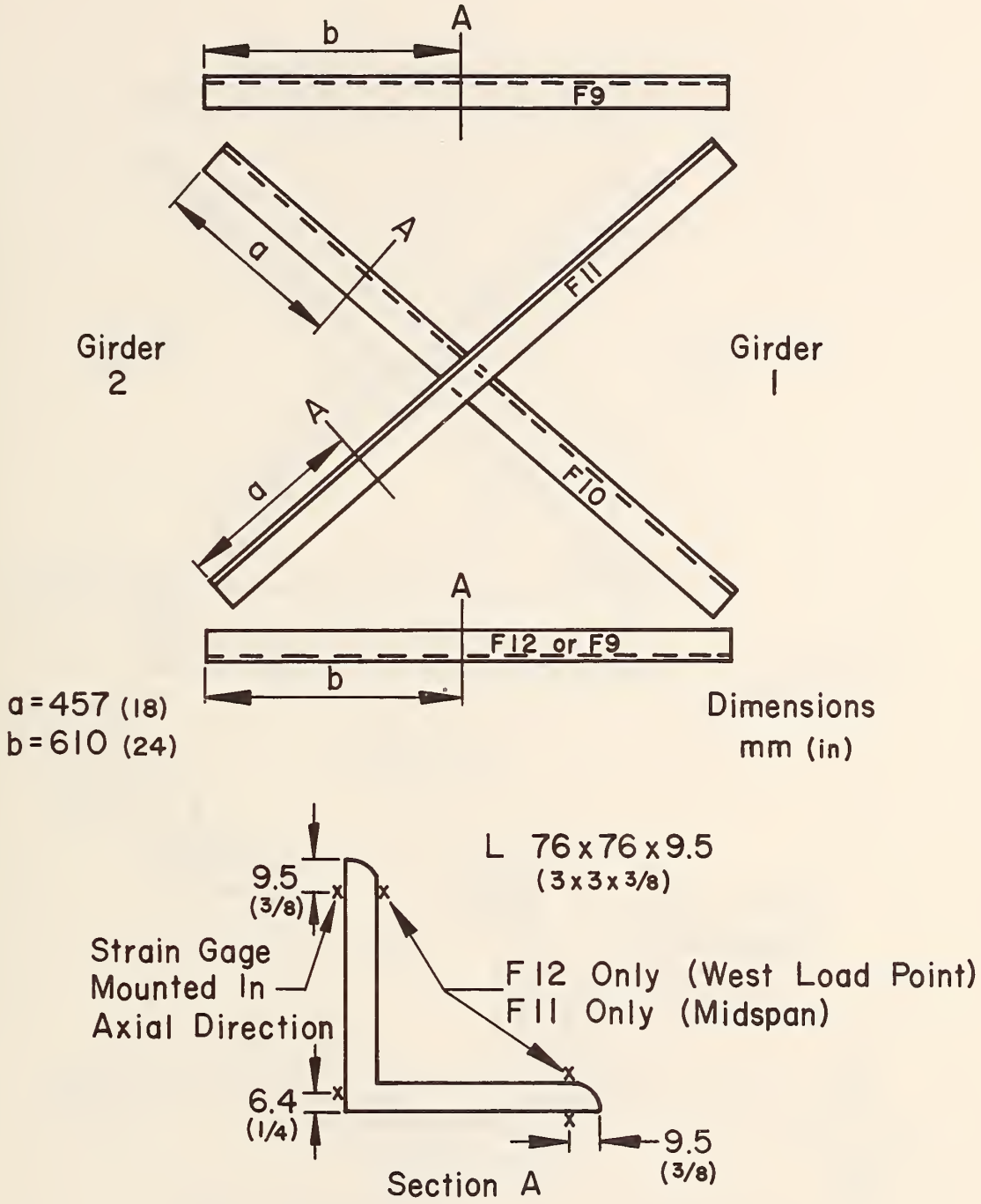

Fig. 20 Strain Gages on Assembly 2 Diaphragms
Between Joints 3 and 4, 5 and 6

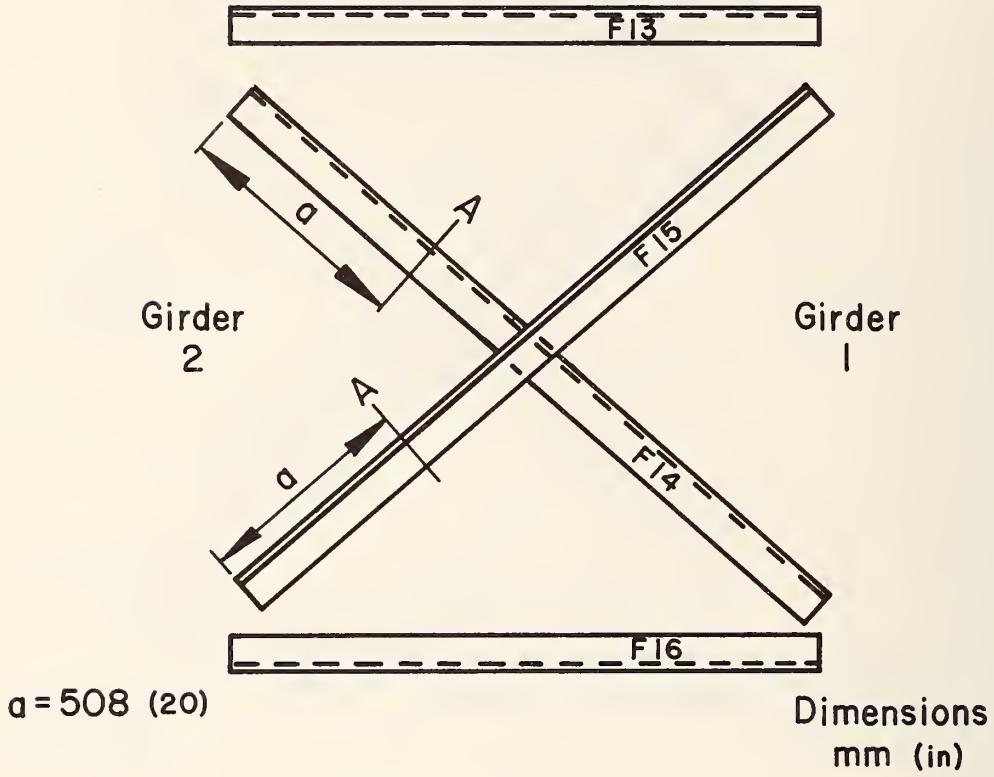

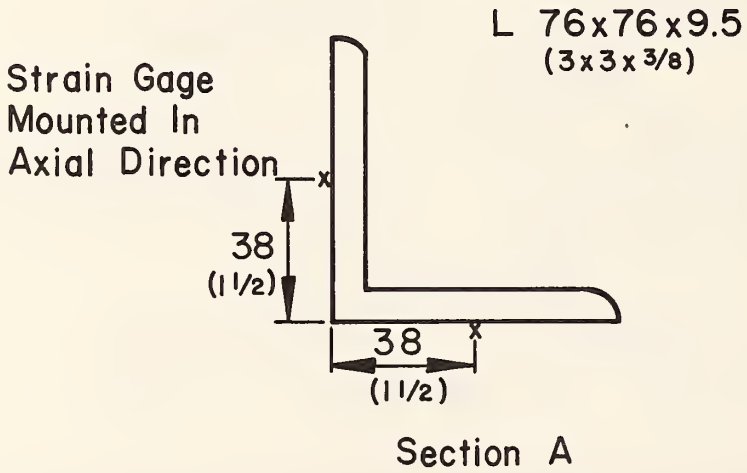

Fig. 21 Strain Gages on Assembly 3 Diaphragms Between Joints 3 and 4, 5 and 6

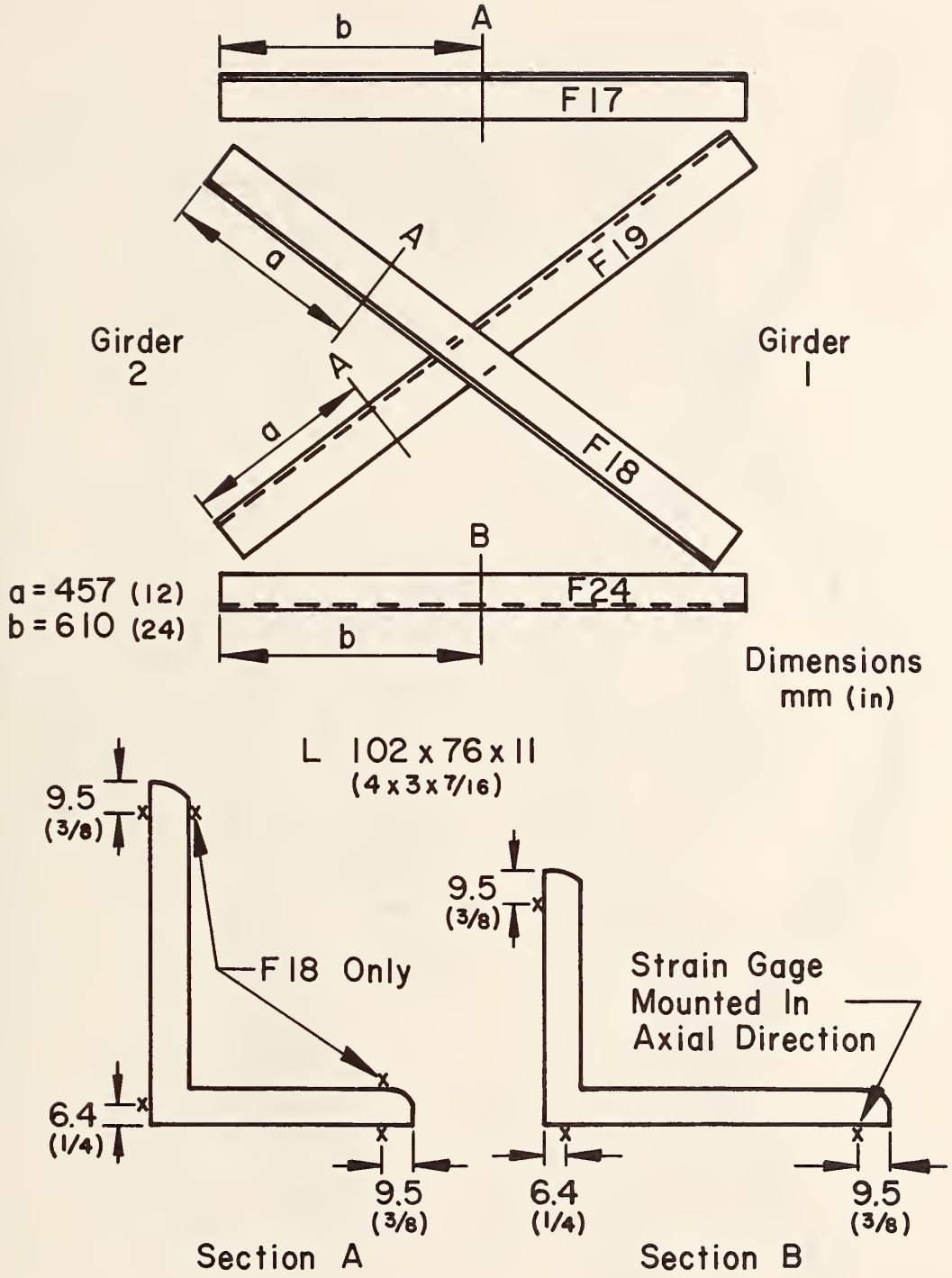

Fig. 22 Strain Gages on Diaphragm Between Joints 5 and 6 on Assemblies 4 and 5

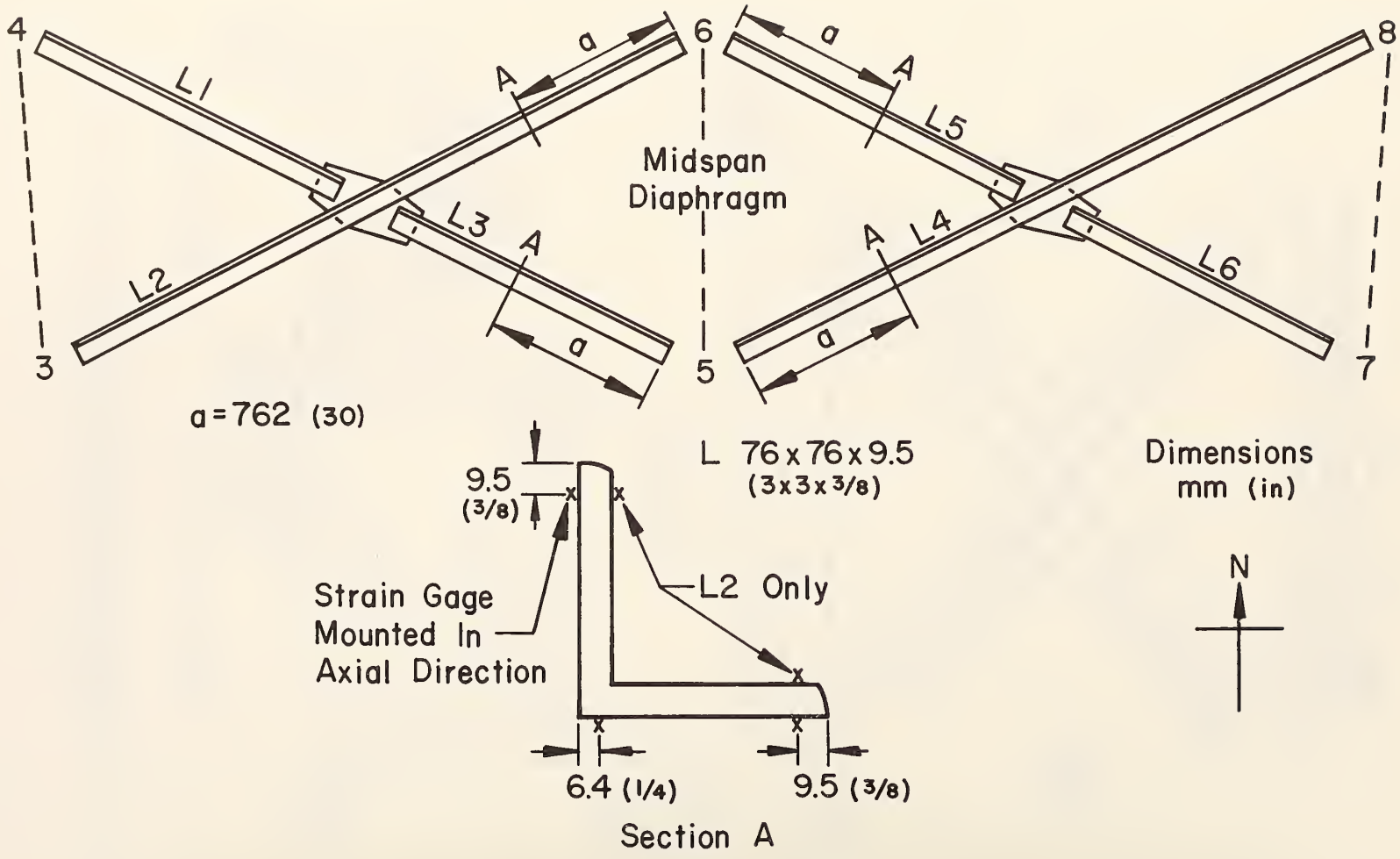

Fig. 23 Strain Gages on Bottom Lateral Bracing on Assemblies 4 and 5

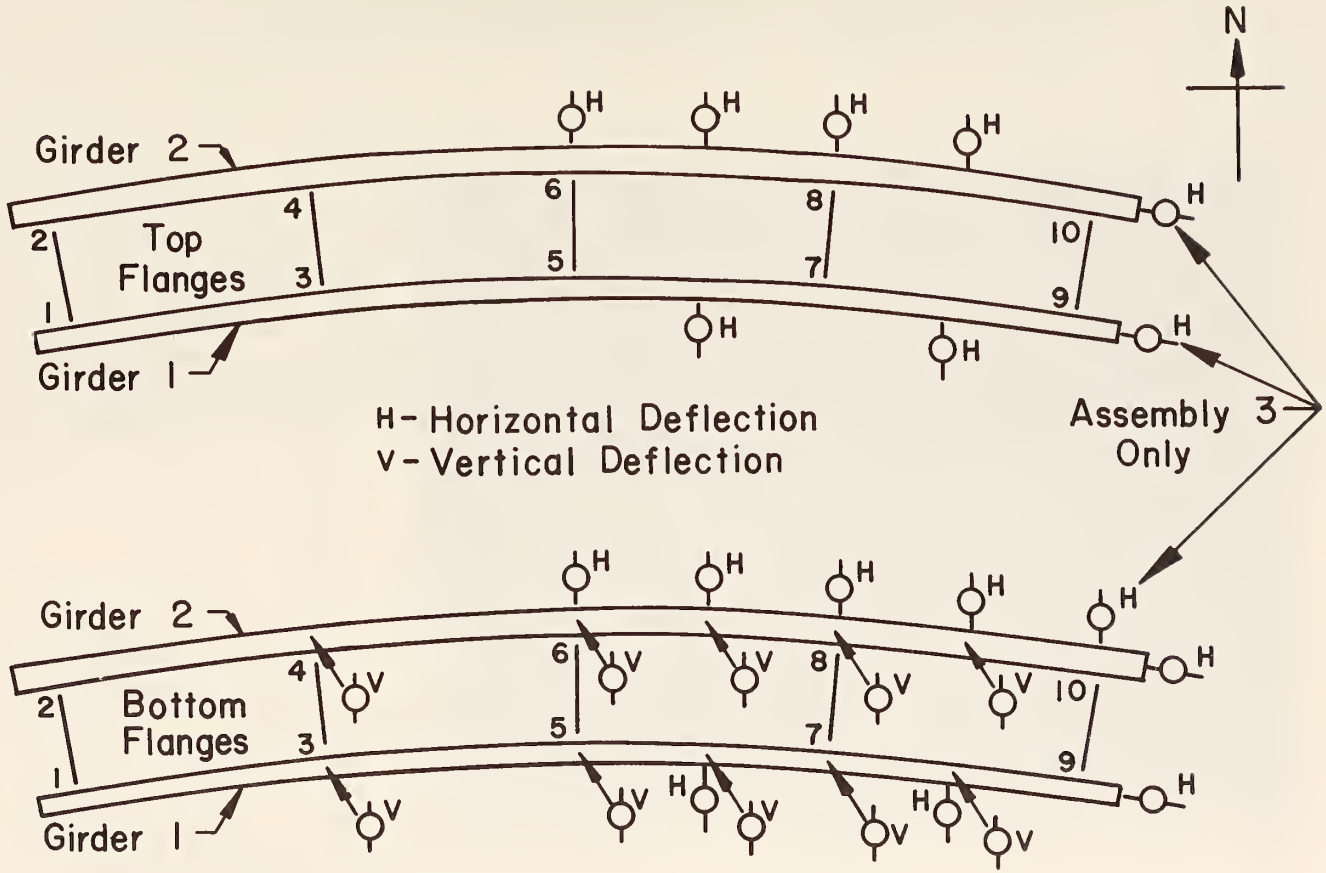

Fig. 24 Deflection Dial Gage Locations - Assemblies 1, 3, and 4

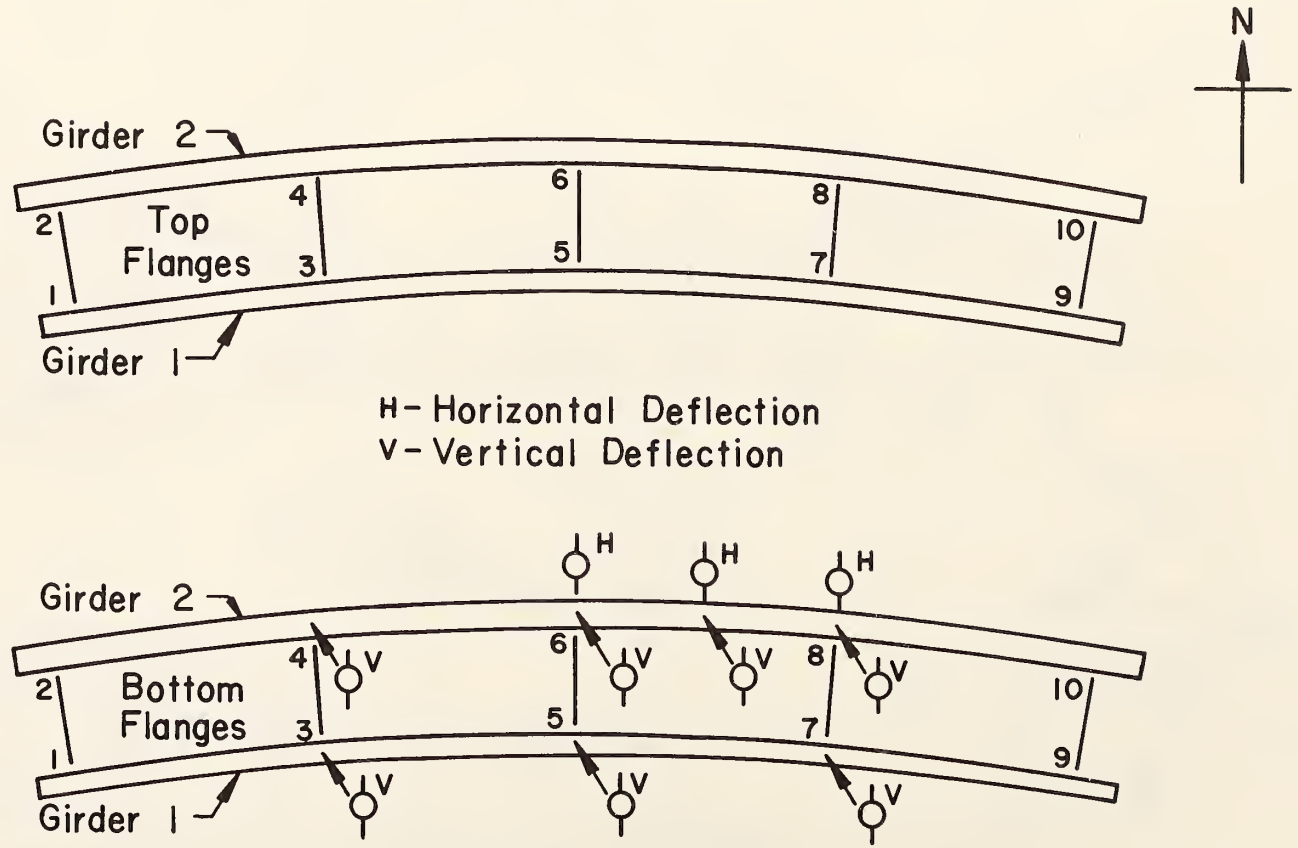

Fig. 25 Deflection Dial Gage Locations - Assemblies 2 and 5

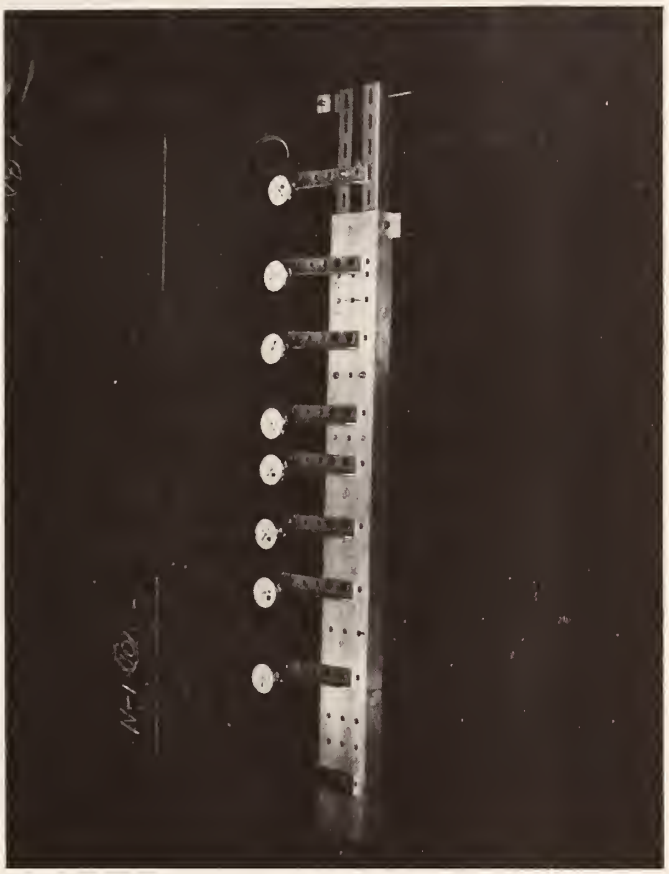

Fig. 26 Dial Gage Rig Measuring Web Deflections

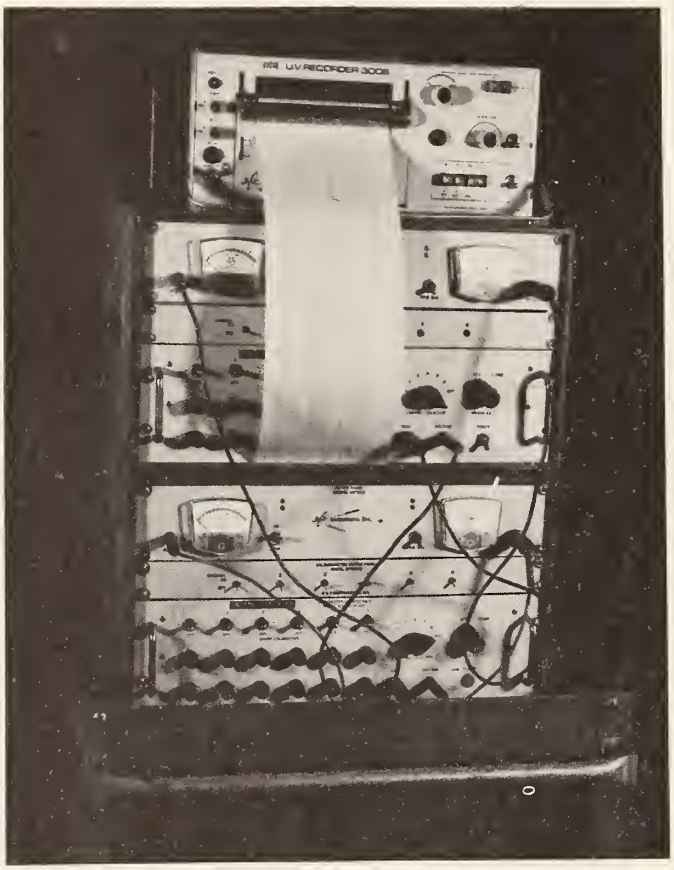

Fig. 27 Ultraviolet Oscillograph Trace Recorder

During dynamic alignment tests strains were recorded by a 12-channel ultraviolet oscillograph trace recorder utilizing light sensitive paper as shown in Fig. 27. From calibration curves and the oscillograph output, the dynamic strain range for each gage is determined and converted into stress range.

In addition to the strain gages shown in Figs. 13 through 23, strain gages were also placed in the vicinity of Group 1 and Group 2 welded details prior to commencing fatigue testing. Table 2 contains the welded details of interest and shows the location and orientation of the linear strain gages near the details. An attempt was made to place the strain gages in positions where the nominal stress ranges at the potential crack locations could be readily determined. At the same time the gages had to be a sufficient distance from the detail so that nominal cross-section stresses were measured without the influence of the stress concentration caused by the welded detail's presence. The stress concentration at the detail is already taken into account in the detail Category[10]. The separation distances of details and strain gages are shown in Table 2.

Strain gages were not mounted adjacent to every Group 1 and Group 2 detail. On each test assembly, the assembly geometry, welded detail locations, and load points were symmetric about the assembly midspan line. Thus, just as in the cross-section strain gage locations shown in Figs. 13 through 17, it was only necessary to gage the welded details on one half of an assembly. All welded details on the western half of a test assembly were monitored with strain gages. A

few strains on the eastern half were also measured to determine if reasonable symmetry of stresses did exist. Figures 28 through 30 show a selection of Group 1 and Group 2 details with their strain gages.

During the fatigue testing of each assembly the midspan vertical deflection of either Girder 1 or Girder 2 was monitored by a double dial gage rig mounted as shown in Fig. 31. The arrangement of the dial gages allowed the deflection range to be monitored to determine if the overall stiffness of an assembly was deteriorated by fatigue crack growth. The lower dial gage also triggered a switch to shut down the hydraulic pulsators if the vertical deflection became too great. This allowed safe operation of the machinery without continuous monitoring by personnel.

Fig. 28 Strain Gages Adjacent to Welded Detail Types I_o and II_o (Table 2)

Fig. 29 Strain Gages Adjacent to Welded Detail Types III_{oa} and III_{ob} (Table 2)

Fig. 30 Strain Gages Adjacent to Welded Detail Types IV_o and V_{oa} (Table 2)

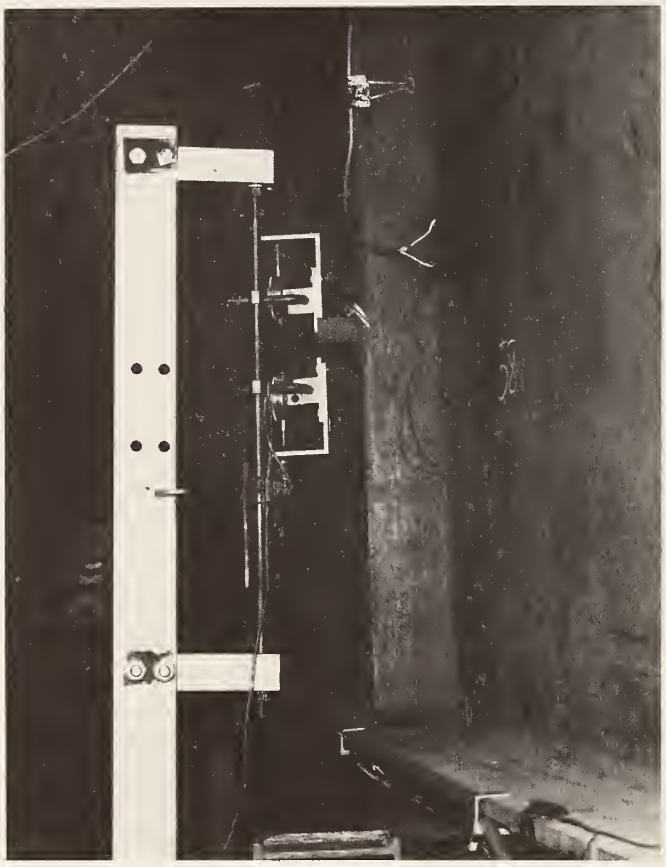

Fig. 31 Double Dial Gage Rig to Monitor Cyclic Deflection and Perform Emergency Shutdown

4. INITIAL STATIC AND CYCLIC LOAD TESTS

4.1 Initial Static Tests

The correlation of static test results with results of a CURVBRG computer program static analysis of each assembly is performed prior to applying cycling loads. This provides an indication of the validity of the analysis results. The static test also provides stress range and deflection range values to be expected during the cyclic load tests and an initial check of an assembly's alignment with respect to the loads.

Figures 32 through 41 show the CURVBRG analytical stress range profiles (Ref. 8) and measured static stresses for the bottom flange of each girder. The profiles (continuous curves) represent the stress range, S_r, corresponding to a static load range of 445 kN (100 kips) for the load conditions shown in Fig. 7. The measured static stresses plotted on the figures (solid circle, triangle, and cross) are obtained from the tension flange strain gages (Figs. 13 through 18).

In each figure, stress range, S_r (ordinate), is plotted with respect to fractions of span length, L (abscissa), with X being the position along the assembly centerline. For each assembly the lengths of Girders 1 and 2 measured at the web-flange junction are, respectively, L_1 and L_2. Profiles are shown for only half of each girder length because of symmetry of geometry and load positions about mid-span. Only stress ranges measured on the western half of an assembly are plotted. The curved stress range profiles in each figure are for the flange tips. The profile consisting of two straight line segments

is for the web-to-tension flange junction. The web profile curve does not cross the flange tip curves at precisely the same location since web stress range values are plotted for the bottom of the web, not for the mid-depth of the flange.

The tension flange strain gage locations (Figs. 13 through 18) do not permit direct measurement of the flange tip stresses. Gages near the edges of the flanges are located 12.7 mm (1/2 in.) from the flange tip. Whenever a flange cross section contains two or three strain gages, a cross-flange stress profile can be plotted. The flange tip stress is computed by extending the cross-flange profile to the flange tip. The same type of cross-flange stress profile is used to measure the middle-of-flange stresses on Assembly 5 where no strain gages are located directly beneath the web. On cross sections having only one flange tip strain gage, the measured stress is extrapolated to the flange tip using the cross-flange stress profile from analytical results for the particular cross section.

Table 3 summarizes vertical and horizontal deflections measured at diaphragm locations during static loading. Horizontal displacements are not computed by the CURVBRG computer analysis.

4.2 Initial Cyclic Tests

After checking the alignment of an assembly under static load, cyclic loading is applied. The jack load range for each assembly is selected by measuring the ability to match the tension flange stress range profiles calculated by the CURVBRG computer program as closely

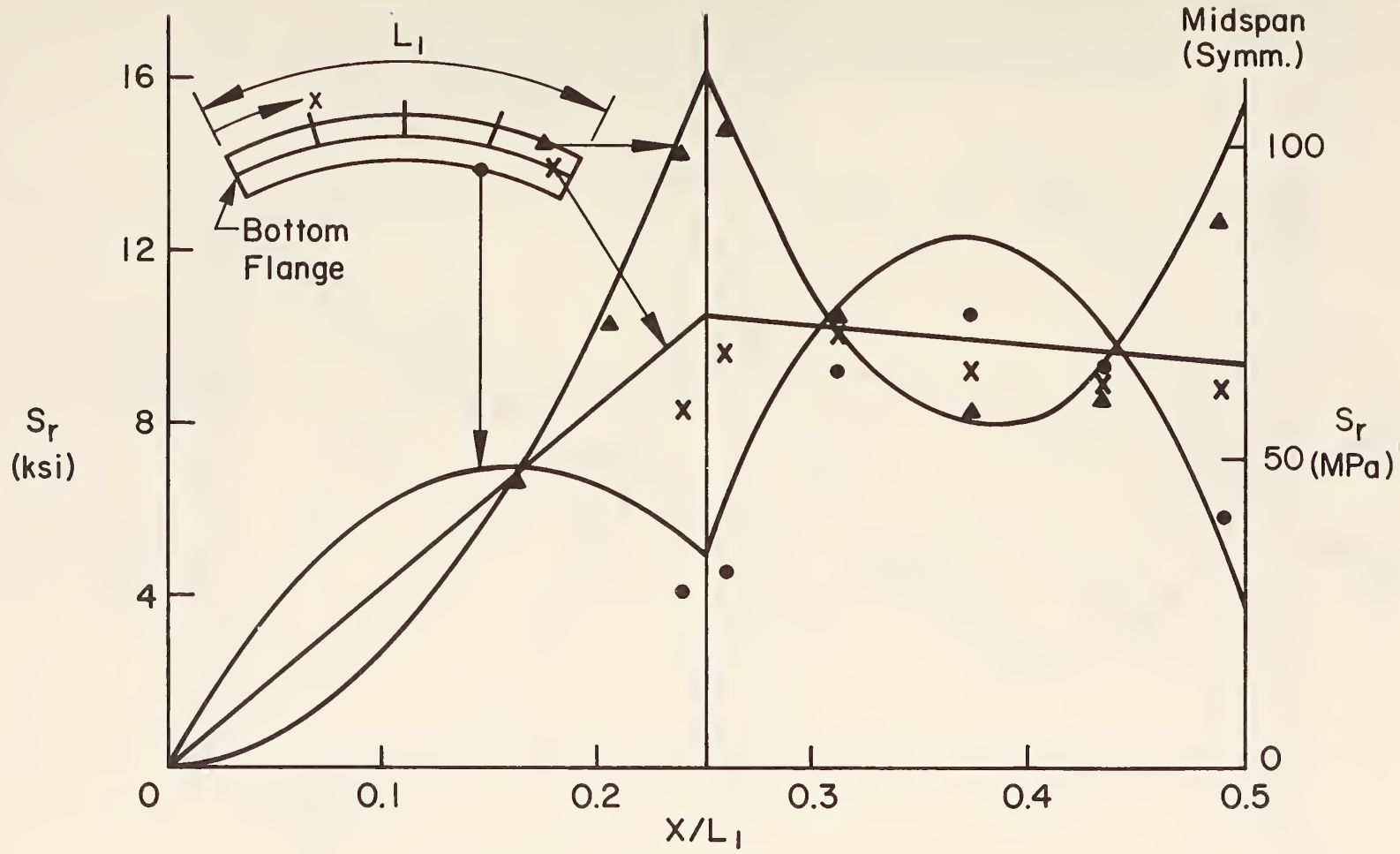

Fig. 32 Stress Range Profiles (From Ref. 8) and Measured Static Stresses for Bottom Flange - Assembly 1 - Girder 1

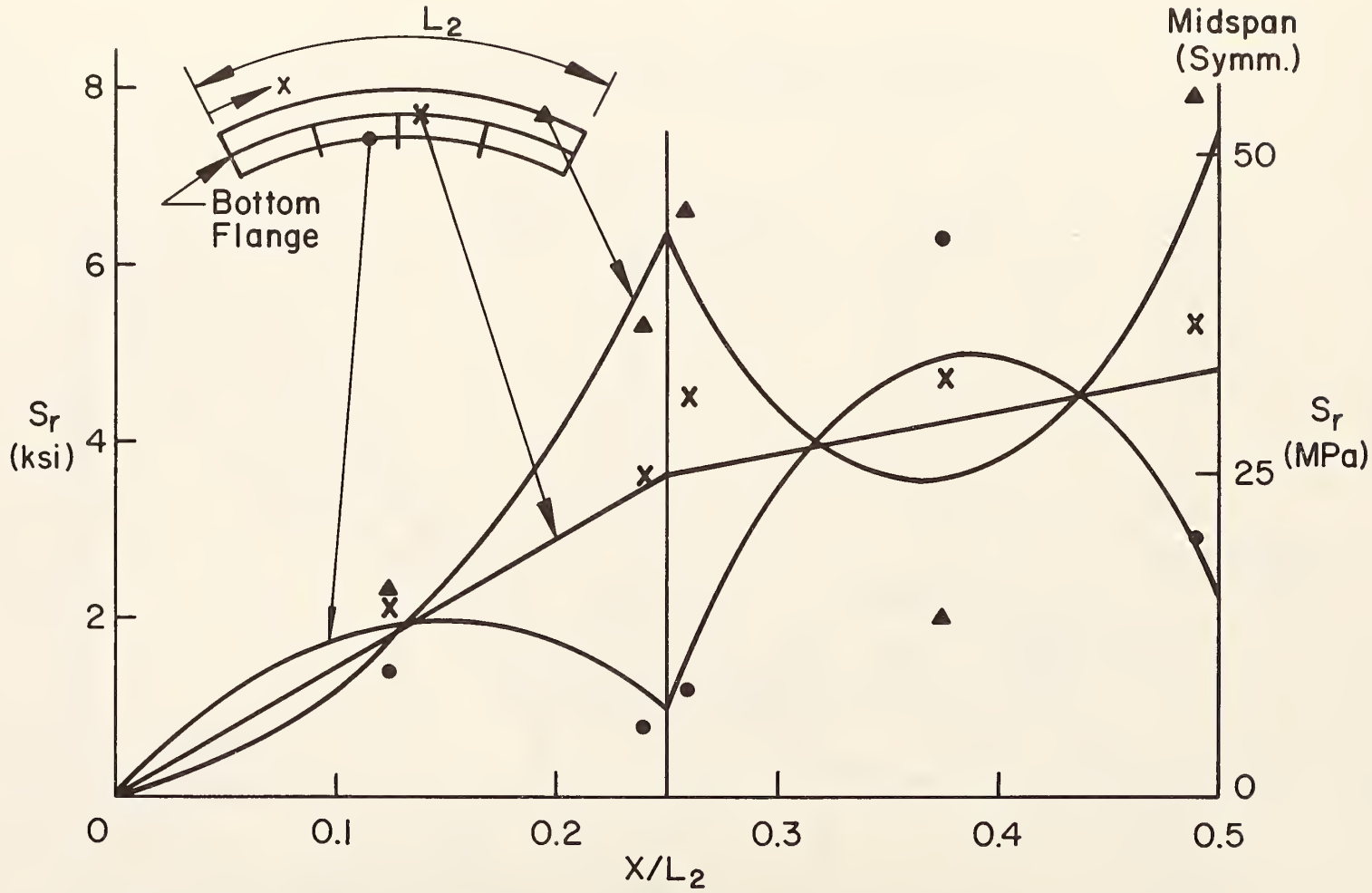

Fig. 33 Stress Range Profiles (From Ref. 8) and Measured Static Stresses for Bottom Flange - Assembly 1 - Girder 2

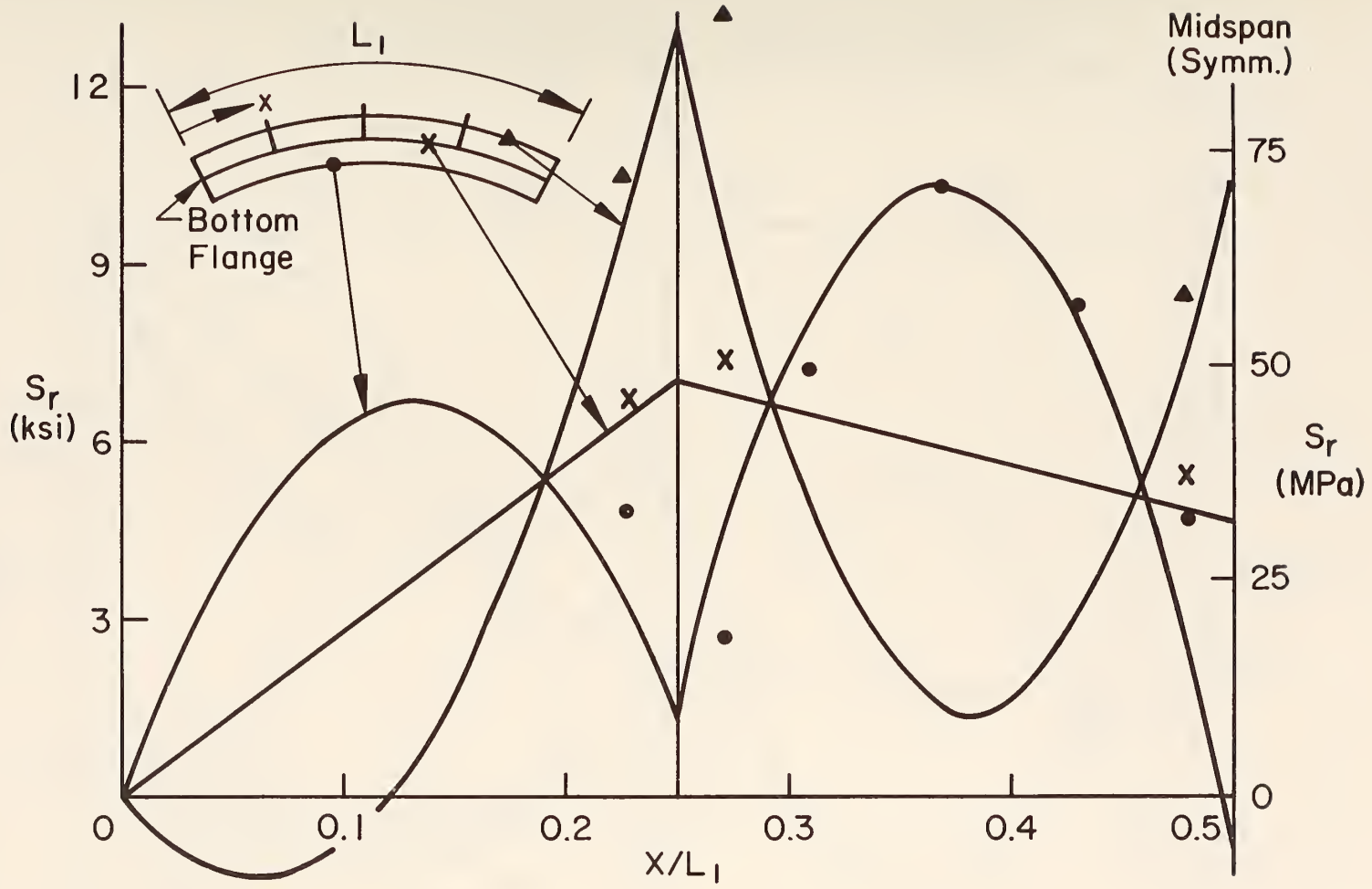

Fig. 34 Stress Range Profiles (From Ref. 8) and Measured Static Stresses for Bottom Flange - Assembly 2 - Girder 1

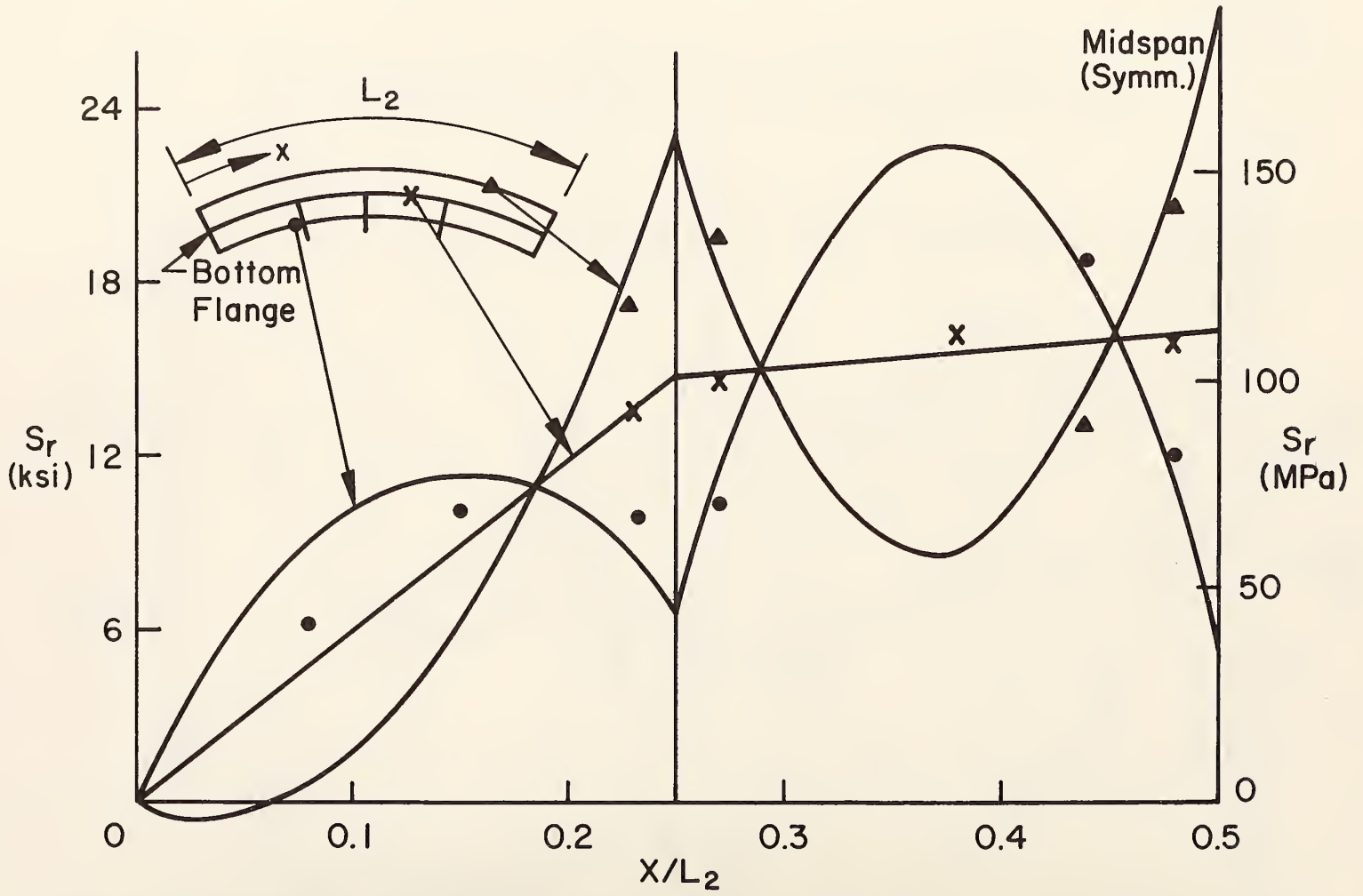

Fig. 35 Stress Range Profiles (From Ref. 8) and Measured Static Stresses for Bottom Flange - Assembly 2 - Girder 2

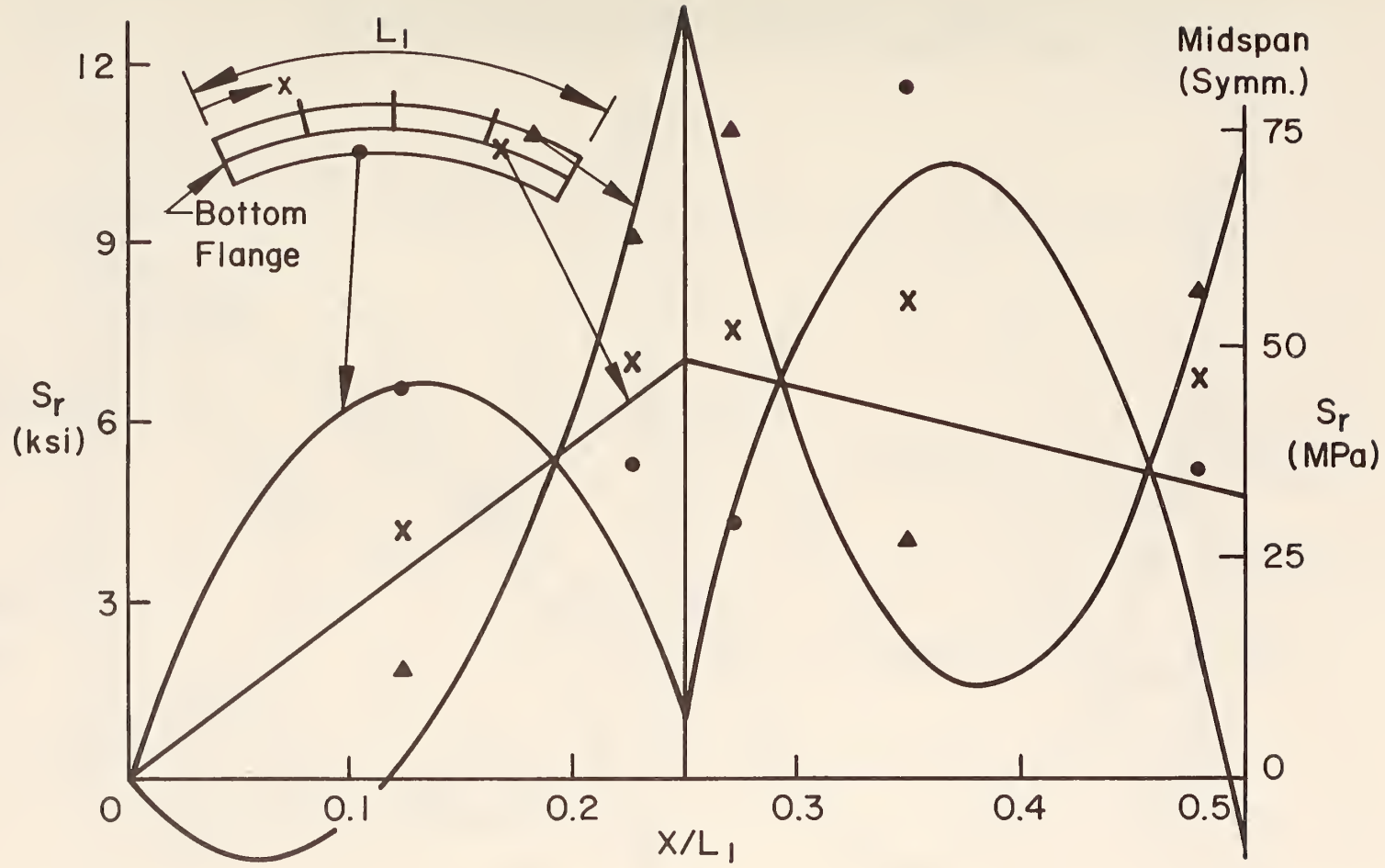

Fig. 36 Stress Range Profiles (From Ref. 8) and Measured Static Stresses for Bottom Flange - Assembly 3 - Girder 1

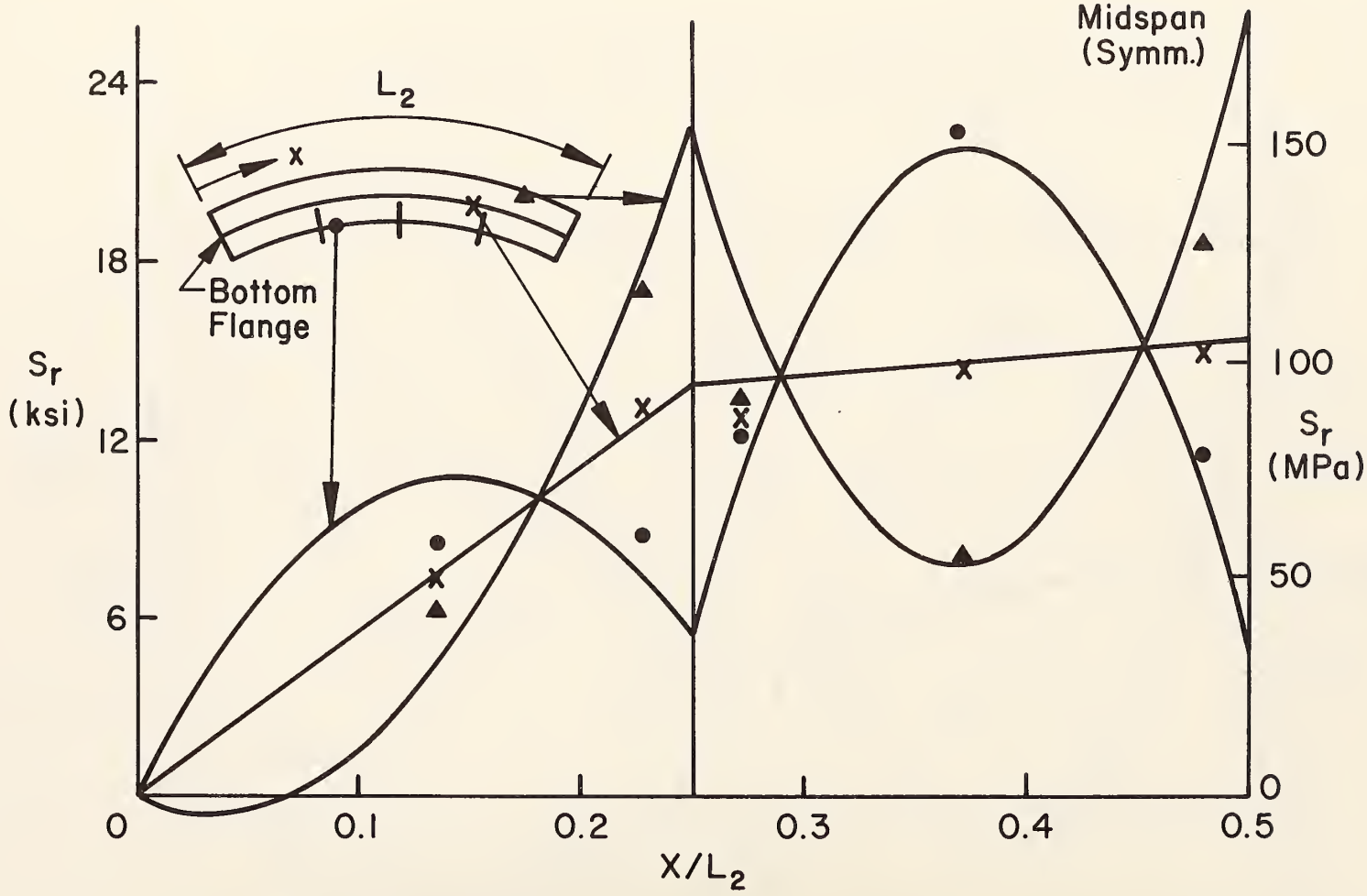

Fig. 37 Stress Range Profiles (From Ref. 8) and Measured Static Stresses for Bottom Flange - Assembly 3 - Girder 2

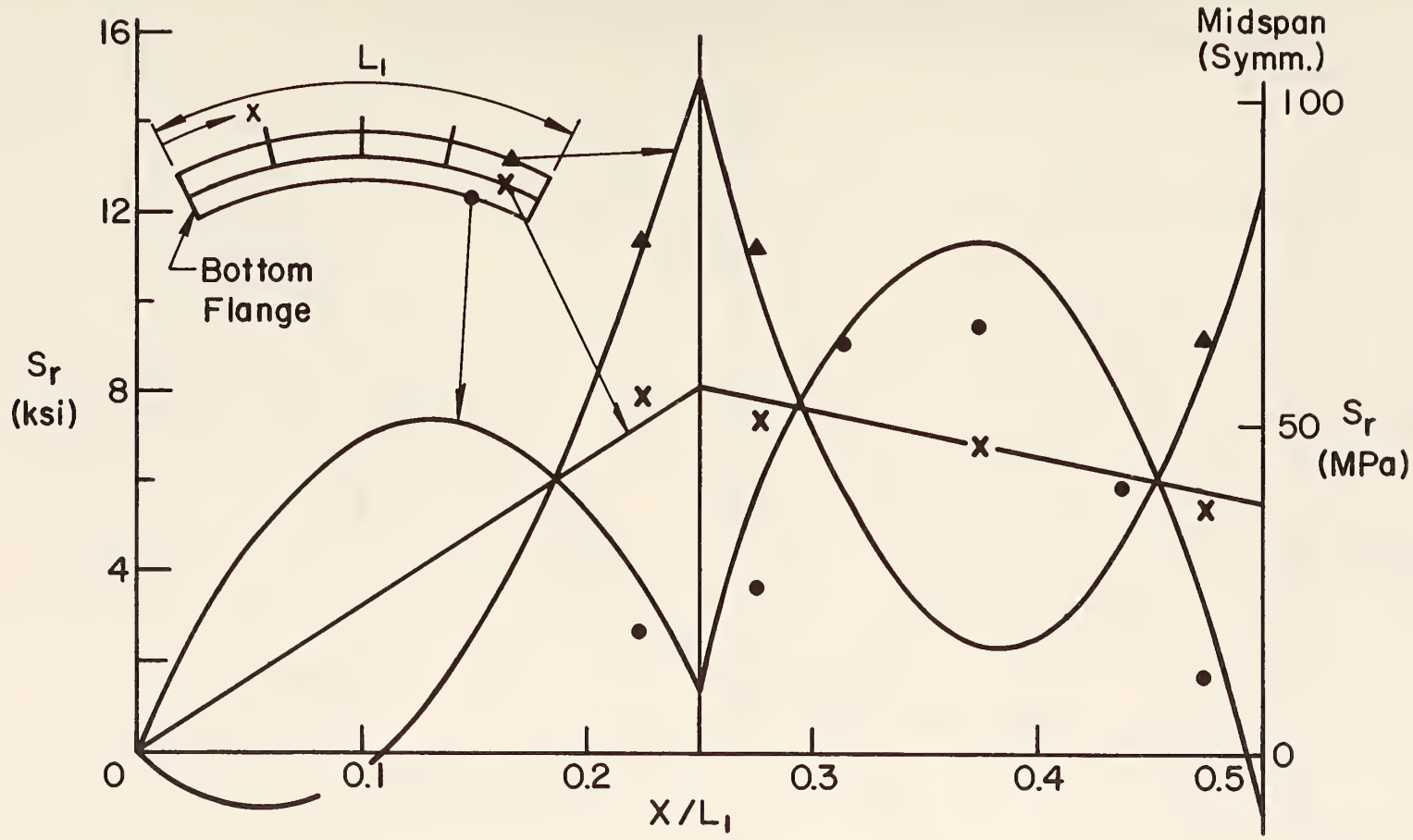

Fig. 38 Stress Range Profiles (From Ref. 8) and Measured Static Stresses for Bottom Flange - Assembly 4 - Girder 1

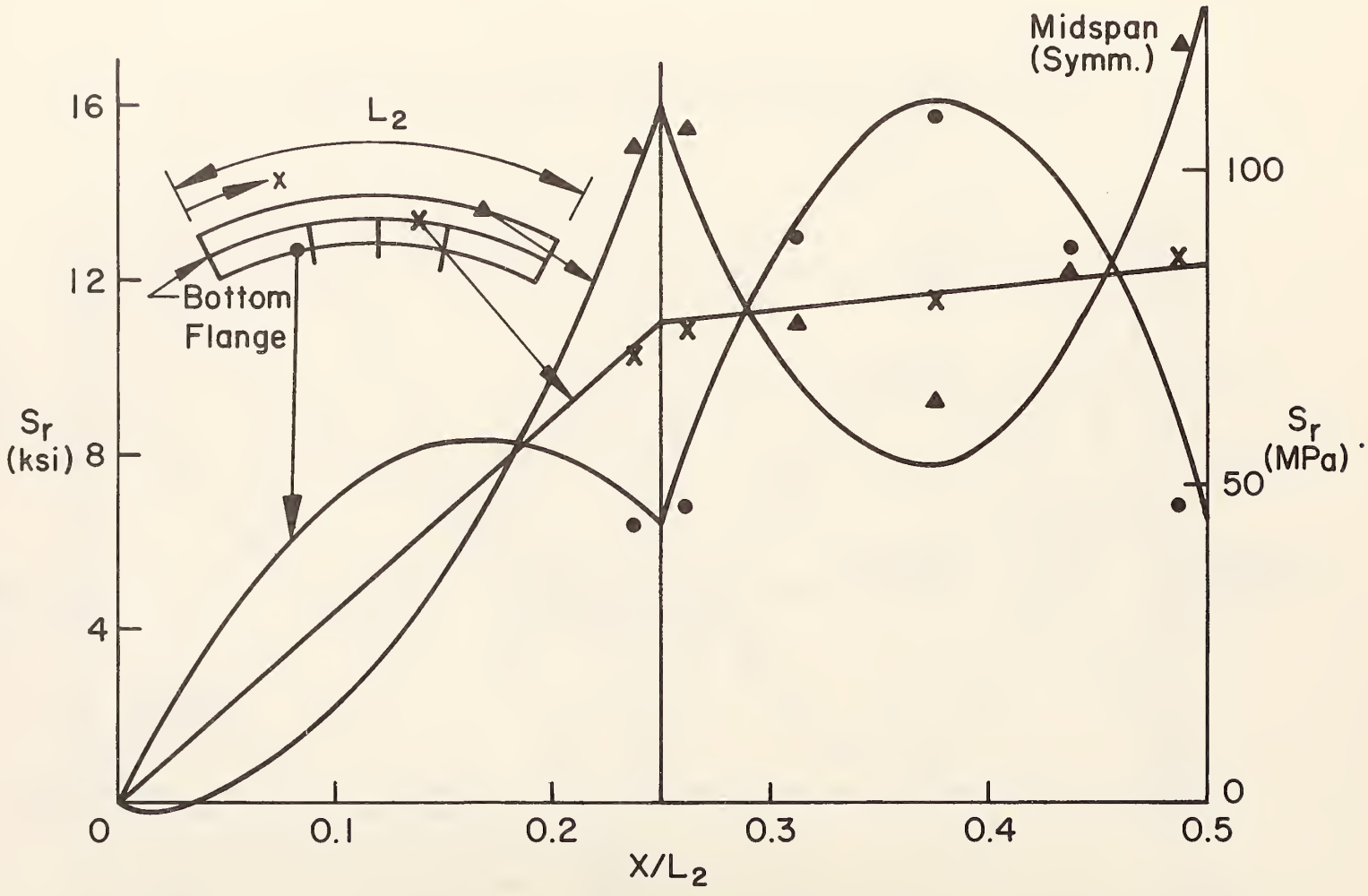

Fig. 39 Stress Range Profiles (From Ref. 8) and Measured Static Stresses for Bottom Flange - Assembly 4 - Girder 2

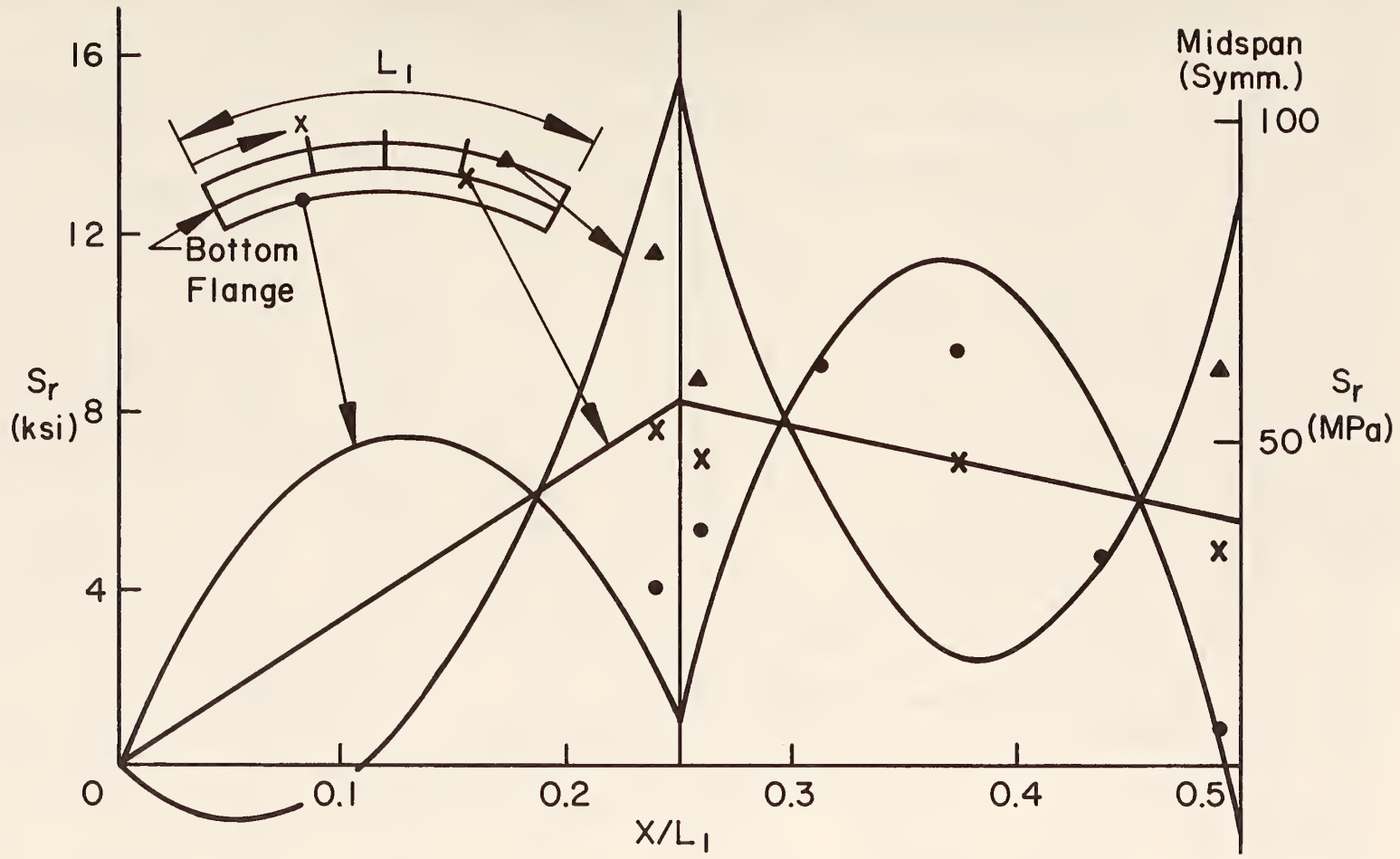

Fig. 40 Stress Range Profiles (From Ref. 8) and Measured Static Stresses for Bottom Flange - Assembly 5 - Girder 1

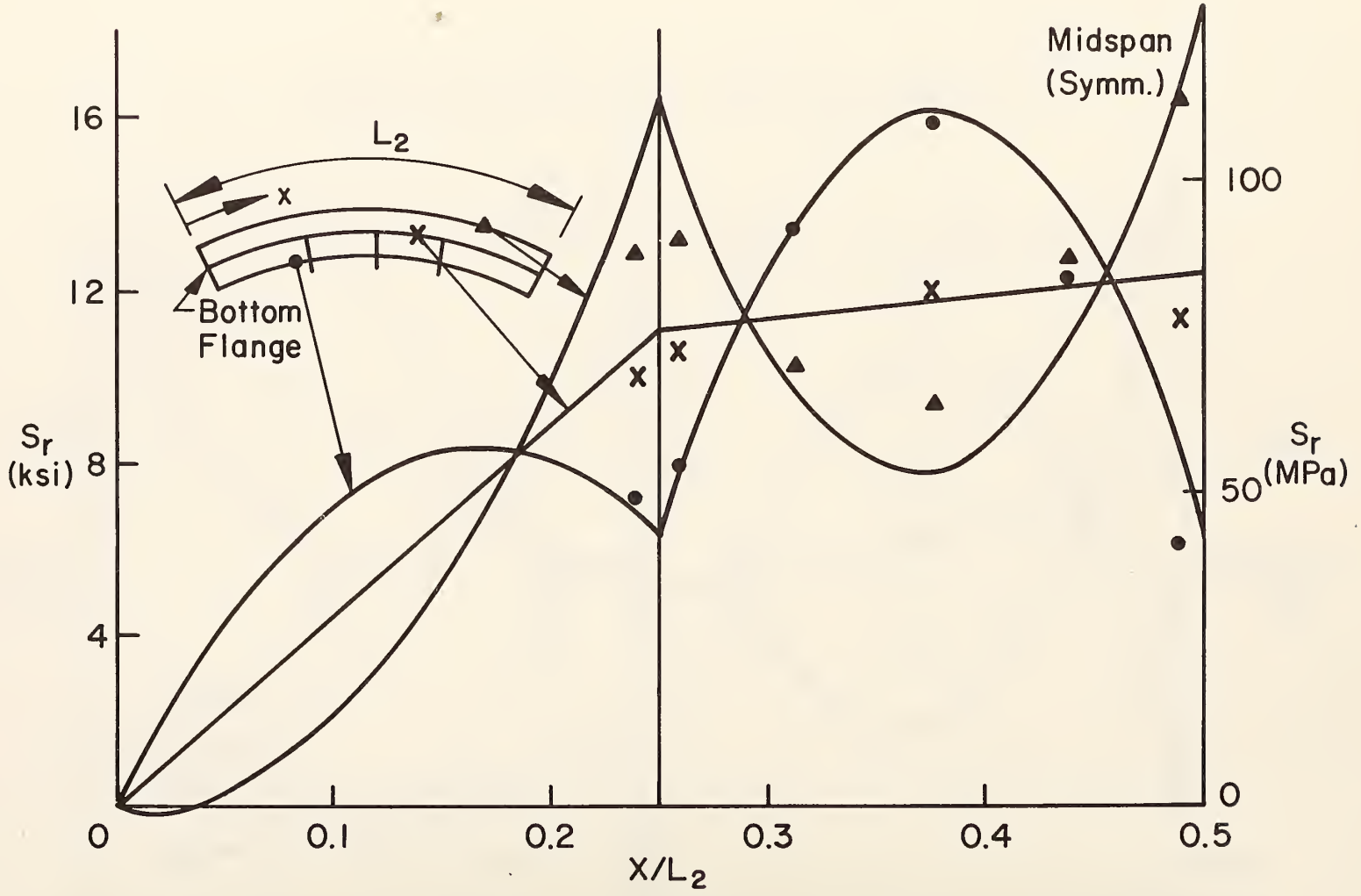

Fig. 41 Stress Range Profiles (From Ref. 8) and Measured Static Stresses for Bottom Flange - Assembly 5 - Girder 2

Table 3 Theoretical and Measured Deflections Under Static 445 kN (100 kip) Jack Loads

Assembly	Joint Number	Theoretical Vertical Deflection mm	(in.)	Measured Vertical Deflection mm	(in.)	Measured Horizontal Deflection Top Flange mm	(in.)	Bottom Flange mm	(in.)
1	5	7.72	(0.304)	8.56	(0.337)	Gage Damaged		N 2.84	(0.112)
	6	2.87	(0.113)	4.06	(0.160)				
	7	6.02	(0.237)	7.75	(0.305)	N 0.74	(0.029)	N 4.70	(0.185)
	8	2.06	(0.081)	3.15	(0.124)				
2	5	7.47	(0.294)	8.71	(0.343)	No Gage		S 4.60	(0.181)
	6	16.76	(0.660)	17.35	(0.683)				
	7	5.64	(0.222)	6.73	(0.265)	No Gage		S 3.45	(0.136)
	8	12.27	(0.483)	13.03	(0.513)				
3	5	7.24	(0.285)	8.76	(0.345)	S 0.89	(0.035)	S 9.40	(0.370)
	6	15.65	(0.616)	15.90	(0.626)				
	7	5.49	(0.216)	6.98	(0.275)	S 1.96	(0.077)	S 7.87	(0.310)
	8	11.43	(0.450)	12.37	(0.487)				
4	5	7.90	(0.311)	9.02	(0.355)	N 6.48	(0.255)	N 0.69	(0.027)
	6	13.56	(0.534)	14.22	(0.560)				
	7	6.02	(0.237)	7.14	(0.281)	N 3.81	(0.150)	N 0.38	(0.015)
	8	9.96	(0.392)	10.67	(0.420)				
5	5	7.90	(0.311)	8.79	(0.346)	No Gage		S 1.98	(0.078)
	6	13.56	(0.534)	14.38	(0.566)				
	7	6.02	(0.237)	7.09	(0.279)	No Gage		S 2.13	(0.084)
	8	9.96	(0.392)	10.69	(0.421)				

as possible. The importance of matching the tension flange stress range profiles cannot be overemphasized. The design and analysis of each assembly (see Ref. 8) culminated in tension flange stress range profiles which would meet the requirements of the fatigue test program. These requirements are discussed in Art. 2.2. For the fatigue tests to be successful the stress ranges measured at the Group 1 details need to be close to the desired values discussed in Art. 2.2, and the measured tension flange stress profile must allow the placement of Group 2 details at locations where they will be subjected to their desired stress ranges.

Figures 42 through 50 show the measured cyclic loading stress ranges and the locations selected for Group 2 details. The continuous curves in the figures are the same stress range profiles presented in Figs. 32 through 41. The profiles for Girder 2 of Assembly 1 are not included because the stress ranges are so low that no Group 1 or 2 details are located on the girder. The load range for each assembly is selected by varying the range until the best match between measured and predicted tension flange stress range profiles is achieved. A minimum load of 44.5 kN (10 kips) under cyclic loading is needed to ensure that uplift at the girder supports does not occur.

The measured stress ranges plotted in Figs. 42 through 50 (solid circles, triangles and crosses) are those computed from the tension flange strain gages while under cyclic load. Only stress ranges measured on the western half of an assembly are plotted because of symmetry of geometry and load positions about midspan. The Group 2 detail locations shown are also symmetric about midspan.

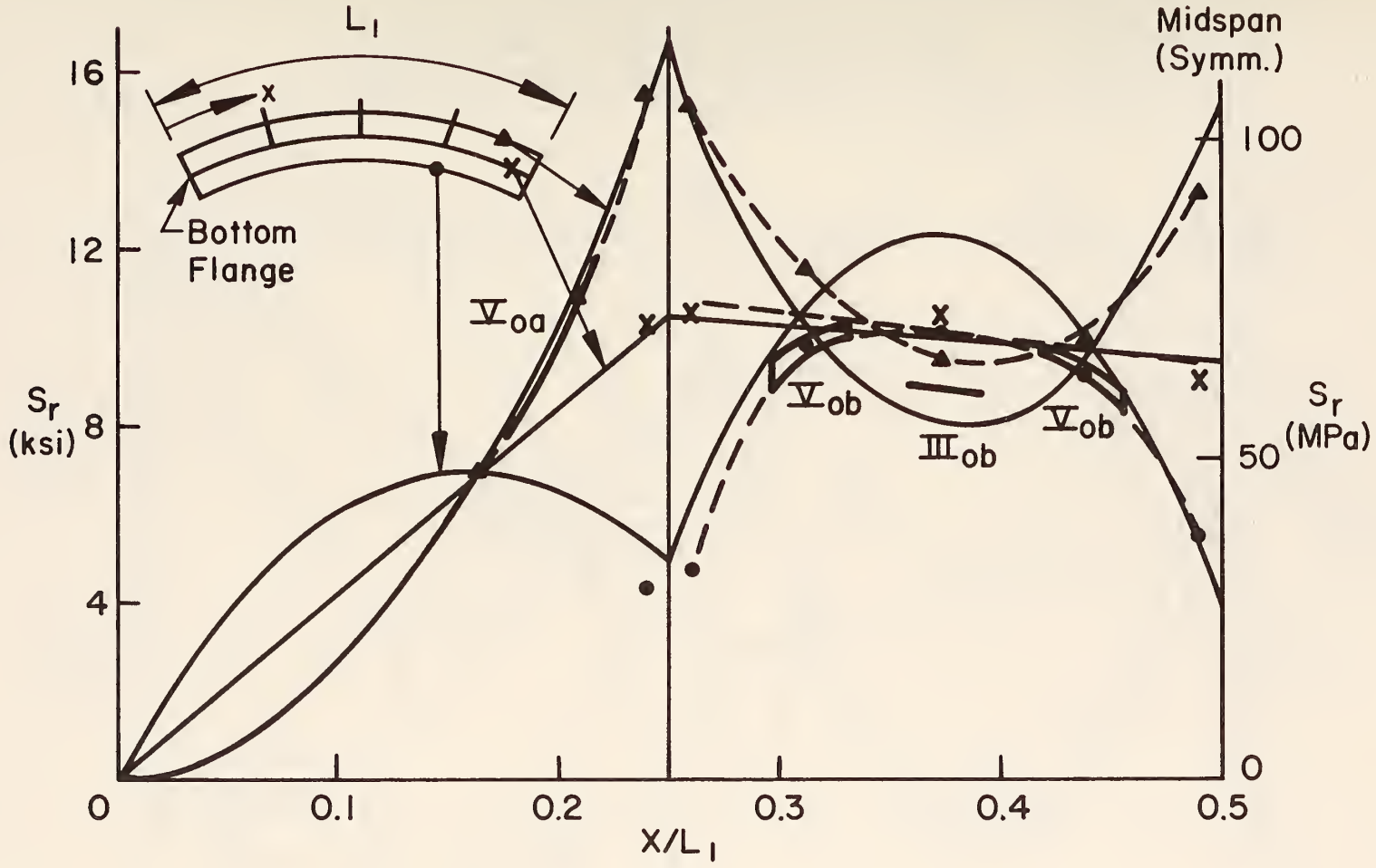

Fig. 42 Stress Range Profiles and Measured Stress Ranges Under Cyclic Loading for Bottom Flange - Assembly 1 - Girder 1
Jack Load Range - 44.5-422.8 kN (10-95 kips)

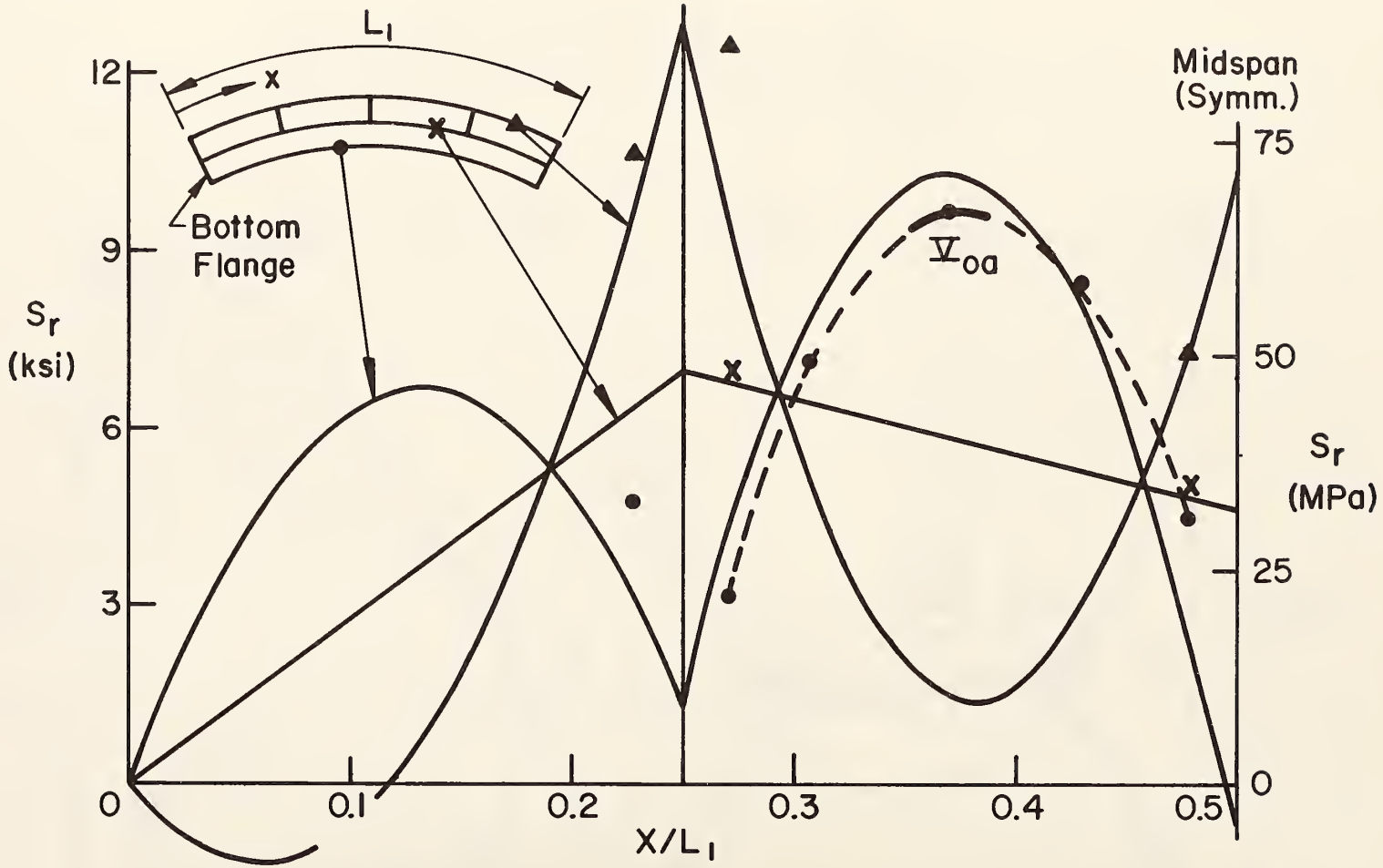

Fig. 43 Stress Range Profiles and Measured Stress Ranges Under Cyclic Loading for Bottom Flange - Assembly 2 - Girder 1
Jack Load Range - 44.5-387.2 kN (10-87 kips)

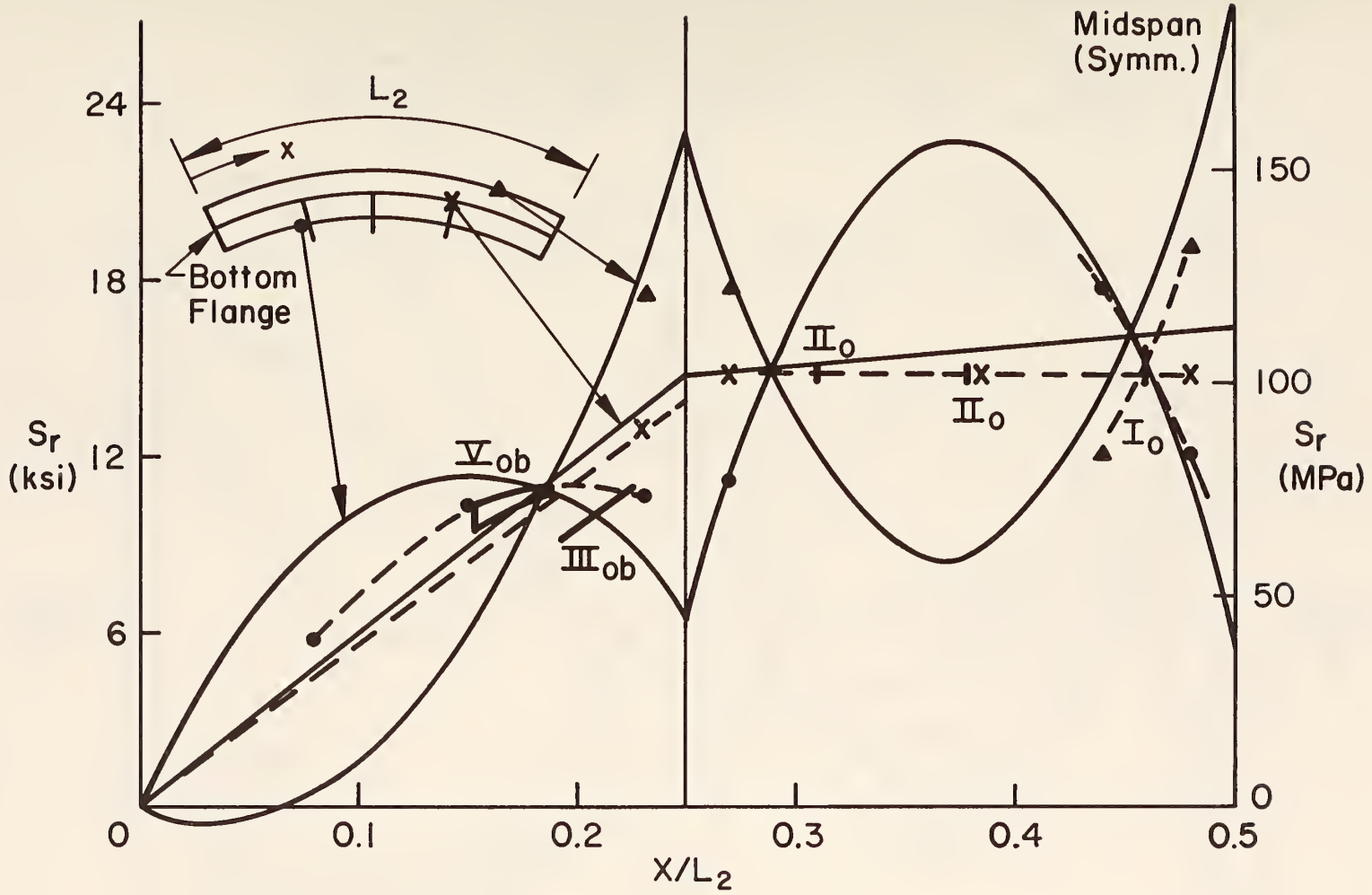

Fig. 44 Stress Range Profiles and Measured Stress Ranges Under Cyclic Loading for Bottom Flange - Assembly 2 - Girder 2
Jack Load Range - 44.5-387.2 kN (10-87 kips)

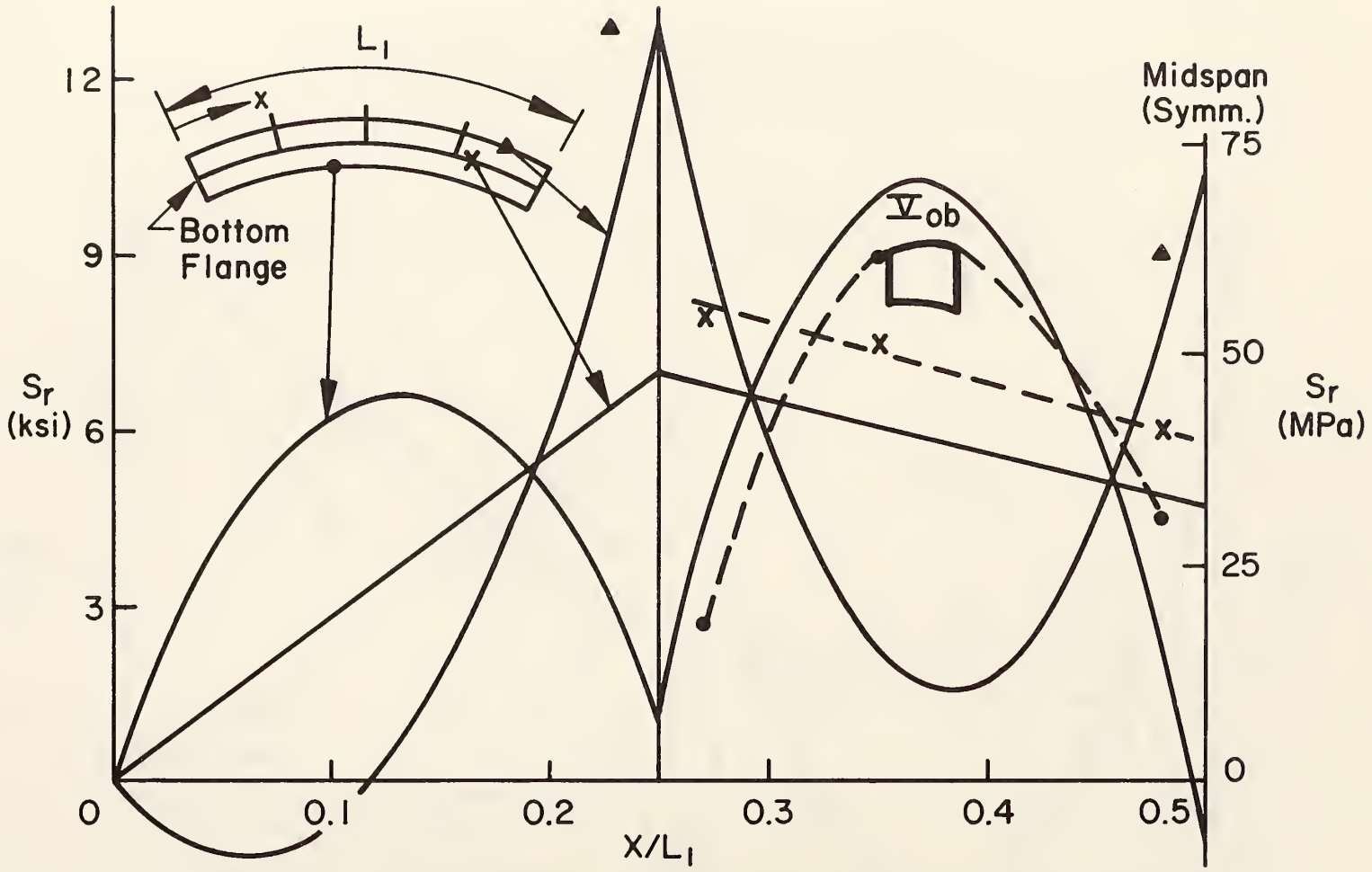

Fig. 45 Stress Range Profiles and Measured Stress Ranges Under Cyclic Loading for Bottom Flange - Assembly 3 - Girder 1
Jack Load Range - 44.5-400.5 kN (10-90 kips)

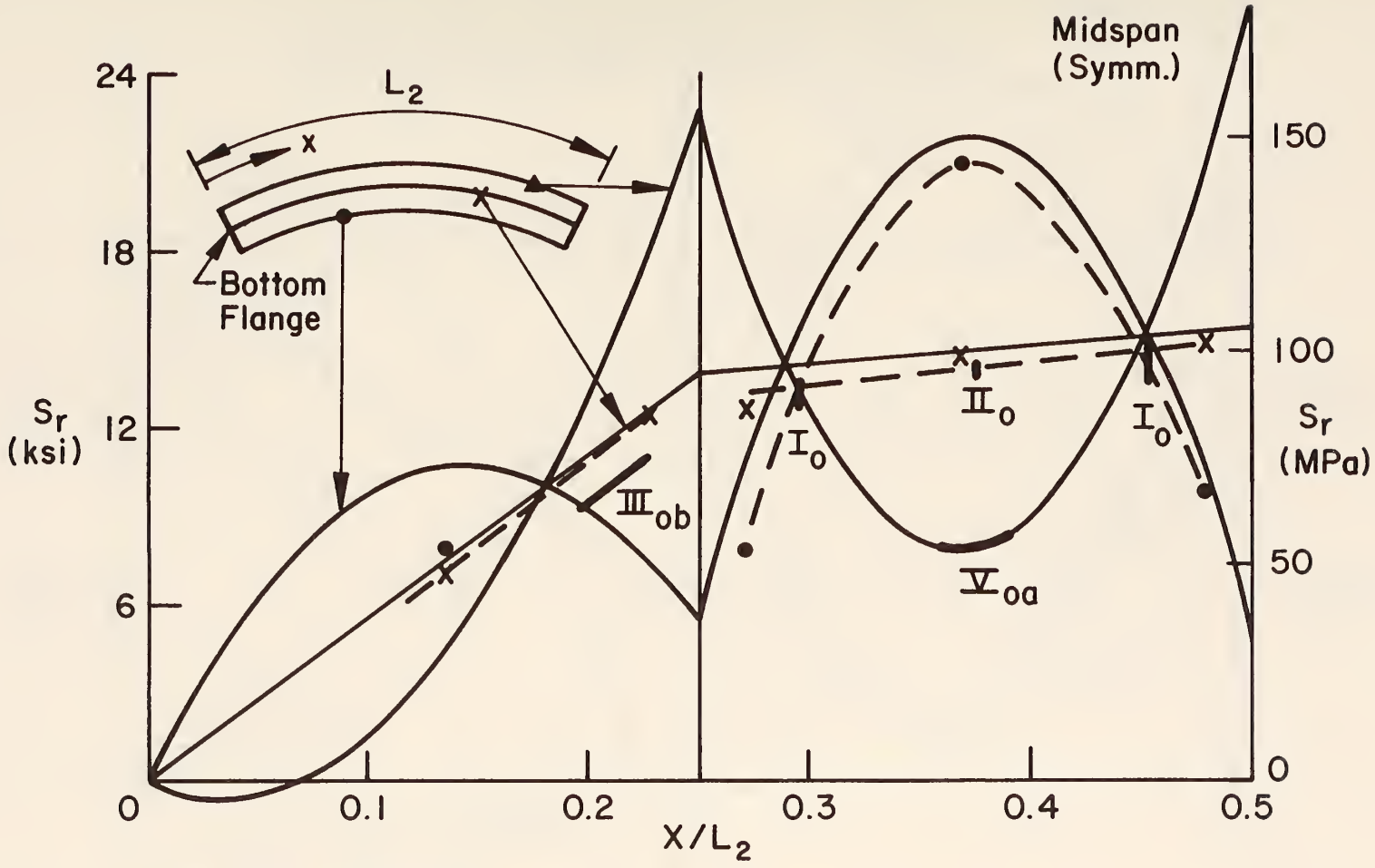

Fig. 46 Stress Range Profiles and Measured Stress Ranges Under Cyclic Loading for Bottom Flange - Assembly 3 - Girder 2
Jack Load Range - 44.5-400.5 kN (10-90 kips)

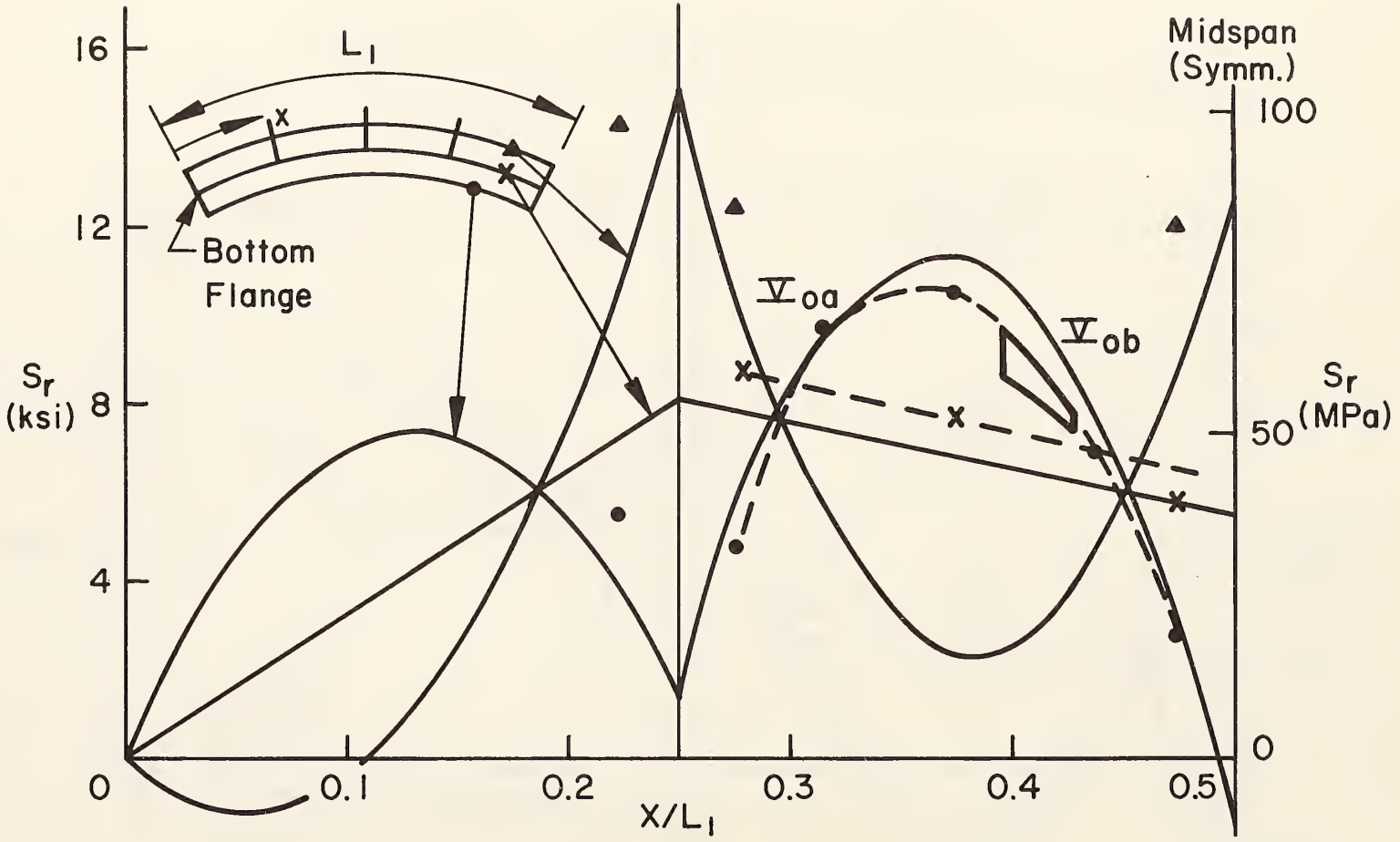

Fig. 47 Stress Range Profiles and Measured Stress Ranges Under Cyclic Loading for Bottom Flange - Assembly 4 - Girder 1
Jack Load Range - 44.5-409.4 kN (10-92 kips)

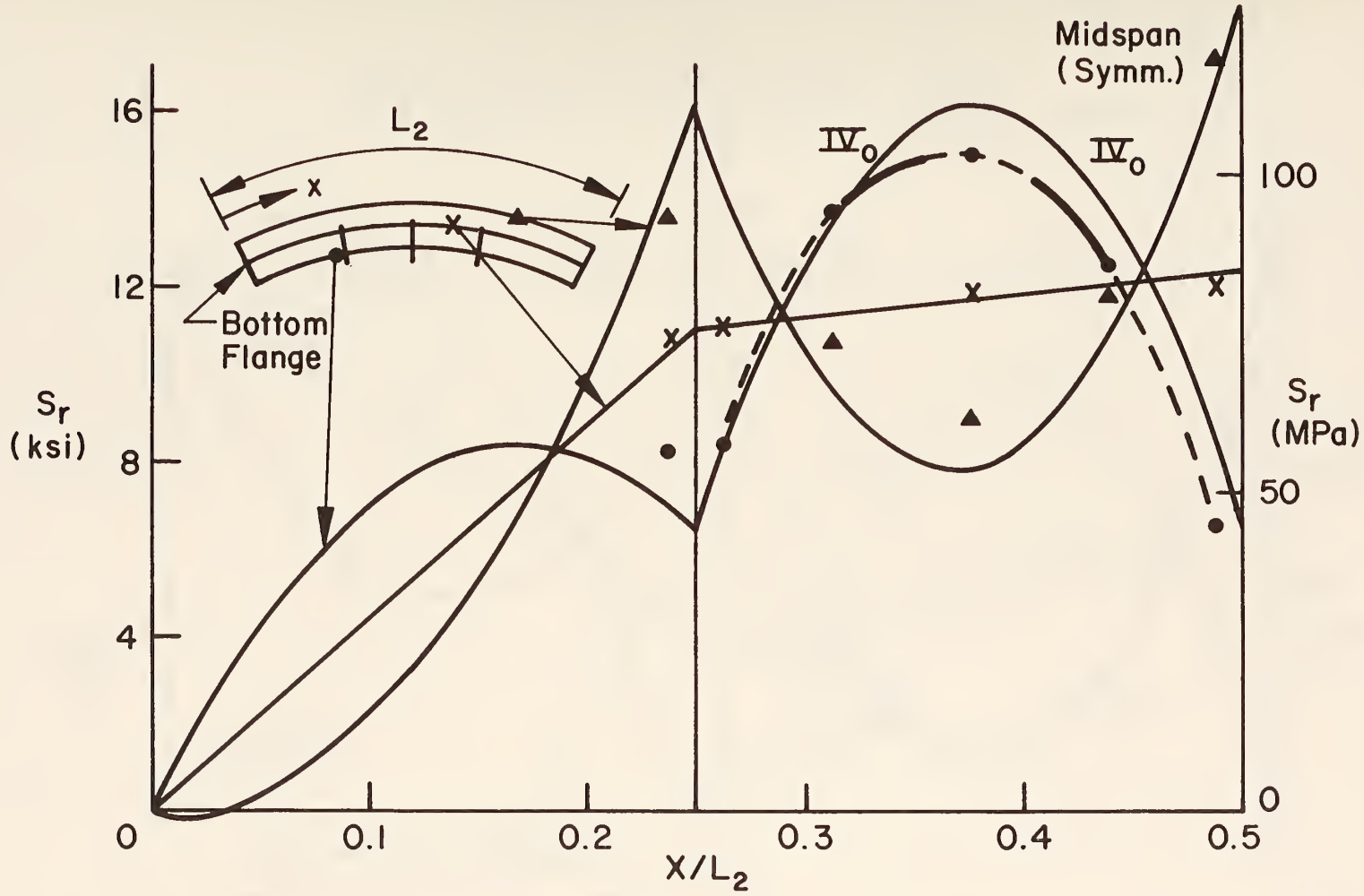

Fig. 48 Stress Range Profiles and Measured Stress Ranges Under Cyclic Loading for Bottom Flange - Assembly 4 - Girder 2
Jack Load Range - 44.5-409.4 kN (10-92 kips)

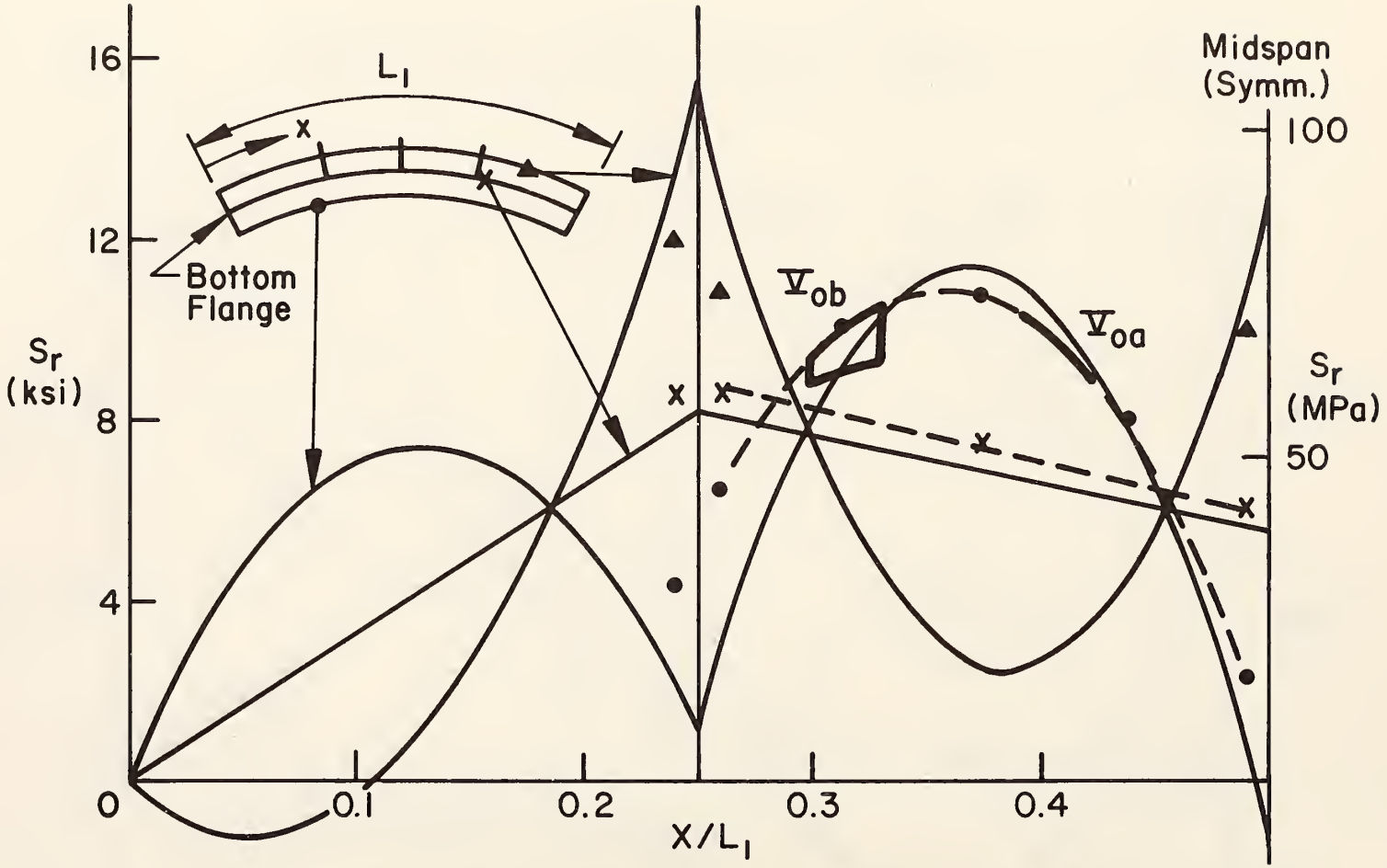

Fig. 49 Stress Range Profiles and Measured Stress Ranges Under Cyclic Loading for Bottom Flange - Assembly 5 - Girder 1
Jack Load Range - 44.5-409.4 kN (10-92 kips)

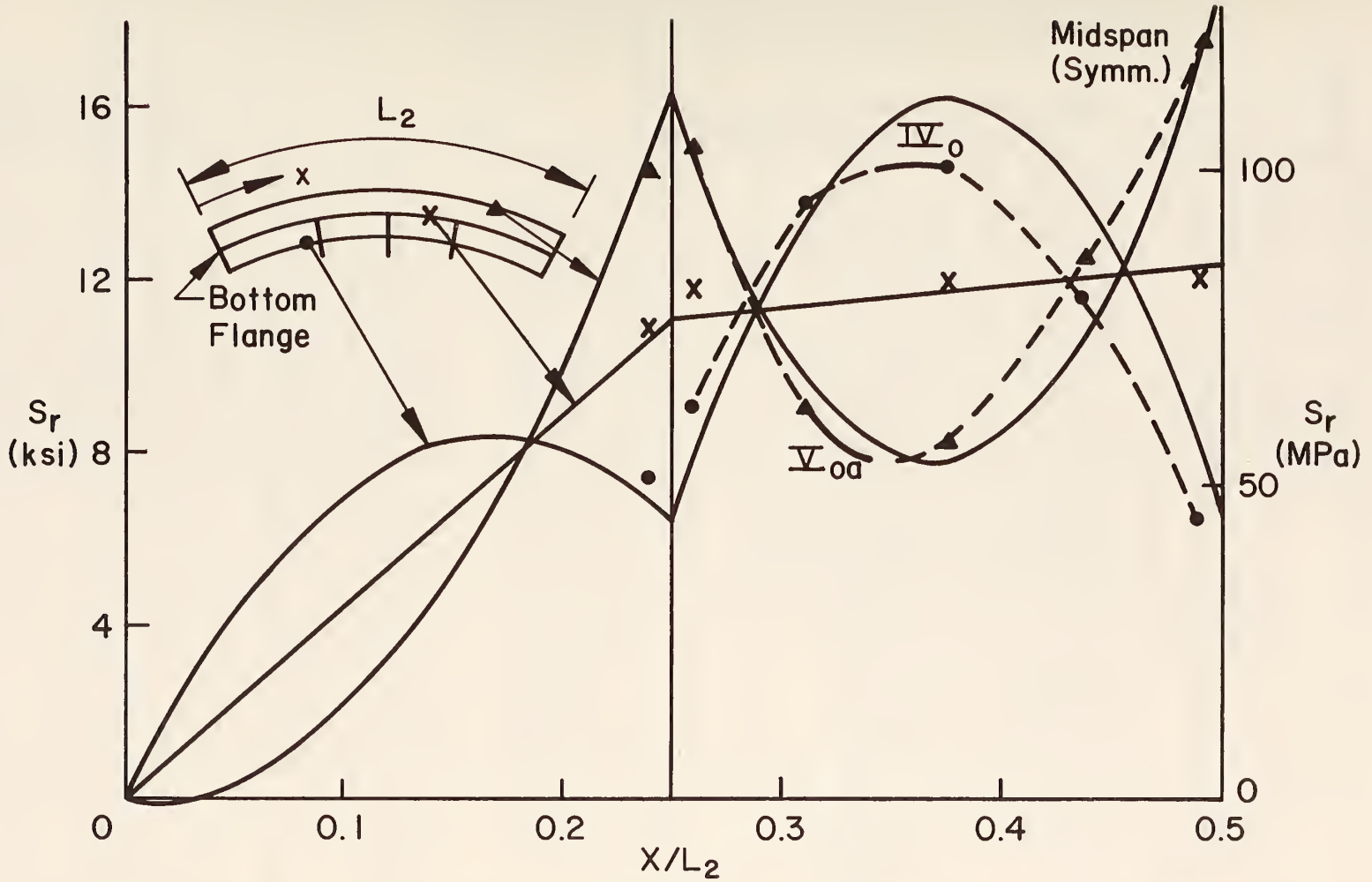

Fig. 50 Stress Range Profiles and Measured Stress Ranges Under Cyclic Loading for Bottom Flange - Assembly 5 - Girder 2
Jack Load Range - 44.5-409.4 kN (10-92 kips)

Table 4 Theoretical and Measured Axial Forces in Diaphragm Members (Figs. 19-22)

Assembly	Diaphragm[a] Location	Member[b]	Theoretical Force[c] kN (kips)	Measured Static[d] Force, kN (kips)	Measured Force Range, kN (kips)	Jack Load Range kN (kips)
1	Joint 3 to Joint 4	F5	-20.0 (- 4.5)	-28.0 (- 6.3)	+ 4.9 (+ 1.1)	44.5-422.8 (10-95)
		F6	+20.0 (+ 4.5)	-17.4 (+ 3.9)	+30.3 (+ 6.8)	
		F7	-55.2 (-12.4)	-35.2 (- 7.9)	-56.1 (-12.6)	
		F8	+55.2 (+12.4)	-35.2 (+ 7.9)	+35.2 (+ 7.9)	
2	Joint 3 to Joint 4	F9	+19.6 (+ 4.4)		+25.8 (+ 5.8)	44.5-387.2 (10-87)
		F10	+50.7 (+11.4)		+48.1 (+10.8)	
		F11	-50.7 (-11.4)		-49.8 (-11.2)	
		F12	-19.6 (- 4.4)		-15.6 (- 3.5)	
	Joint 5 to Joint 6	F9	+27.1 (+ 6.1)	+36.0 (+ 8.1)	+37.4 (+ 8.4)	
		F10	+58.7 (+13.2)	+69.4 (+15.6)	+64.1 (+14.4)	
		F11	-58.7 (-13.2)	-51.6 (-11.6)	-51.6 (-11.6)	
		F12	-27.1 (- 6.1)	-25.4 (- 5.7)	-23.6 (- 5.3)	
4	Joint 5 to Joint 6	F17	+30.7 (+ 6.9)	+38.3 (+ 8.6)	+42.3 (+ 9.5)	44.5-409.4 (10-92)
		F18	+63.2 (+14.2)	+30.7 (+ 6.9)	+36.9 (+ 8.3)	
		F19	-63.2 (-14.2)	-61.4 (-13.8)	-66.3 (-14.9)	
		F24	-30.7 (- 6.9)	-60.5 (-13.6)	-59.6 (-13.4)	
5	Joint 5 to Joint 6	F25	+30.7 (+ 6.9)	+33.4 (+ 7.5)	+40.9 (+ 9.2)	44.5-409.4 (10-92)
		F26	+63.2 (+14.2)	+35.6 (+ 8.0)	+36.9 (+ 8.3)	
		F27	-63.2 (-14.2)	-48.5 (-10.9)	-47.2 (-10.6)	
		F32	-30.7 (- 6.9)	-58.7 (-13.2)	-54.7 (-12.3)	

a-Refer to Fig. 1
b-Refer to Figs. 19 to 22
c-CURVBRG Computer Program
d-Jack Loads of 445 kN (100 kips)

4.3 Group 2 Welded Detail Locations

The broken lines in Figs. 42 through 50 are constructed through plotted data points to obtain stress ranges needed for locating the Group 2 details. The type of detail (refer to Table 2) is shown on the figures adjacent to its location on the girders. Type I_o and II_o details are represented by single vertical lines (Fig. 44, for example) while the remaining details appear on the figures as lines or irregularly shaped envelopes whose lengths equal that of the details. As discussed in Art. 2.2, the Category C details (I_o, II_o, IV_o) are to be subjected to a stress range of 103.4 MPa (15 ksi). Category E details (III_o, V_o) are to have a stress range of 69.0 MPa (10 ksi). The length of most of the details prohibits each potential crack location from being subjected to the desired stress range. Thus the midpoint of the detail's weld is usually located at the desired stress range with the weld termination points being at slightly higher and lower stress ranges.

The single vertical line for detail type I_o and II_o crosses either one or two profile curves depending on the attachment position. A type I_o detail is attached across nearly half of the flange width. Thus its vertical line crosses the web profile and the flange tip profile of the side on which it is placed. Detail II_o is a web detail and its vertical line crosses only the web-to-flange junction profile.

Detail III_{ob} is a web detail placed 101.6 mm (4 in.) above the tension flange. Its location appears as a line parallel to the web-to-flange junction profile but at a reduced stress range. Type IV_o and

V_{oa} details are attached only to the flange tips. Their location lines lie on the flange tip profiles. Detail type V_{ob} overlaps the flange by 50.8 mm (2 in.) and has four potential crack locations. The location symbol for a V_{ob} detail shows the irregularly shaped stress range envelope experienced by the detail. The corners of the envelope are the four potential crack locations.

The Group 2 detail locations shown in Figs. 42 through 50 are not identical to those presented in Appendix D of Ref. 8. The difference between the predicted stress range profiles and the measured profiles required a modest relocation of many Group 2 details to satisfy their stress range requirements.

4.4 Diaphragm and Lateral Bracing Members

Table 4 summarizes the theoretical and measured axial forces in the members of the X-type diaphragms. The theoretical force is taken directly from the CURVBRG computer program analysis. The measured axial force is computed from the stress or stress range profile recorded by the three strain gages on a cross section (Figs. 19-22). No measured forces are available for the diaphragm members on Assembly 3. A minimum of two strain gages are required on the leg of the angle primarily subjected to bending in order to determine the stress profile. The diaphragm members on Assembly 3 have only one strain gage per leg (Fig. 21).

Table 5 summarizes the measured axial forces in the bottom lateral bracing members on Assemblies 4 and 5. No theoretical values of

axial forces for the bottom lateral bracing members are available from the computer analysis.

Table 5 Measured Axial Forces in Bottom Lateral Bracing (Fig. 23)

Assembly	Member[a]	Measured Static[b] Force, kN (kips)	Measured Force Range, kN (kips)	Jack Load Range kN (kips)
4	L2	+28.9 (+6.5)	+40.5 (+9.1)	44.5-409.4 (10-92)
	L3	+34.3 (+7.7)	+36.0 (+8.1)	
	L4	+34.7 (+7.8)	+43.2 (+9.7)	
	L5	+27.1 (+6.1)	+34.7 (+7.8)	
5	L2	+21.8 (+4.9)	+24.9 (+5.6)	44.5-409.4 (10-92)
	L3	+44.5 (+10.0)	+44.9 (+10.1)	
	L4	+37.8 (+8.4)	+53.8 (+12.1)	
	L5	+27.1 (+6.1)	+21.8 (+4.9)	

a-Refer to Fig. 23
b-Jack Loads of 445 kN (100 kips)

5. FATIGUE TESTING

5.1 General Procedure

After attaching the Group 2 details in Fritz Laboratory an assembly is ready for fatigue testing. Each of the five assemblies was subjected to approximately two million constant amplitude load cycles while periodically inspecting for fatigue cracks. The cyclic load range for each assembly was selected as described in Art. 4.2.

The order in which the assemblies were tested is as follows: Assembly 3, Assembly 2, Assembly 5, Assembly 4, Assembly 1. Assembly 1 was last on the list because it required a different alignment of loading jacks and assembly. Assemblies 4 and 5 are the only assemblies with type IV_o details. Thus it was desirable to have the fatigue testing program running smoothly before testing the assemblies with the limited number of type IV_o details.

The fatigue testing of Assembly 3 required the greatest length of time. Loading frame vibration and excessive rocking of the supports were problems which were solved after several trial solutions. No problems were encountered during cycling of the four remaining assemblies.

5.2 Crack Detection and Repair

During the fatigue testing, an assembly was frequently inspected for visible fatigue cracks. The inspections were done at approximately 100,000 cycle intervals and normally under a static load of about

222.5 kN (50 kips) per jack. Most visual inspections were made with a 10X magnifying glass and a cleaner fluid. The cleaner fluid is sprayed on the metal surface and seeps into a crack if one is present. As the fluid on the flat surface rapidly evaporates the distinct line of a crack still remains due to the liquid in the crack. This inspection method proves very efficient and productive in inspecting the large number of potential crack locations on each assembly.

The frequent visual inspections concentrated on locating fatigue cracks at the potential crack locations at Group 1 and Group 2 details. At times a magnetic particle probe was also used. In addition to inspections of the Group 1 and Group 2 details, several visual inspections of the other welds on an assembly were made during the fatigue testing.

When a visible crack is discovered its location is recorded along with the present number of load cycles on the assembly. If the crack is not through the thickness of a web or flange no repairs are done immediately, but the crack's growth is monitored. When a crack has grown through the web or flange thickness or is initially discovered as a through crack then repairs are made to prevent premature failure of the assembly. The crack repair could consist of drilling a hole to blunt the crack tip as in Figs. 51 and 52, or clamping a splice plate over the cracked section as in Fig. 52, or a combination. The extent of the repair and the sizes of drilled hole and/or splice plate depend upon the location and size of the fatigue crack. The objective is to maintain the integrity of the assembly until at least two million load cycles have been applied.

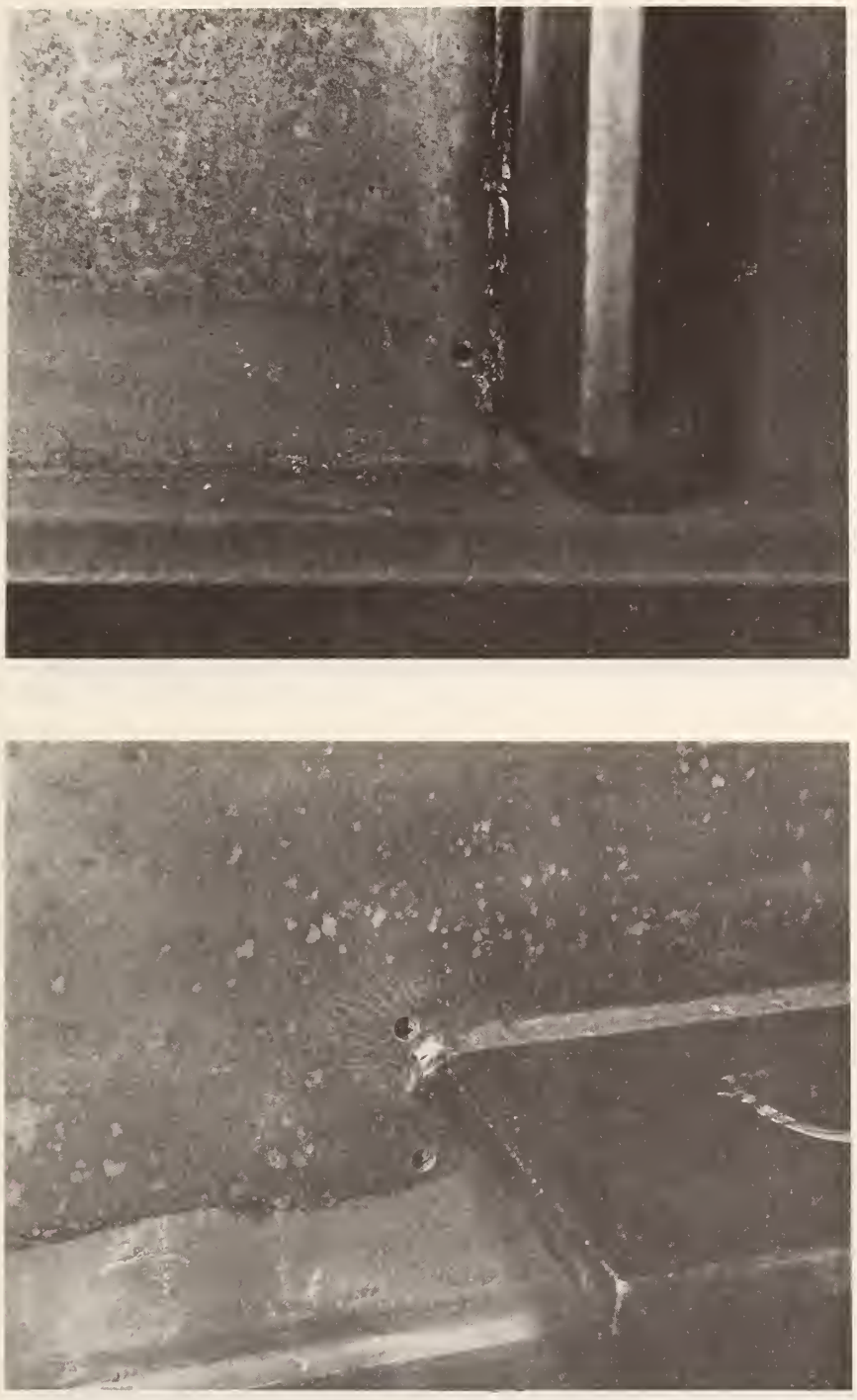

Fig. 51 Typical Web Crack Repairs - Drilled Holes at Type II_o and III_{ob} Details

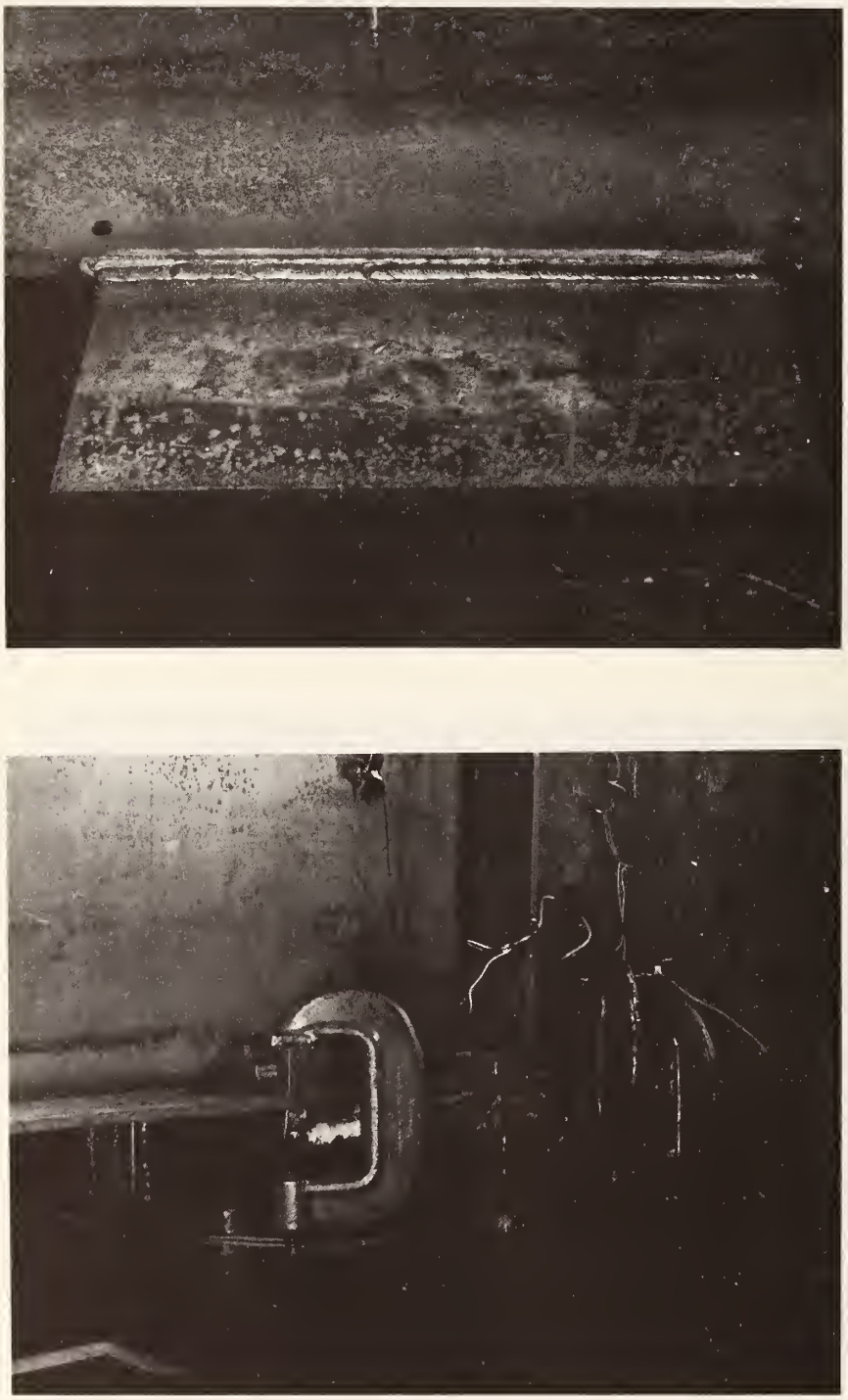

Fig. 52 Typical Flange Crack Repairs - Drilled Holes at Type V_{oa} Detail - Splice Plates Clamped to Flange

6. RESULTS OF FATIGUE TESTS

6.1 Primary Fatigue Cracks

Figures 53 through 57 are schematic diagrams showing the Group 1 and Group 2 welded details on each assembly. The side view of each girder is the south side. Each potential primary fatigue crack location is assigned a letter or letters. The Group 2 details in Figs. 53 through 57 are positioned as shown on the stress range profiles (Figs. 42 through 50) with the exception of two type V_{ob} details on Assembly 3. The V_{ob} details in Fig. 55 with potential crack locations u through bb were welded on the wrong edge of the flange and remained there during the fatigue tests.

The nominal stress ranges computed from measured stress data for all potential crack locations are presented in Tables 6 through 10. The number of cycles at which the visible and through-thickness cracks were discovered is also presented in the right-hand columns of the tables. Potential crack locations which do not develop visible cracks by the end of approximately two million load cycles have no entries in these columns. Some of the cracks propagated through other potential crack locations thus eliminating the chance of fatigue cracks initiating from the locations. These locations carry the notations regarding "interference" in the tables.

The nominal stress ranges at the potential crack locations were computed from strains measured by the strain gages located near the welded details (Table 2). The computations made use of the measured

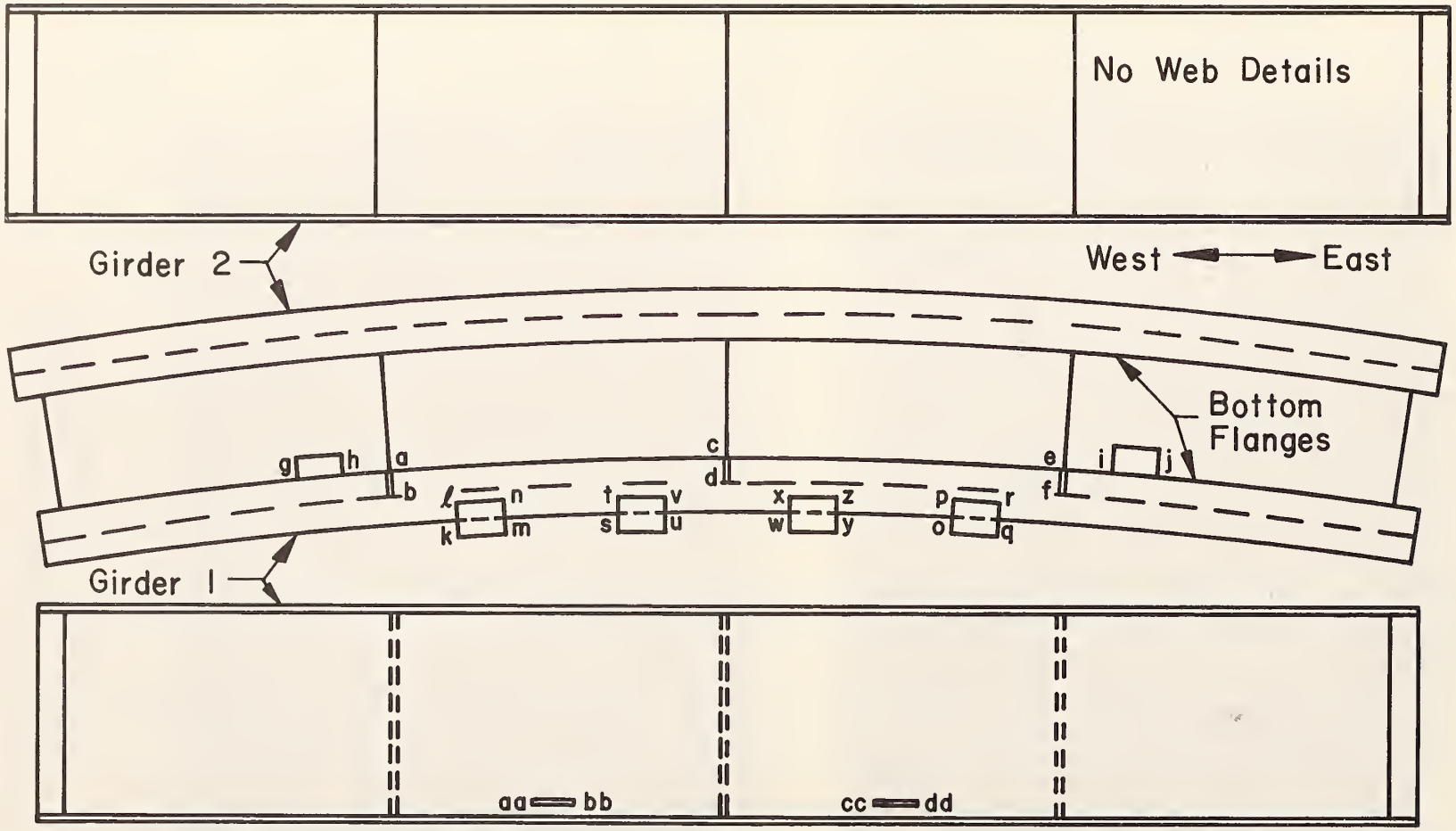

Fig. 53 Group 1 and Group 2 Welded Details on Assembly 1

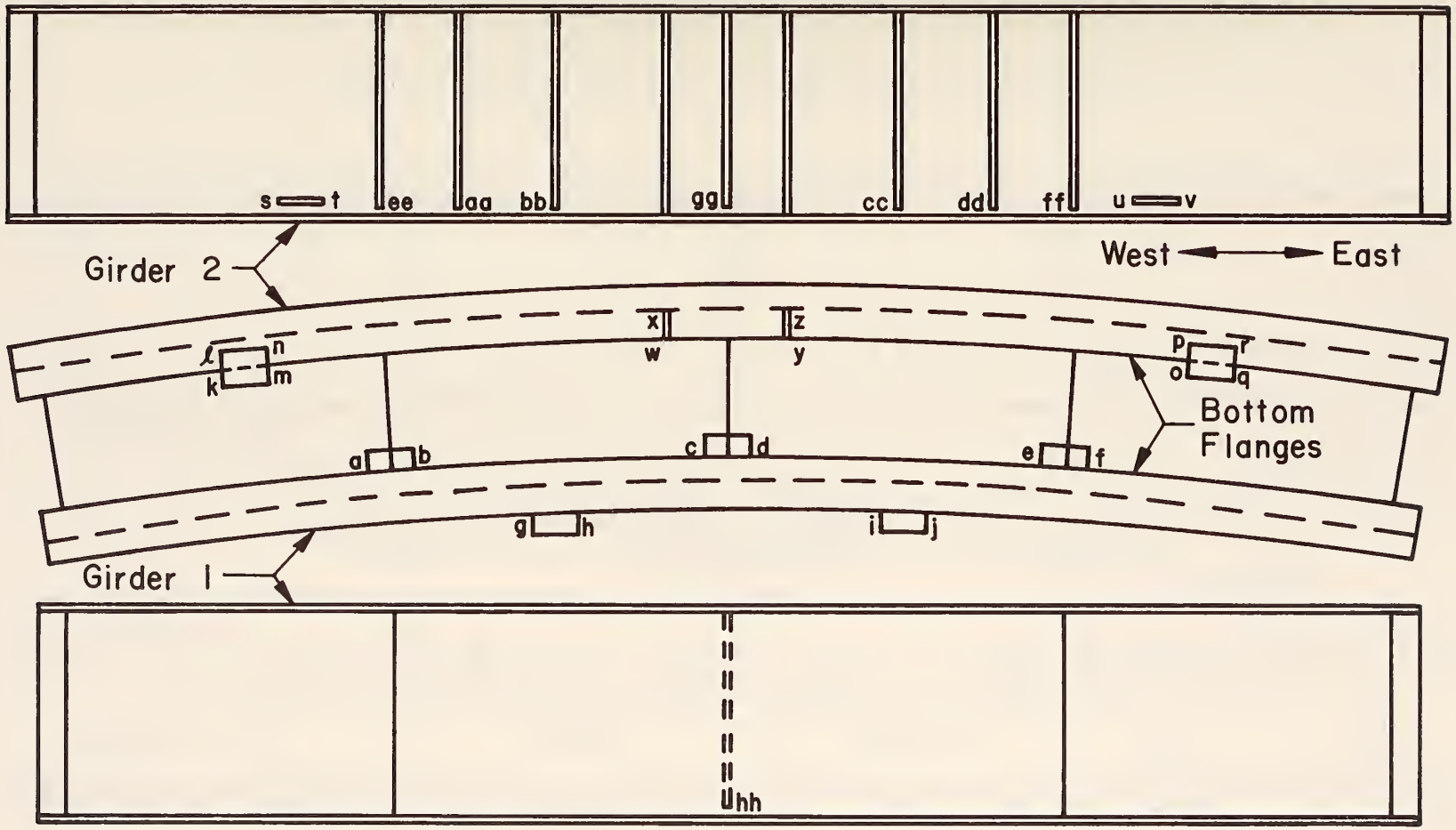

Fig. 54 Group 1 and Group 2 Welded Details on Assembly 2

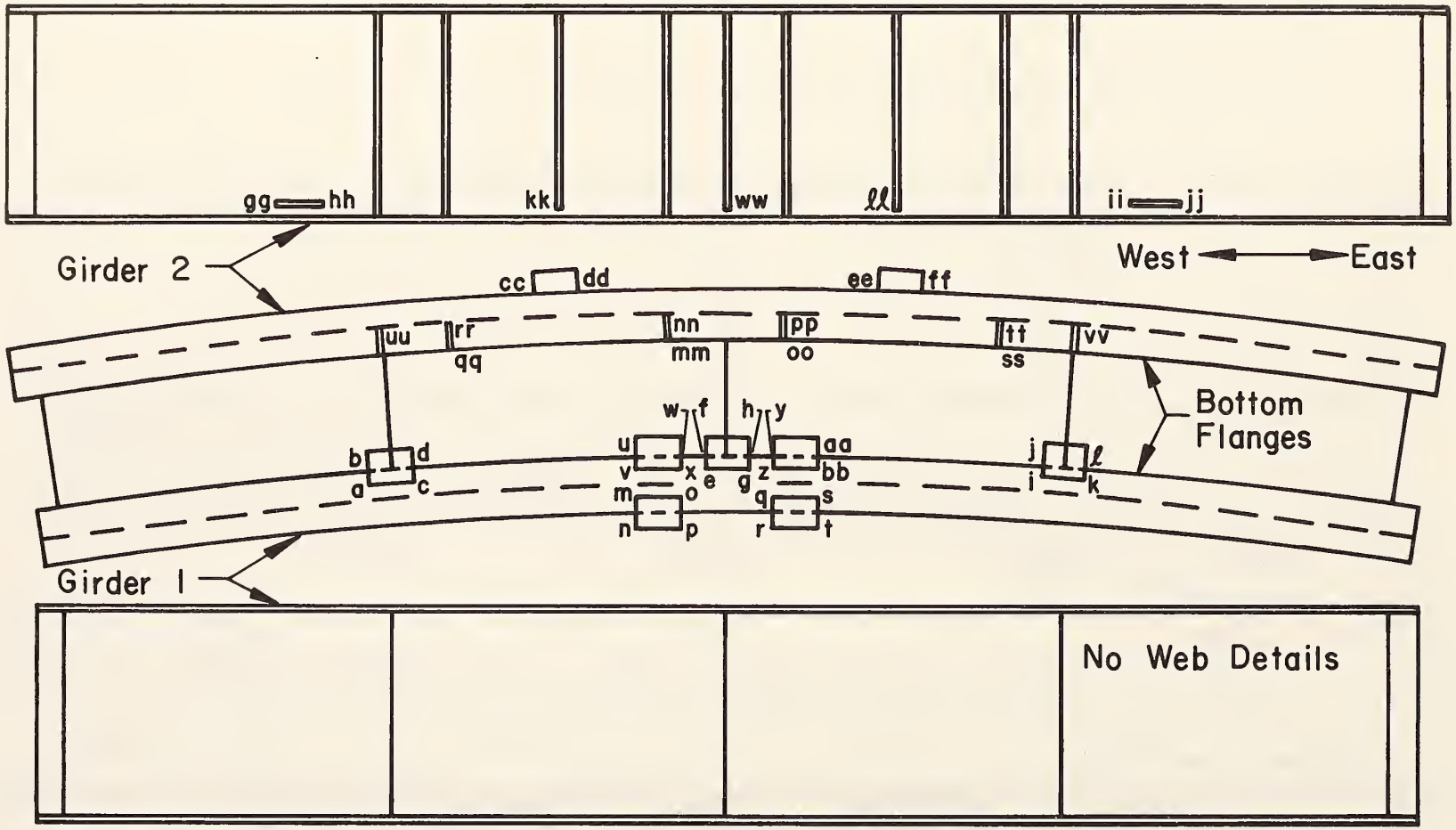

Fig. 55 Group 1 and Group 2 Welded Details on Assembly 3

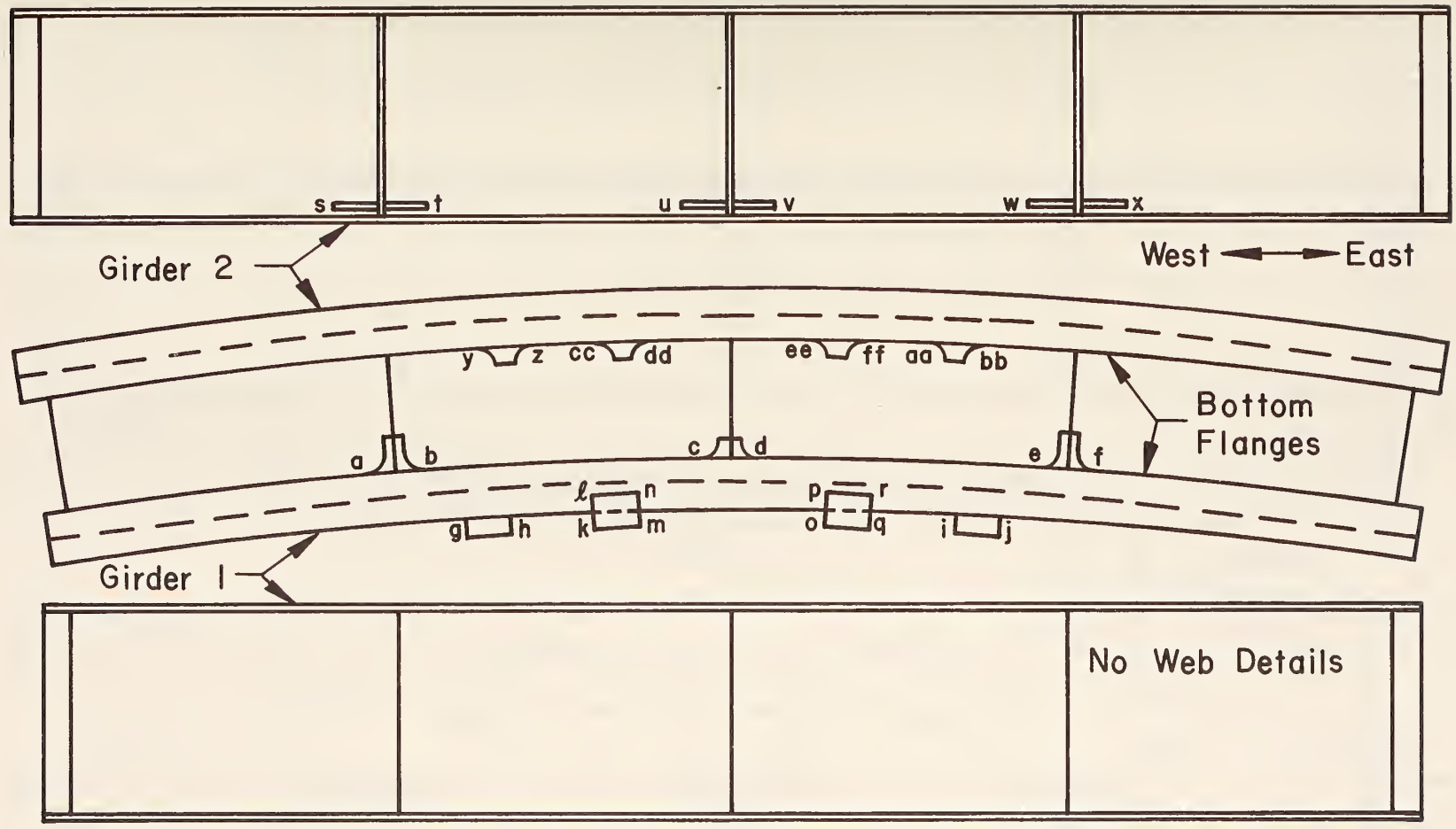

Fig. 56 Group 1 and Group 2 Welded Details on Assembly 4

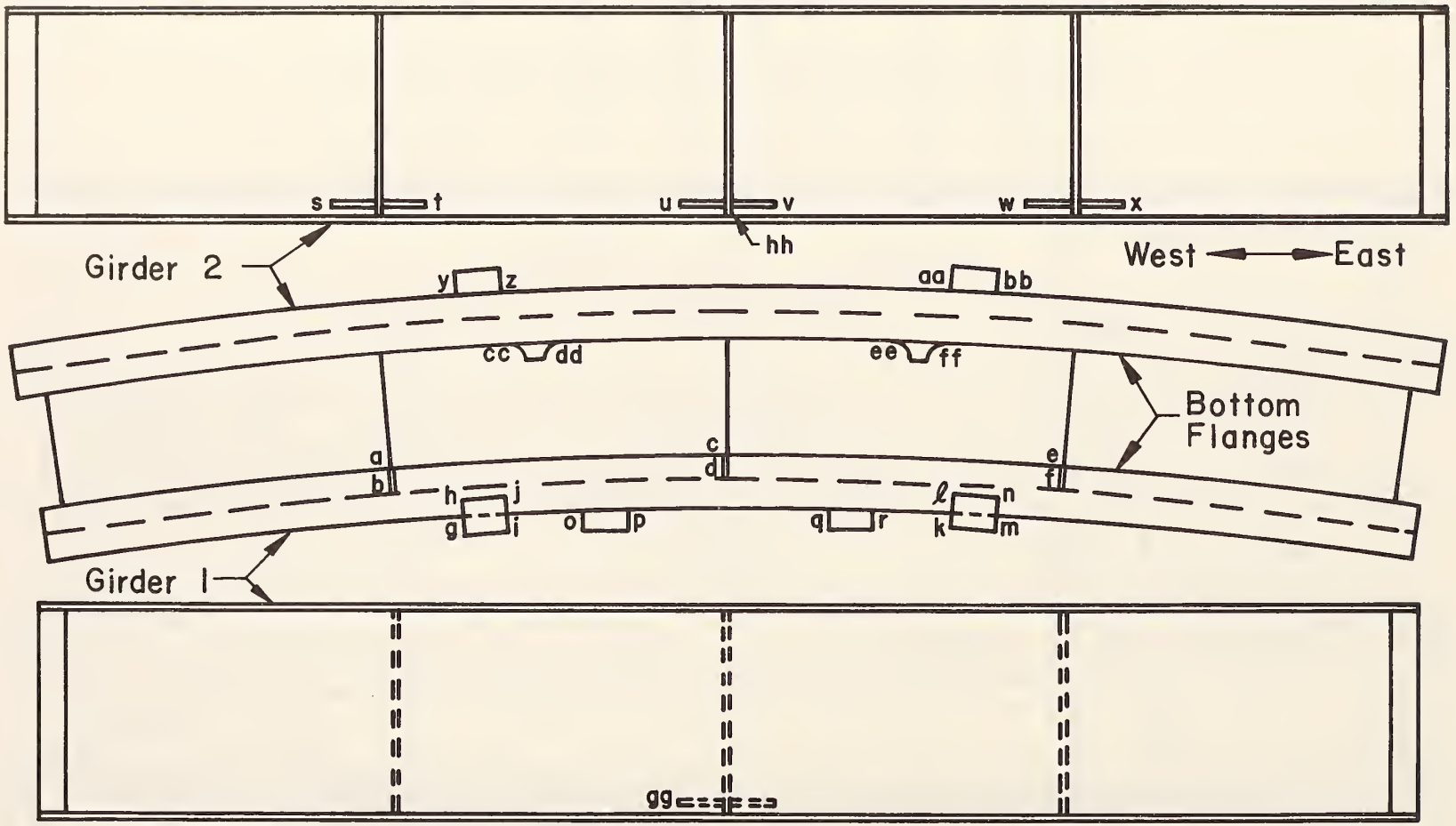

Fig. 57 Group 1 and Group 2 Welded Details on Assembly 5

Table 6 Measured Nominal Stress Ranges at All Potential Crack Locations and Cycles to Visible and Through Cracks - Assembly 1

AASHTO Fatigue Category	Detail Type	Potential Crack Location	Measured S_r (MPa)	Measured S_r (ksi)	Cycles (10^6) Visible Crack	Cycles (10^6) Through Crack
C	I_o	a	100.7	14.6	1.61	
		b	71.7	10.4		
		c	83.4	12.1		
		d	<69.0	<10		
		e	100.7	14.6		
		f	71.7	10.4		
E	V_{oa}	g	57.2	8.3	1.45	
		h	79.3	11.5	0.64	0.76
		i	79.3	11.5	0.64	0.95
		j	57.2	8.3	2.03	
E	V_{ob}	k	77.9	11.3	*0.95	
		ℓ	59.3	8.6		
		m	73.8	10.7	*0.64	
		n	73.1	10.6		
		o	73.8	10.7	0.64	0.95
		p	Interference from crack at o			
		q	73.1	10.6	1.45	
		r	59.3	8.6		
		s	81.4	11.8	0.95	1.61
		t	Interference from crack at s			
		u	64.1	9.3		
		v	64.8	9.4		
		w	64.1	9.3	*0.64	
		x	64.8	9.4		
		y	81.4	11.8	0.95	1.61
		z	67.6	9.8		
E	III_{ob}	aa	58.6	8.5		
		bb	51.7	7.5		
		cc	51.7	7.5	2.03	
		dd	58.6	8.5		

*Crack develops only in weld material, not in flange material.

Assembly 2

AASHTO Fatigue Category	Detail Type	Potential Crack Location	Measured S_r (MPa)	Measured S_r (ksi)	Cycles (10^6) Visible Crack	Cycles (10^6) Through Crack
E	V_{oa}	a	69.6	10.1	2.03	
		b	80.7	11.7		
		c	54.5	7.9		
		d	53.8	7.8		
		e	75.8	11.0	1.09	1.27
		f	60.7	8.8		
		g	74.5	10.8	1.45	1.86
		h	79.3	11.5	1.94	
		i	79.3	11.5	1.52	
		j	74.5	10.8		1.45
E	V_{ob}	k	96.5	14.0	2.03	
		ℓ	71.7	10.4		
		m	73.8	10.7	2.03	
		n	68.3	9.9		
		o	73.8	10.7	2.03	
		p	68.3	9.9		
		q	96.5	14.0		
		r	71.7	10.4		
E	III_{ob}	s	60.0	8.7		
		t	73.8	10.7	1.09	1.38
		u	60.0	8.7	2.03	
		v	55.8	8.1	1.52	
C	I_o	w	101.4	14.7		
		+x	93.8	13.6	1.52	
		y	101.4	14.7		
		+z	93.8	13.6	1.52	
C	II_o	aa	93.1	13.5	1.38	
		bb	90.3	13.1		
		cc	90.3	13.1	1.86	
		dd	93.1	13.5		
		ee	88.9	12.9	**	
		ff	90.3	13.1	**	
		gg	*	*		0.86
		hh	*	*		0.86

\+ Cracks develop in web weld material and not at potential locations on flange.

* Cracks develop due to out-of-plane bending of web (Article 6.2).

** No visible cracks were observed at the ends of the ⊥-type connection (Article 6.2 and Figure 62) although the stress range at the web-to-flange weld is approximately 13.7 ksi at ee and 13.9 ksi at ff.

Table 8 Measured Nominal Stress Ranges at All Potential Crack Locations and Cycles to Visible and Through Cracks - Assembly 3

AASHTO Fatigue Category	Detail Type	Potential Crack Location	Measured S_r (MPa)	Measured S_r (ksi)	Cycles (10^6) Visible Crack	Cycles (10^6) Through Crack
E	V_{ob}	a	Interference from crack at b			
		b	82.7	12.0	1.40	
		c	91.0	13.2		1.02
		d	Interference from crack at c			
		e	65.5	9.5		
		f	82.1	11.9		
		g	62.7	9.1		
		h	93.1	13.5		
		i	74.5	10.8		
		j	87.6	12.7		
		k	Interference from crack at ℓ			
		ℓ	95.8	13.9		1.60
		n	56.5	8.2		
		t	56.5	8.2		
		w	66.9	9.7		
		x	65.5	9.5		
		y	77.9	11.3	1.36	
		z	Interference from crack at y			
E	V_{oa}	cc	63.4	9.2		
		dd	60.0	8.7		
		ee	60.0	8.7	1.66	2.07
		ff	63.4	9.2		
E	III_{ob}	gg	60.7	8.8		
		hh	73.1	10.6		
		ii	73.1	10.6	1.51	1.60
		jj	60.7	8.8	1.66	
C	II_o	kk	84.1	12.2		
		ℓℓ	84.1	12.2		
C	I_o	mm	99.3	14.4		
		nn	100.0	14.5		
		oo	99.3	14.4		
		pp	100.0	14.5		
		qq	99.3	14.4		
		rr	103.4	15.0		
		ss	99.3	14.4		
		tt	103.4	15.0		
		uu	71.7	10.4		
		vv	71.7	10.4		
C	II_o	ww	*	*		0.32

*Cracks develop due to out-of-plane bending of web (Article 6.2).
Note: The measured S_r at locations m and s is <48.3 MPa (7 ksi). The measured S_r at locations o, p, q, r, u, v, aa, bb is <34.5 MPa (5 ksi).

Table 9 Measured Nominal Stress Ranges at All Potential Crack Locations and Cycles to Visible and Through Cracks - Assembly 4

AASHTO Fatigue Category	Detail Type	Potential Crack Location	Measured S_r (MPa)	Measured S_r (ksi)	Cycles (10^6) Visible Crack	Cycles (10^6) Through Crack
C	IV_o	a	114.6	16.6		0.68
		b	105.5	15.3		1.64
		c	77.9	11.3		
		d	85.5	12.4		
		e	101.4	14.7		
		f	102.7	14.9		0.35
E	V_{oa}	g	58.6	8.5		
		h	81.4	11.8	0.68	0.79
		i	81.4	11.8	0.68	0.79
		j	58.6	8.5		1.32
E	V_{ob}	k	69.0	10.0		
		ℓ	65.5	9.5		
		m	62.7	9.1		
		n	53.1	7.7		
		o	62.7	9.1		
		p	53.1	7.7		
		q	69.0	10.0	1.12	1.32
		r	Interference from crack at q			
E	III_{oa}	s	63.4	9.2	1.32	1.64
		t	73.1	10.6	1.32	1.64
		u	80.0	11.6		
		v	78.6	11.4		
		w	73.1	10.6	1.64	
		x	63.4	9.2		
C	IV_o	y	104.8	15.2		
		z	113.1	16.4		1.32
		aa	113.1	16.4		
		bb	104.8	15.2		
		cc	102.7	14.9		
		dd	78.6	11.4		
		ee	78.6	11.4		
		ff	102.7	14.9		

Table 10 Measured Nominal Stress Ranges at All Potential Crack Locations and Cycles to Visible and Through Cracks - Assembly 5

AASHTO Fatigue Category	Detail Type	Potential Crack Location	Measured S_r (MPa)	Measured S_r (ksi)	Cycles (10^6) Visible Crack	Cycles (10^6) Through Crack
C	I_o	a	89.6	13.0		
		b	69.0	10.0		
		c	77.9	11.3		
		d	51.0	7.4		
		e	82.7	12.0		
		f	61.4	8.9		
E	V_{ob}	g	78.6	11.4		
		h	65.5	9.5		
		i	91.7	13.3		
		j	71.7	10.4		
		k	91.7	13.3	1.82	2.14
		ℓ	Interference from crack at k			
		m	78.6	11.4		
		n	65.5	9.5		
E	V_{oa}	o	75.8	11.0		1.27
		p	52.4	7.6	2.14	
		q	52.4	7.6	1.82	
		r	75.8	11.0		1.27
E	III_{oa}	s	69.0	10.0	1.82	
		t	71.7	10.4		
		u	77.2	11.2	1.82	2.14
		v	80.7	11.7	1.82	
		w	71.7	10.4	1.56	2.14
		x	69.0	10.0		
E	V_{oa}	y	66.2	9.6	1.56	
		z	60.7	8.8	2.14	
		aa	60.7	8.8	2.14	
		bb	66.2	9.6	1.82	2.14
C	IV_o	cc	106.2	15.4		0.44
		dd	106.2	15.4		1.56
		ee	117.2	17.0		0.93
		ff	113.8	16.5	1.82	2.14
E	III_{oa}	gg	40.7	5.9	1.82	
C	II_o	hh	84.1	12.2	2.14	

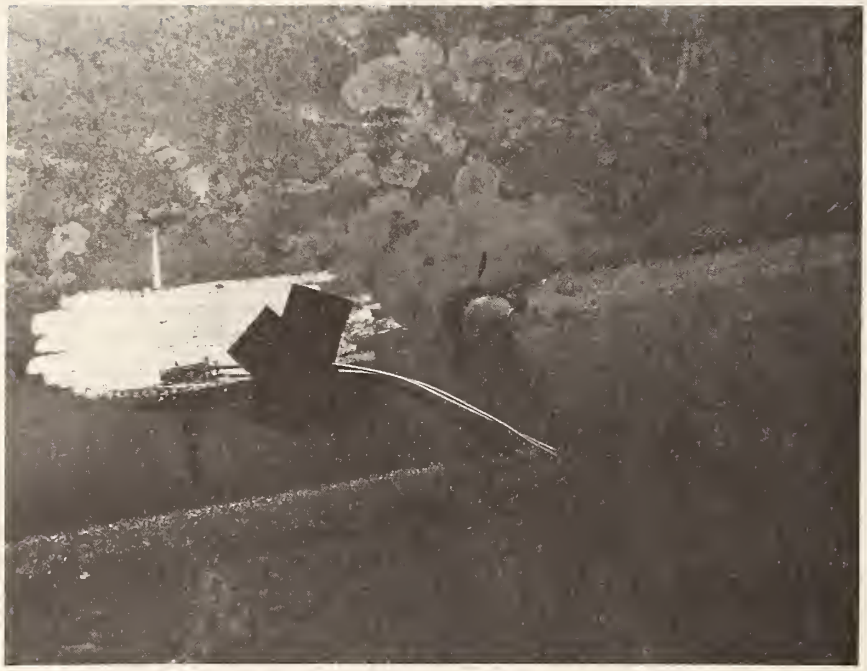

Fig. 58 Typical Fatigue Cracks - Details III_{ob} and IV_{o}

Fig. 59 Typical Fatigue Cracks - Details V_{oa} and V_{ob}

Fig. 60 Web Crack Repairs - Location ww on Girder 2 of Assembly 3

stress range profiles (broken lines in Figs. 42 through 50) to adjust the strains to account for the distance between the strain gage and the potential crack location.

Several fatigue cracks are shown in Figs. 58 and 59. Figure 58 shows cleaner fluid evaporating from the web surface and leaving outlines of cracks growing from the weld termination on a type III_{ob} detail. The flange crack in Fig. 58 has grown from the circular transition detail IV_o and propagated through the hole drilled to halt its growth. The flange cracks shown in Fig. 59 developed at type V_{oa} and V_{ob} details. The drilled hole has halted the small crack at the type V_{oa} detail. The crack initiating at the V_{ob} fillet weld has propagated across half the flange width.

6.2 Secondary Fatigue Cracks

In addition to the potential primary fatigue cracks associated with the Group 1 and Group 2 details, some secondary fatigue cracking occurred due to out-of-plane bending of the web.

Secondary fatigue cracks on Assembly 3, the first assembly tested, were visible after 320,000 cycles. These cracks developed in the web in a 25.4 mm (1 in.) gap between the bottom of a type II_o detail and the bottom flange. The crack location is labeled ww on Girder 2 in Fig. 55. The cracks damaged a strain gage before the stress range at the weld toe could be measured. The cracks were through the web thickness. Repairs consisted of drilling holes through the web at the crack tips and welding the stiffener to a plate which in turn is welded

to the bottom flange as shown in Fig. 60. The cause of the early fatigue damage in the web is the out-of-plane web bending stresses in the small gap between the stiffener and the bottom flange. The stresses are displacement induced with the displacement resulting from the relative lateral motion of the diaphragm which is connected to the stiffener and the bottom flange directly below the stiffener. No relative motion exists at a type I_o detail since the stiffener is welded to the flange.

The bending stresses out of the plane of the web in the gap between a cut-short type II_o detail and the bottom flange were measured on Assembly 2. A strip of ten strain gages in a 19.1 mm (0.75 in.) distance was aligned vertically beneath the type II_o detail shown in Fig. 61. Wires leading to the oscillograph recorder are attached to the terminals mounted to the left of the type II_o detail. Strip gages were mounted on both web faces at the type II_o details at midspan of each girder on Assembly 2. Out-of-plane bending stress ranges as high as 551.6 MPa (80 ksi) were computed from the measured strains. The large stress ranges resulted in web cracking at both locations after only 86,200 cycles. Repairs consisted of drilling holes and connecting the type II_o details to the bottom flange with welded plates as described for Assembly 3. Reference 14 contains an analytical study of the stresses to be expected in the gap between a web transverse stiffener and the bottom flange.

Figure 62 shows two views of a $\perp$-type connection to join cut-short transverse stiffeners to the bottom flange. The connection was

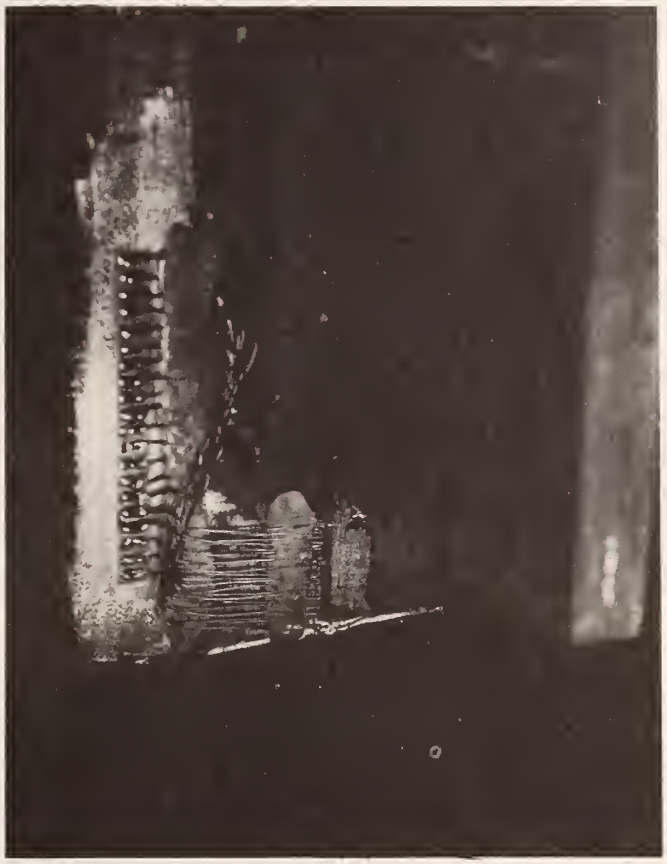

Fig. 61 Strip of Ten Strain Gages in Gap Shown Beneath a Type II_o Detail

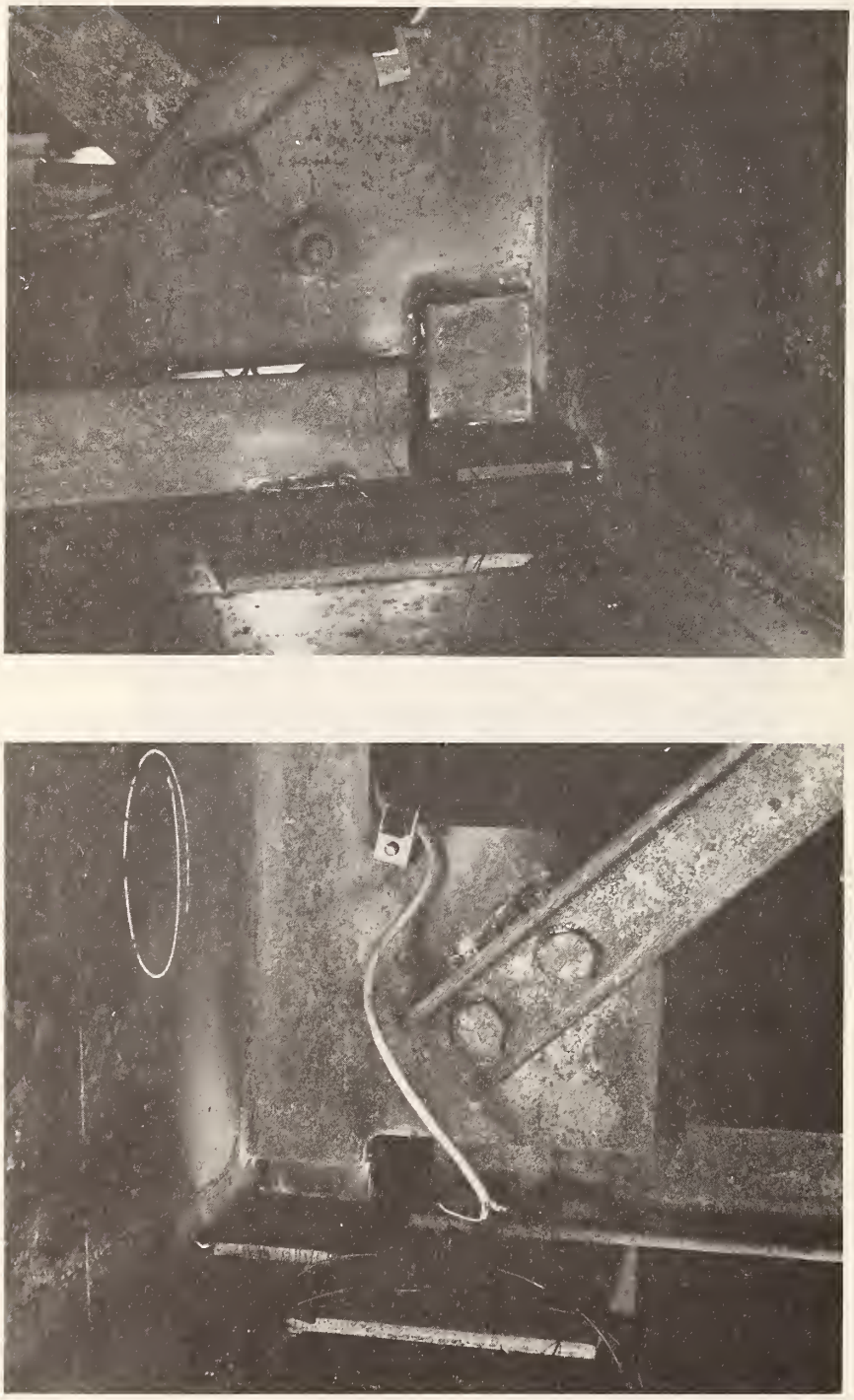

Fig. 62 Trial $\perp$-Type Connection to Join Type II_o Detail to Bottom Flange

used on the type II_o details at joints 3, 4, 7, and 8 on Assembly 2. In Fig. 62 the horizontal and diagonal diaphragm members are not connected at the joint thus allowing lateral out-of-plane motion of the type II_o stiffener before installation of the ⊥-type connection. The horizontal leg of the ⊥ is welded to the web-to-flange junction. The vertical leg is then welded to the stiffener. Such a connection may be practical only when the flange tip stress range is too large to consider extending the web stiffener and welding it directly to the flange, as is done for type I_o details. The ⊥-type details used at joints 4 and 8 on Assembly 2 (ee and ff in Table 7) have approximately 4 inch long horizontal plates, placing them into a Category D detail. Although σ_r varied from 13.7 to 13.9 ksi at these details no visible cracks were observed at the end of the test (2.03×10^6 cycles).

Out-of-plane displacement induced stresses in the web can also be significant in the cope of the type III_{oa} detail (Table 2). One midspan type III_{oa} detail on Girder 2 of Assembly 4 was modified by disconnecting the detail from the transverse stiffener by flame cutting. Again a strip of ten strain gages was mounted on each face of the web. This time the gages were oriented horizontally. Figure 63 shows each side of the web on Girder 2 where the strain gages are mounted horizontally at the level of the type III_{oa} detail. The figure also shows wires leading to the oscillograph recorder. Forces in the bottom lateral bracing member and the diaphragm contribute to the out-of-plane bending of the web. Web fatigue cracks developed after 790,000 cycles with out-of-plane bending stresses measured as high as 222 MPa (32.2 ksi). Repairs consisted of drilling holes at the crack tips and rewelding the gusset plate to the transverse stiffener.

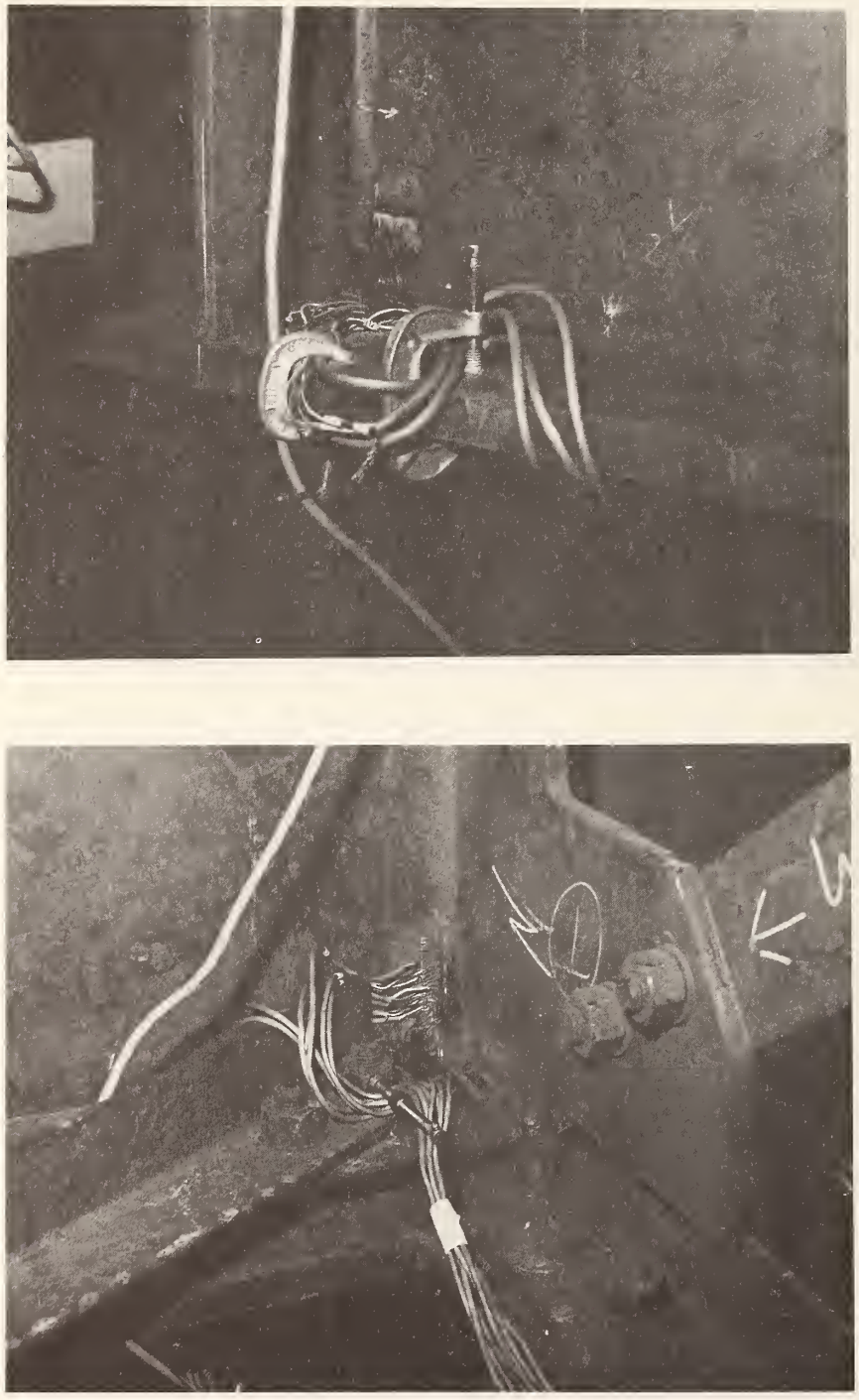

Fig. 63 Strips of Ten Strain Gages Mounted on North and South Faces of Web - Midspan - Assembly 4 - Girder 2

Table 11 Web Panel Properties and Measured Lateral Deflections

Assembly	Girder	Web Panel	D_w/t_w	d/D_w	Maximum δ		Maximum δ/t_w
					mm	(in.)	
1	1	End	144	1.31	2.67	(0.105)	0.28
	2	End	192	1.28	1.98	(0.078)	0.28
2	1	Center	155	2.03	2.59	(0.102)	0.27
	2	End	186	1.05	3.40	(0.134)	0.43
3	1	Center	155	2.03	2.64	(0.104)	0.28
	2	End	155	1.05	2.69	(0.106)	0.28
4	1	Center	139	2.27	1.75	(0.069)	0.18
	2	Center	139	2.37	1.93	(0.076)	0.20
5	1	Center	139	2.27	1.85	(0.073)	0.19
	2	Center	139	2.37	1.40	(0.055)	0.15

D_w - Web Depth

t_w - Web Thickness

d - Transverse Stiffener Spacing

δ - Web Lateral Deflection Under 445 kN (100 kip) Load

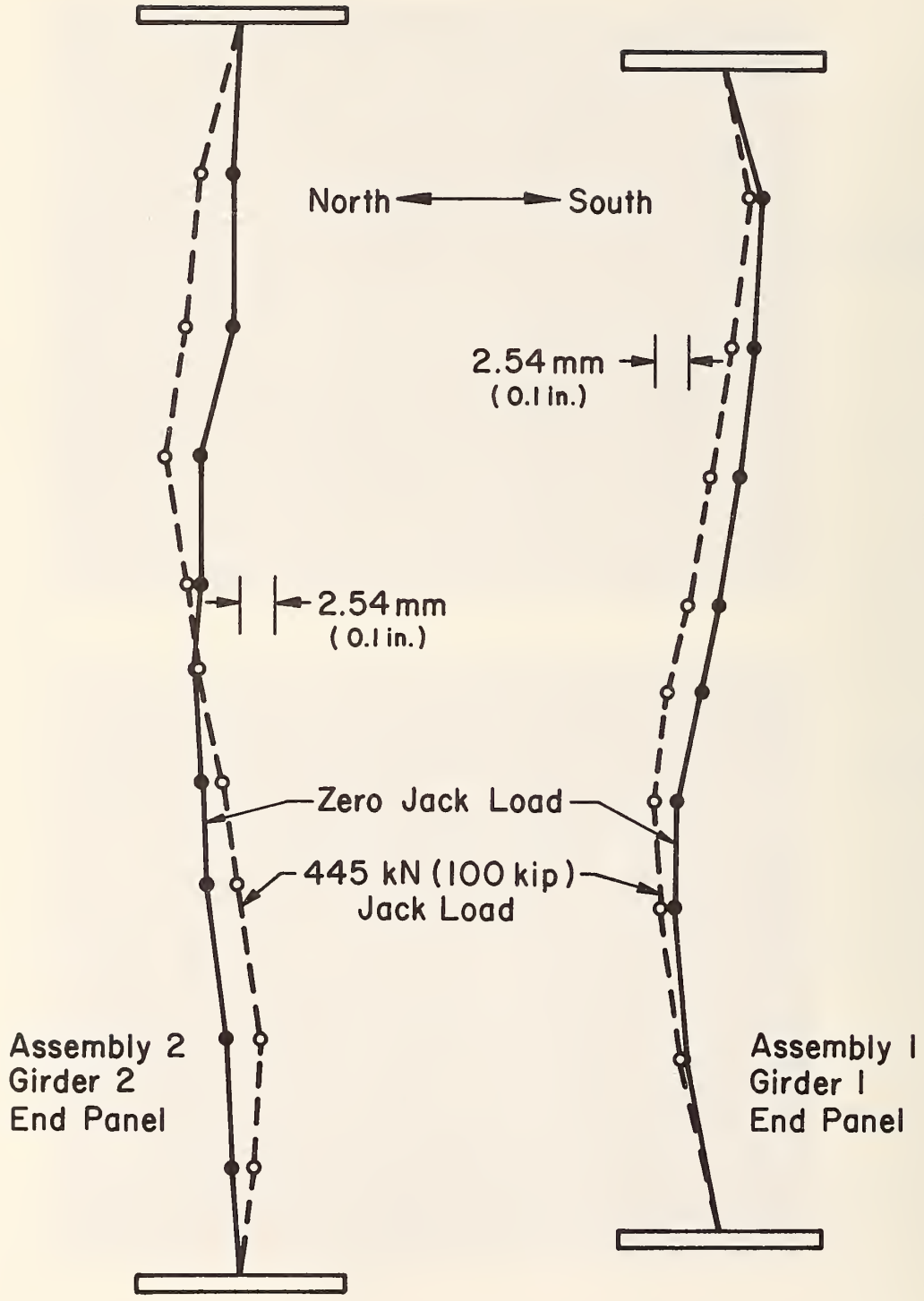

Fig. 64 Typical Deflected Shapes of Webs

6.3 Web Performance

For the purpose of studying web performance under fatigue loading, various web slenderness ratios and transverse stiffener spacings are used on the test assemblies[8]. The actual ratios and spacings exceed the suggested allowable values on most of the assemblies. The differing web and web panel geometries provide the opportunity to observe the so-called "oil canning" effect under various conditions. The "oil canning" effect or "panting" of the web did not cause any visually detectable fatigue cracking of the web boundary welds on any of the five assemblies.

The web lateral deflections were not measured during cyclic loading. Web deflections were measured under static load. The dial gage rig shown in Fig. 26 measures the lateral deflections relative to the top and bottom web-flange junctions. The measurements were normally taken about every 381 mm (15 in.) along the east half of each girder. Table 11 contains the maximum measured web deflections, δ, for each assembly under 445 kN (100 kip) jack loads. The web panel on which the maximum lateral deflection occurred is tabulated in the third column. The end panels are between either joints 7 and 9 or 8 and 10 while the center panels are bounded by joints 5 and 7 or 6 and 8. The ratios of deflection to web thickness, δ/t_w, and the aspect ratio of transverse stiffener spacing to web depth, d/D_w, are also tabulated. The web slenderness ratio is constant for each girder. The deflections of two typical web sections are shown in Fig. 64.

7. DISCUSSION OF TEST RESULTS

The primary fatigue test results summarized in Tables 6 through 10 are plotted in Figs. 65 through 74. Separate Category C and Category E plots are included for each of the five assemblies. Table 1.7.2A1 of Ref. 9 provides the straight girder Category C and Category E AASHTO allowable stress range curves. The solid line and two dashed lines above the allowable stress range curve in each figure are respectively the mean regression line and 95 percent confidence limits for the straight girder tests reported in Refs. 15 and 16. Equation 1 in Chapter 3 of Ref. 15 provides the curves for Category C. The equation for Model D under All Welded End Cover Plates in Table F-18 of Ref. 16 defines the Category E curves. The secondary fatigue cracks discussed in Art. 6.2 which became through-thickness web cracks at less than 500,000 load cycles are not plotted in the figures.

7.1 Detail Type I_o

Figure 75 combines the type I_o detail fatigue test results for all five assemblies. A large percentage of the potential crack locations experienced nominal stress ranges below the two million cycle allowable 89.6 MPa (13 ksi). Based on the satisfactory fatigue performance of the type I_o details with nominal stress ranges greater than 89.6 MPa (13 ksi), the lower stressed details should also achieve a fatigue life characteristic of a Category C detail. Thus the AASHTO straight girder Category C is applicable to the type I_o details on the five curved plate girder assemblies.

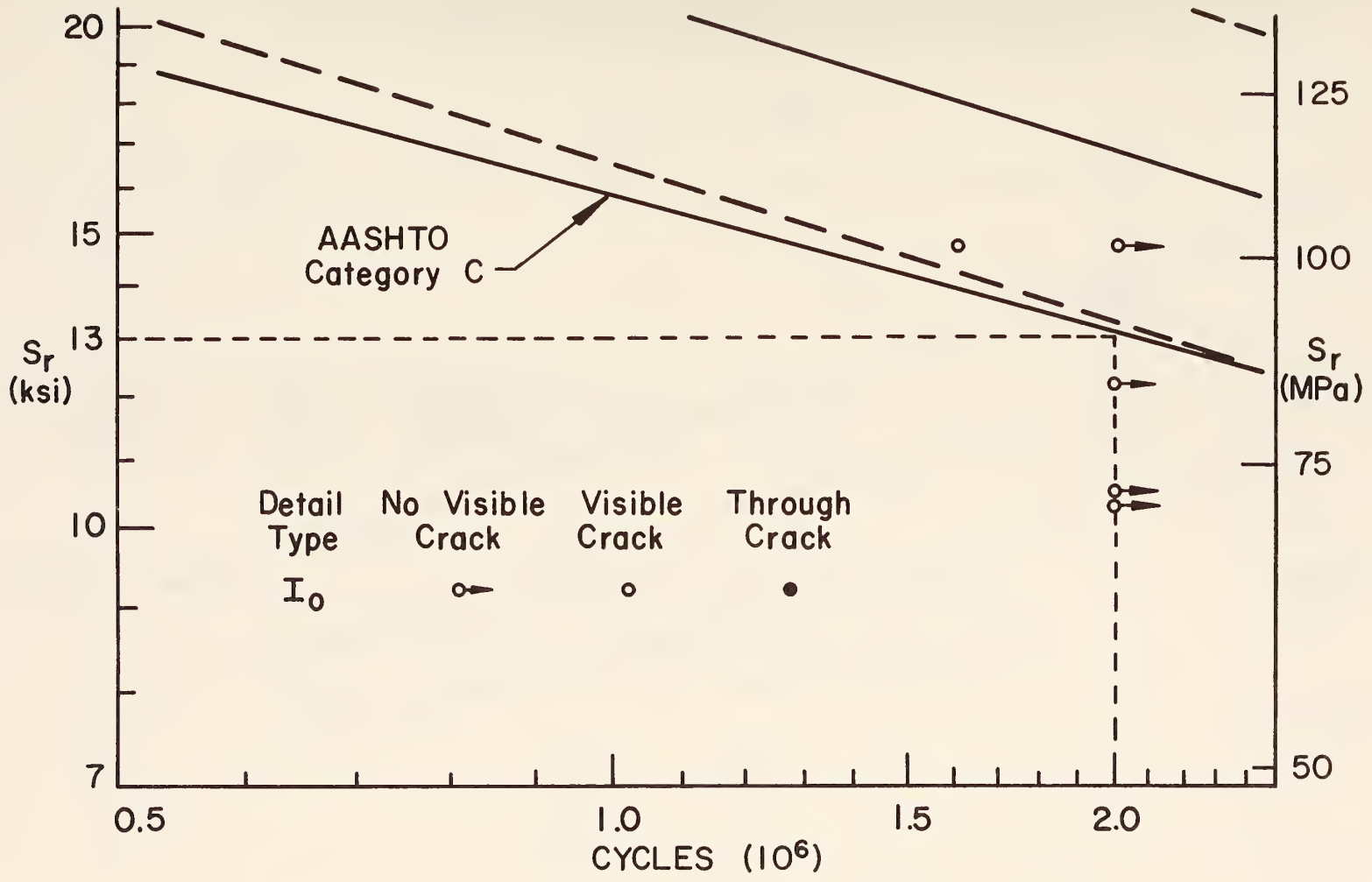

Fig. 65 Fatigue Results - Assembly 1 Category C Details

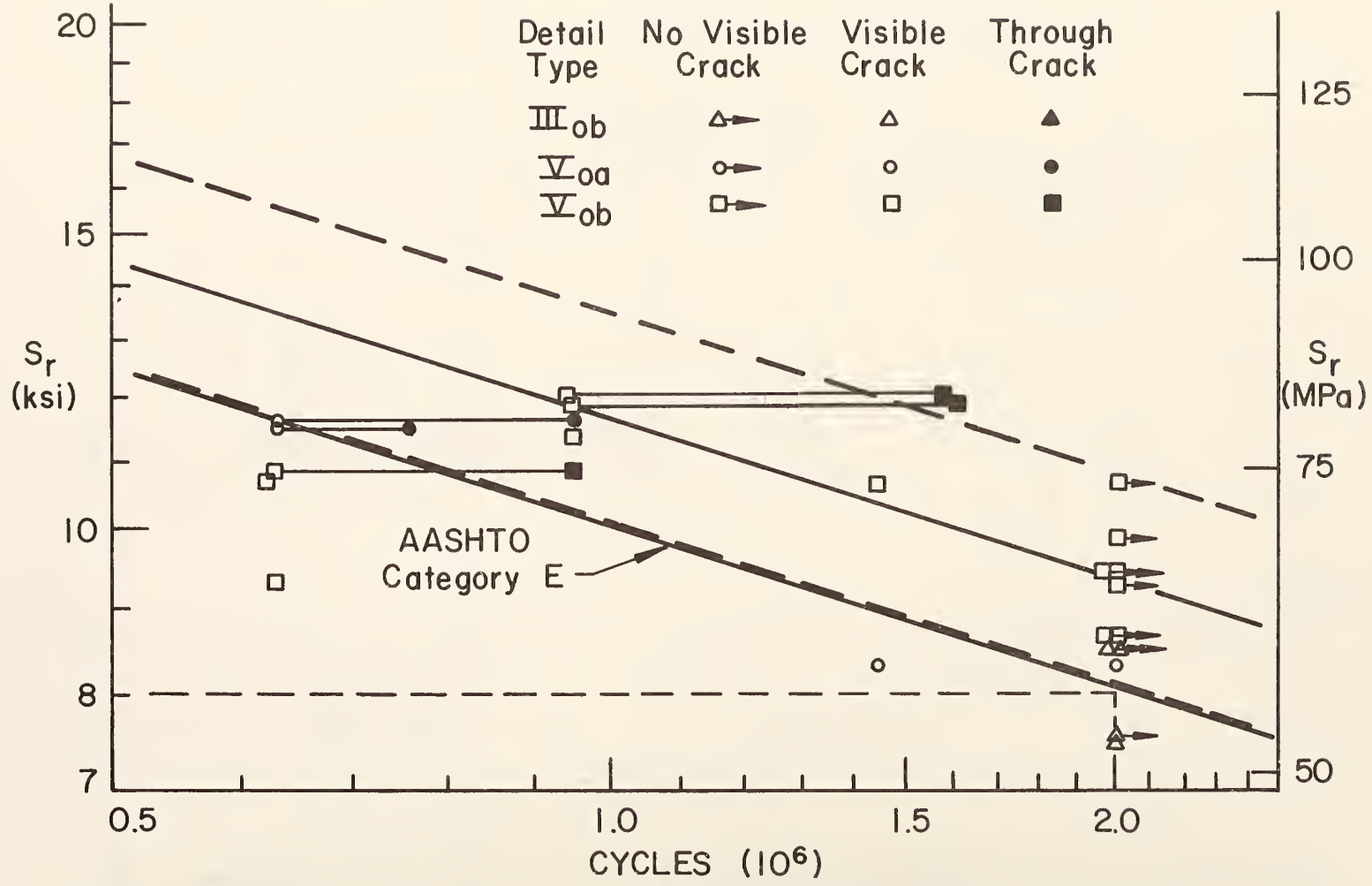

Fig. 66 Fatigue Results - Assembly 1 Category E Details

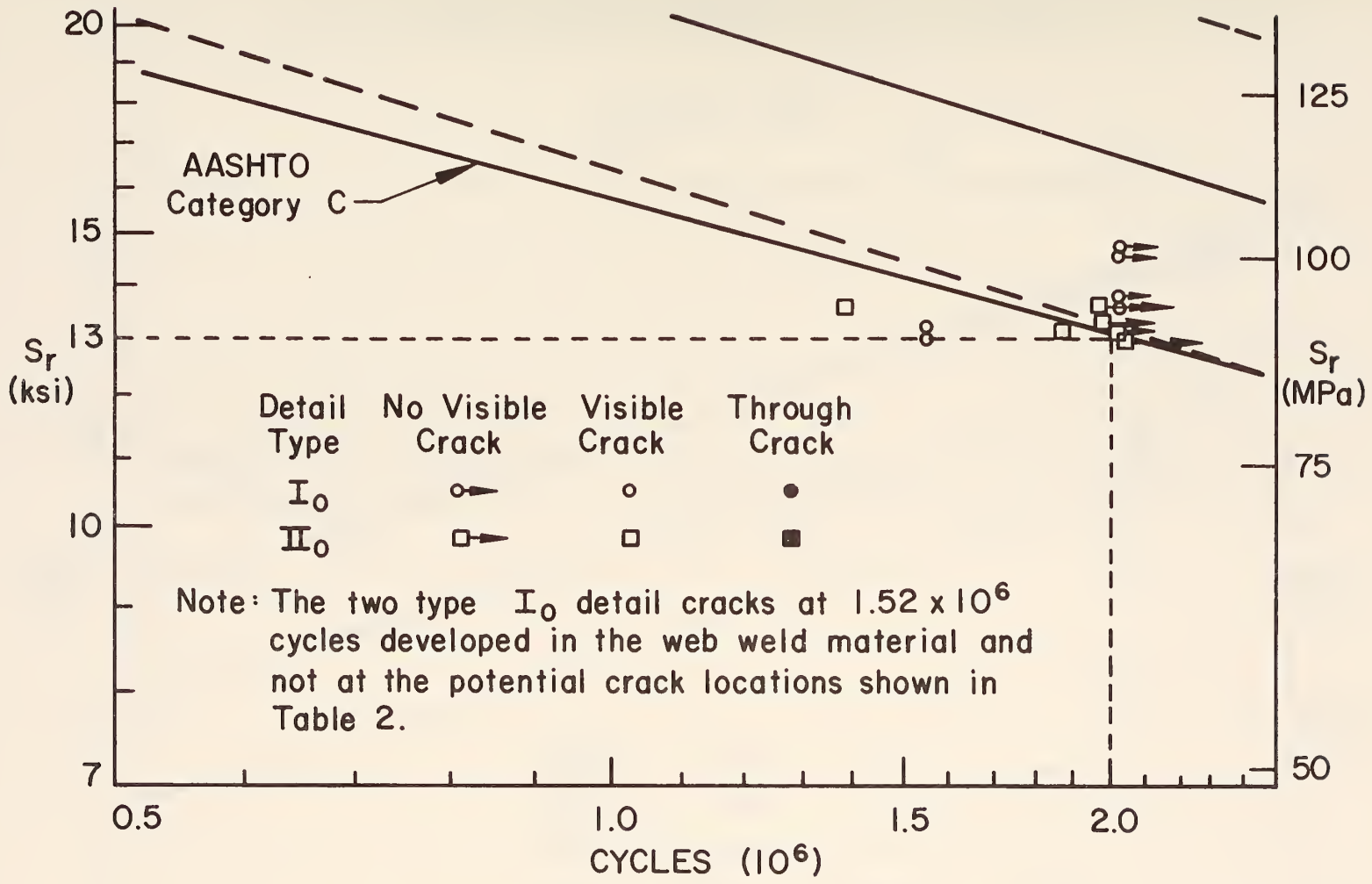

Fig. 67 Fatigue Results - Assembly 2 Category C Details

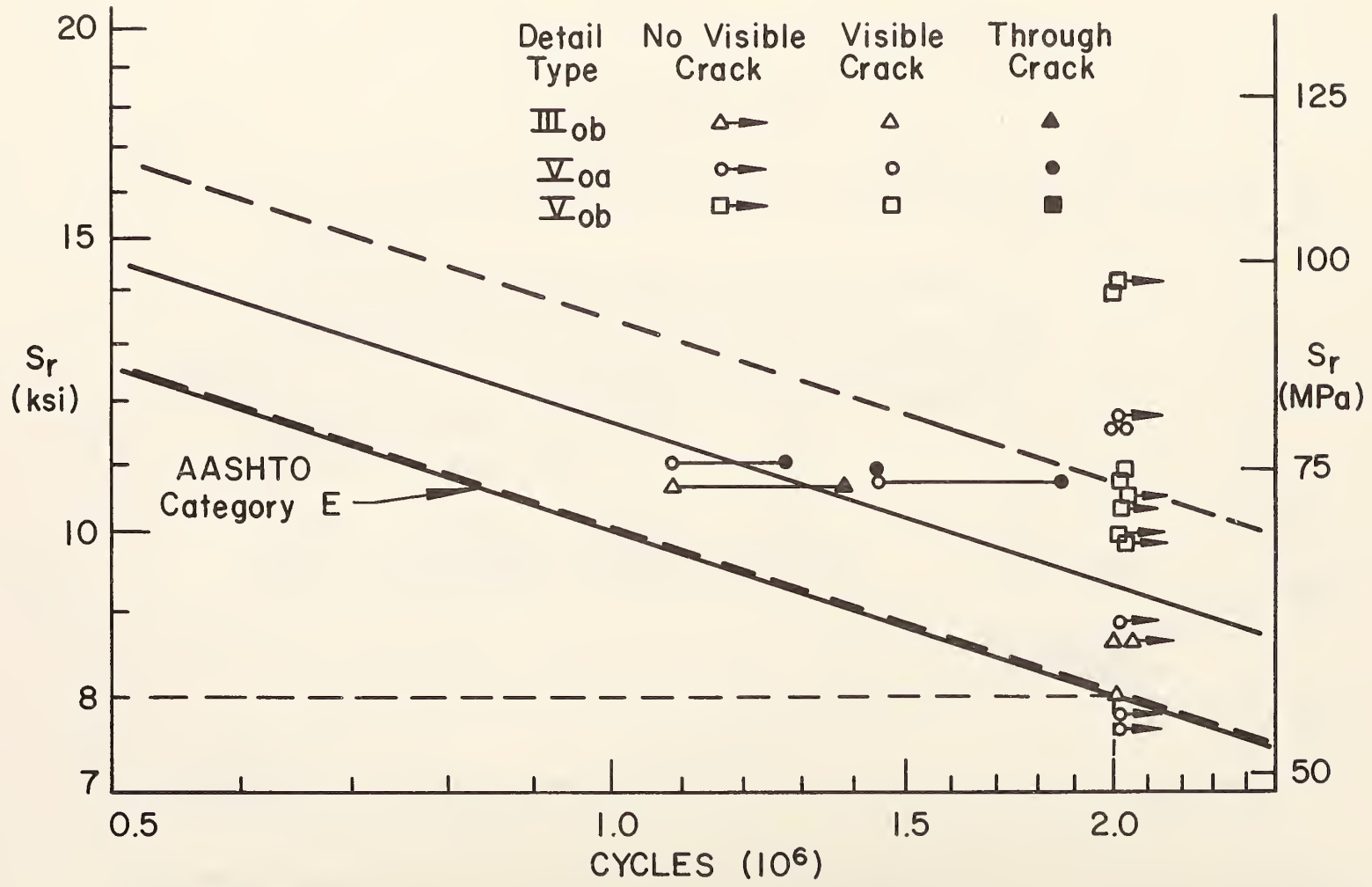

Fig. 68 Fatigue Results - Assembly 2 Category E Details

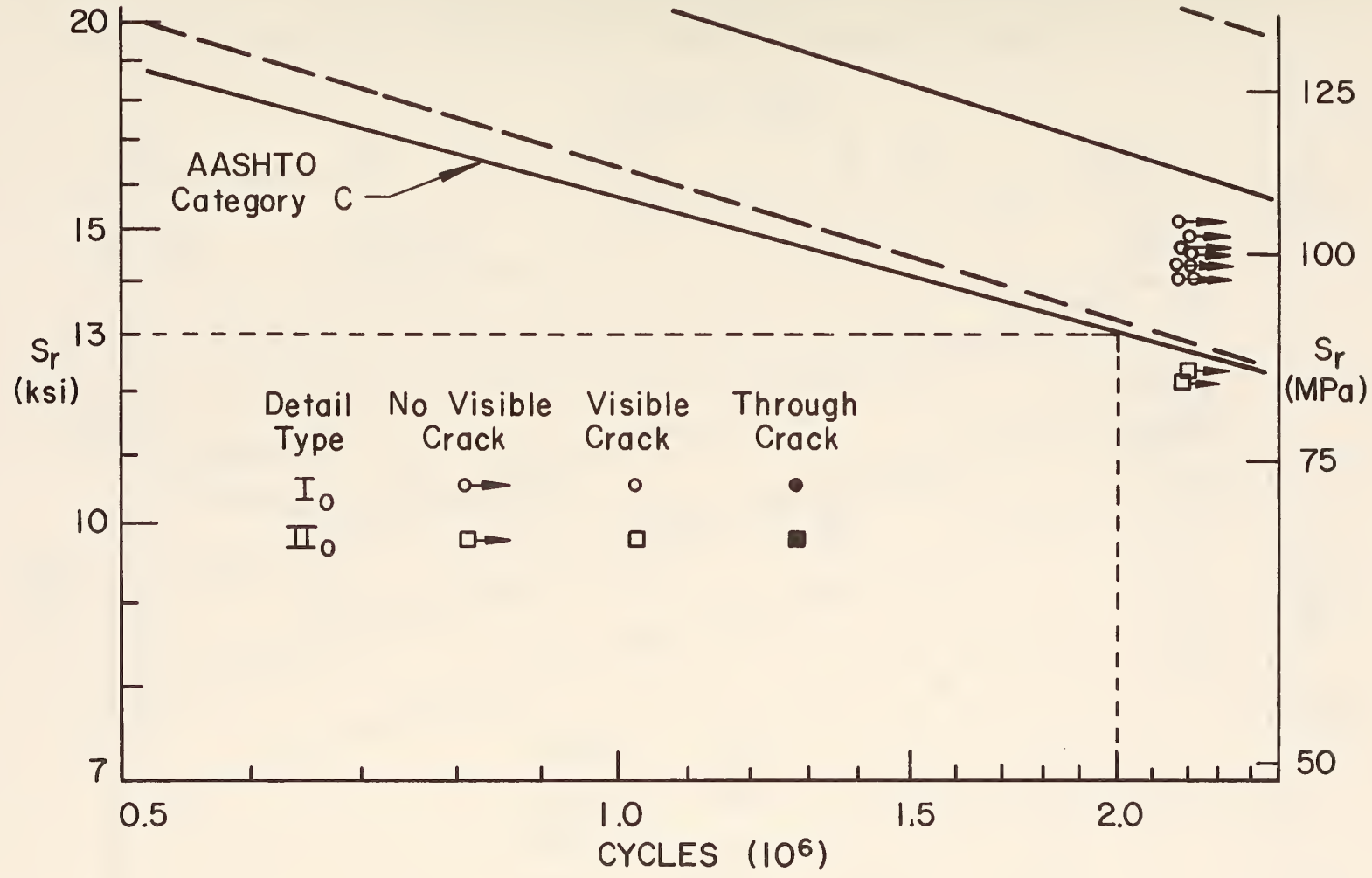

Fig. 69 Fatigue Results - Assembly 3 Category C Details

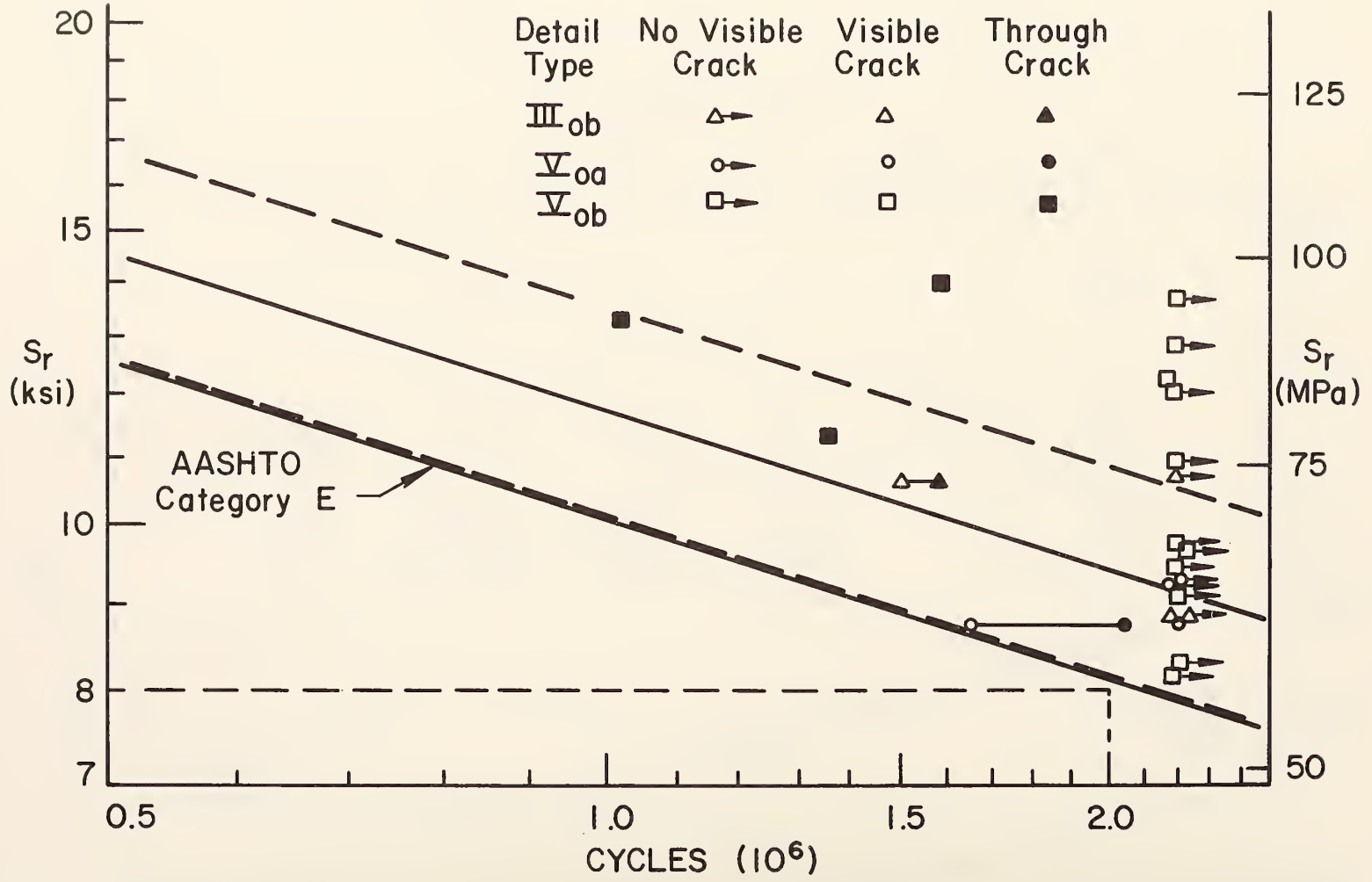

Fig. 70 Fatigue Results - Assembly 3 Category E Details

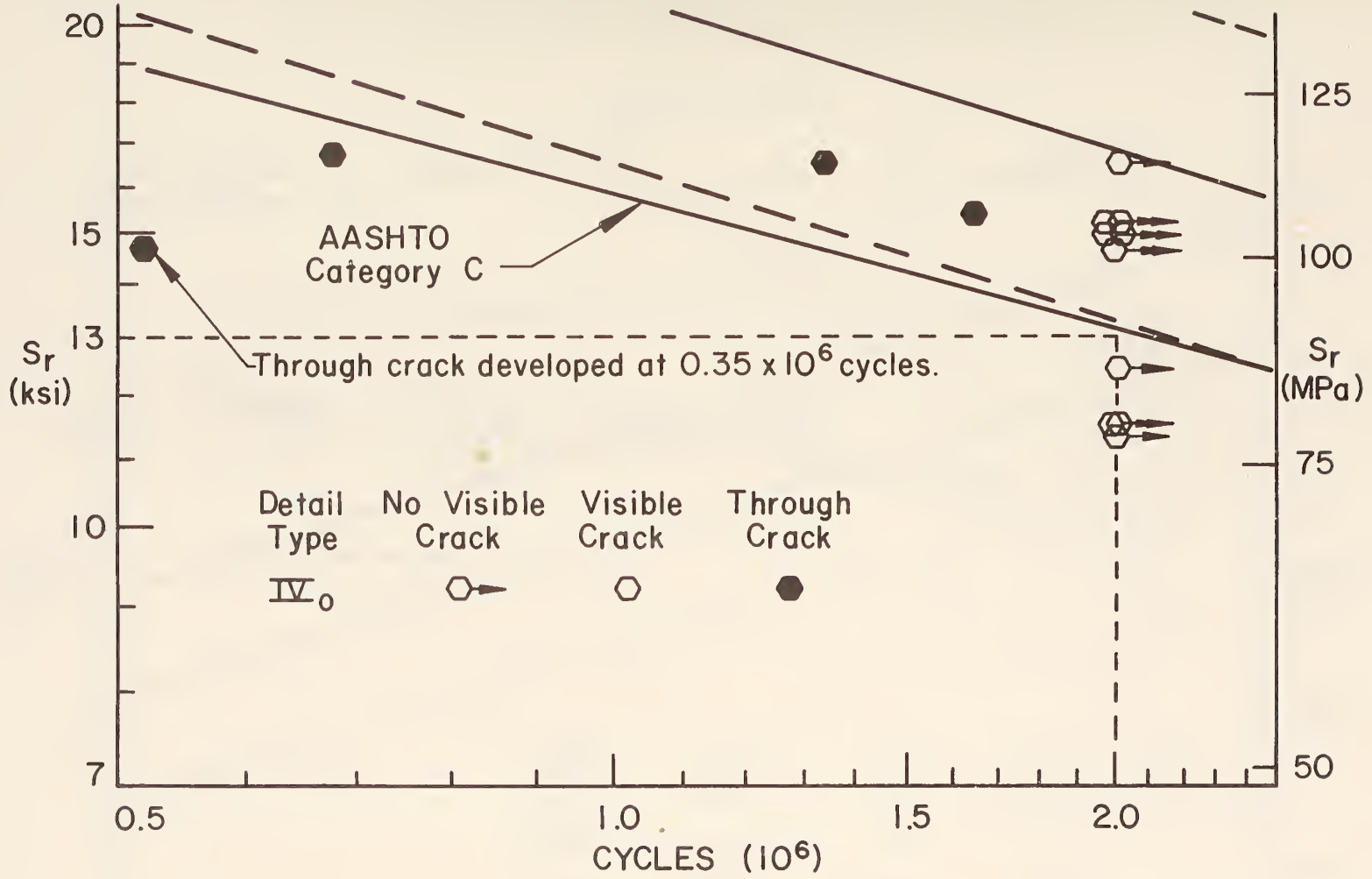

Fig. 71 Fatigue Results - Assembly 4 Category C Details

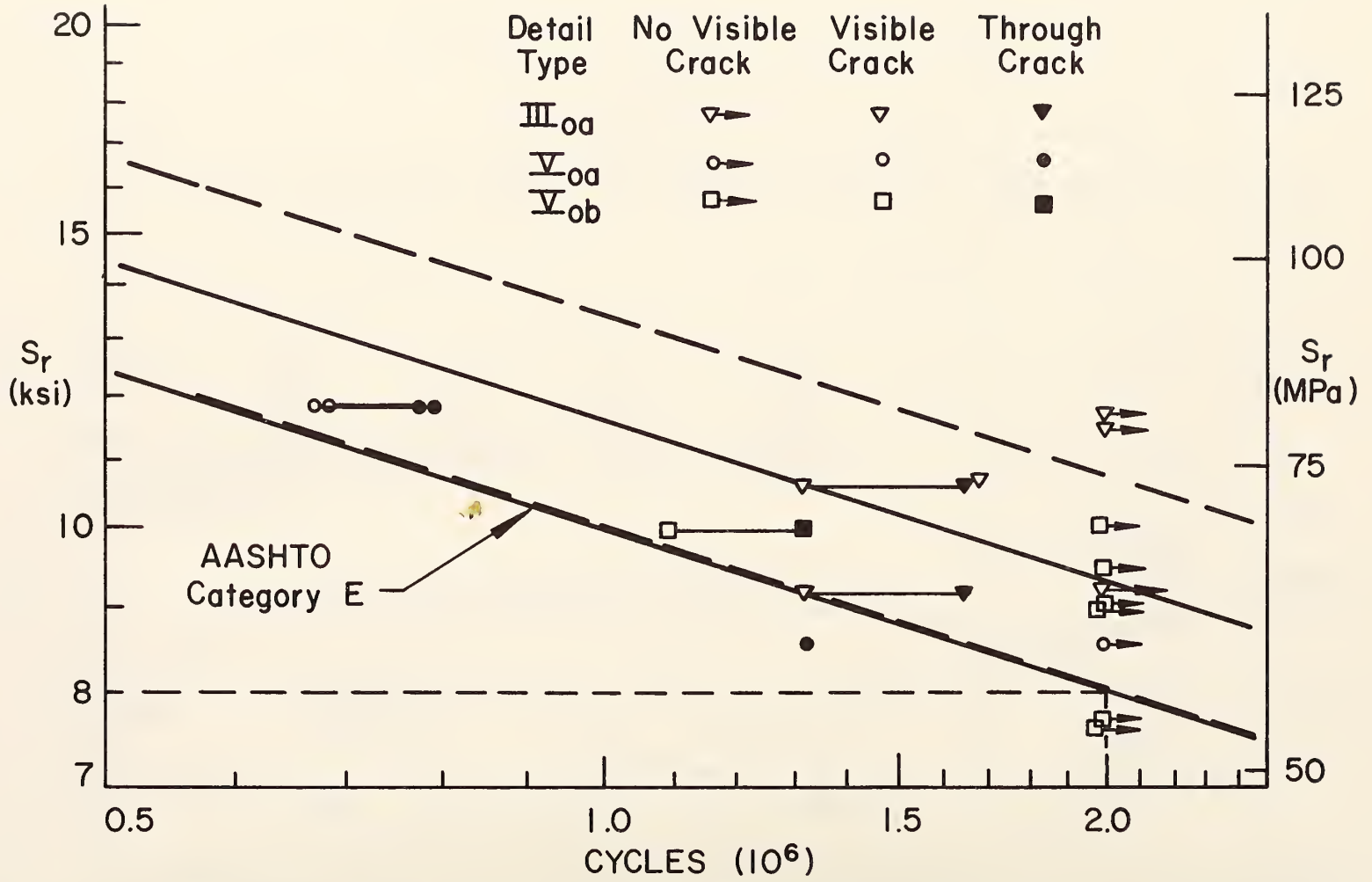

Fig. 72 Fatigue Results - Assembly 4 Category E Details

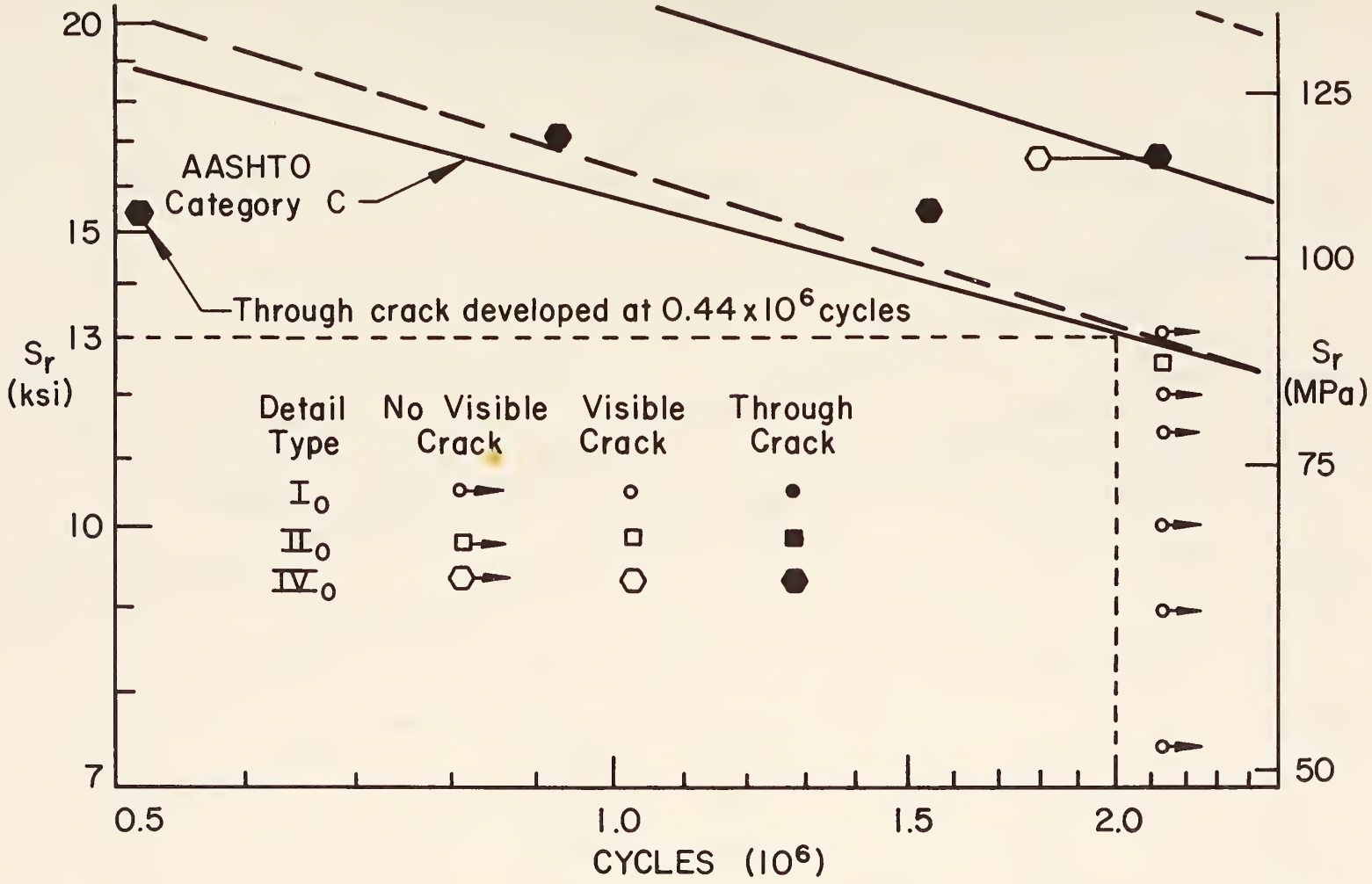

Fig. 73 Fatigue Results - Assembly 5 Category C Details

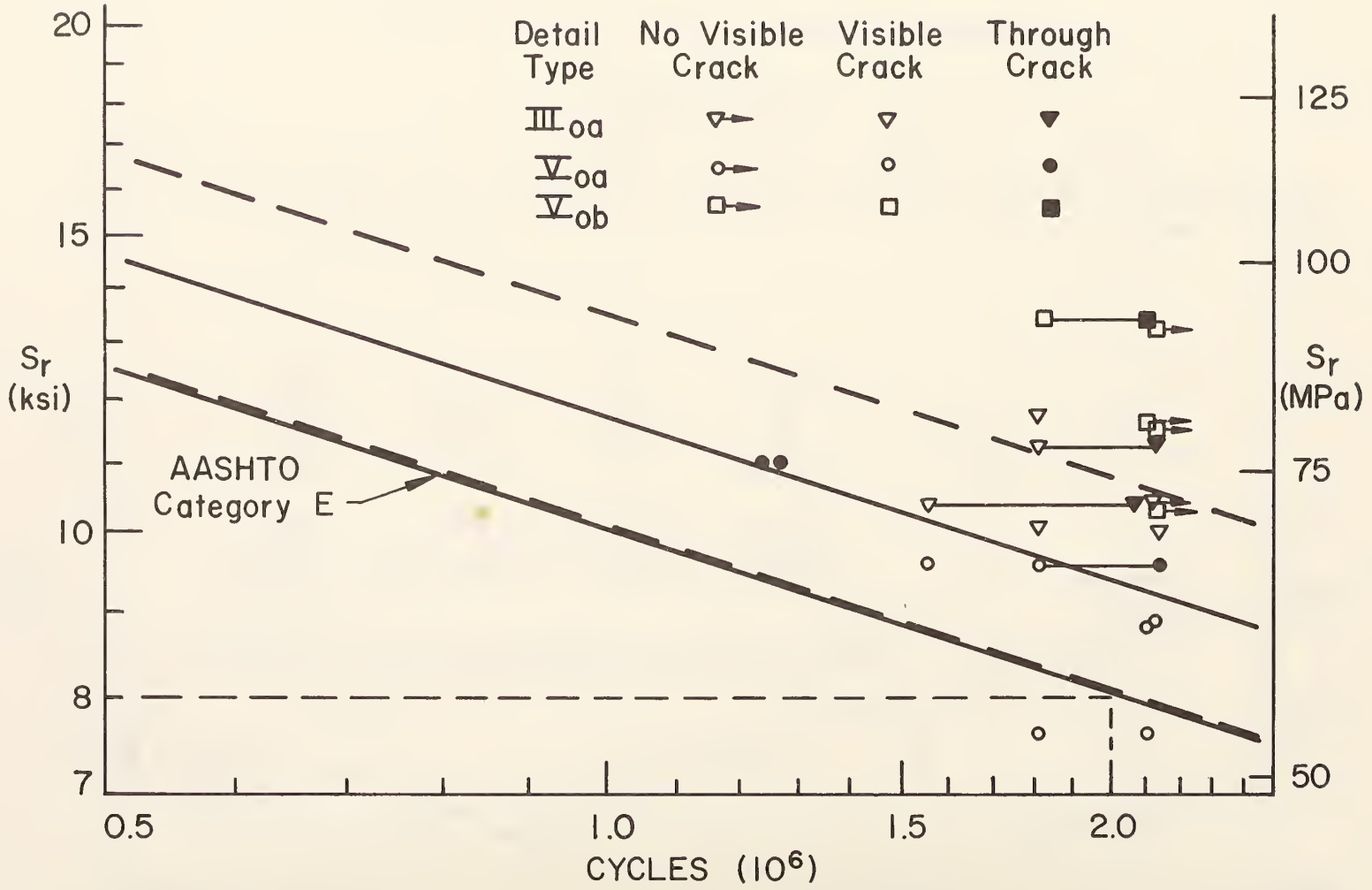

Fig. 74 Fatigue Results - Assembly 5 Category E Details

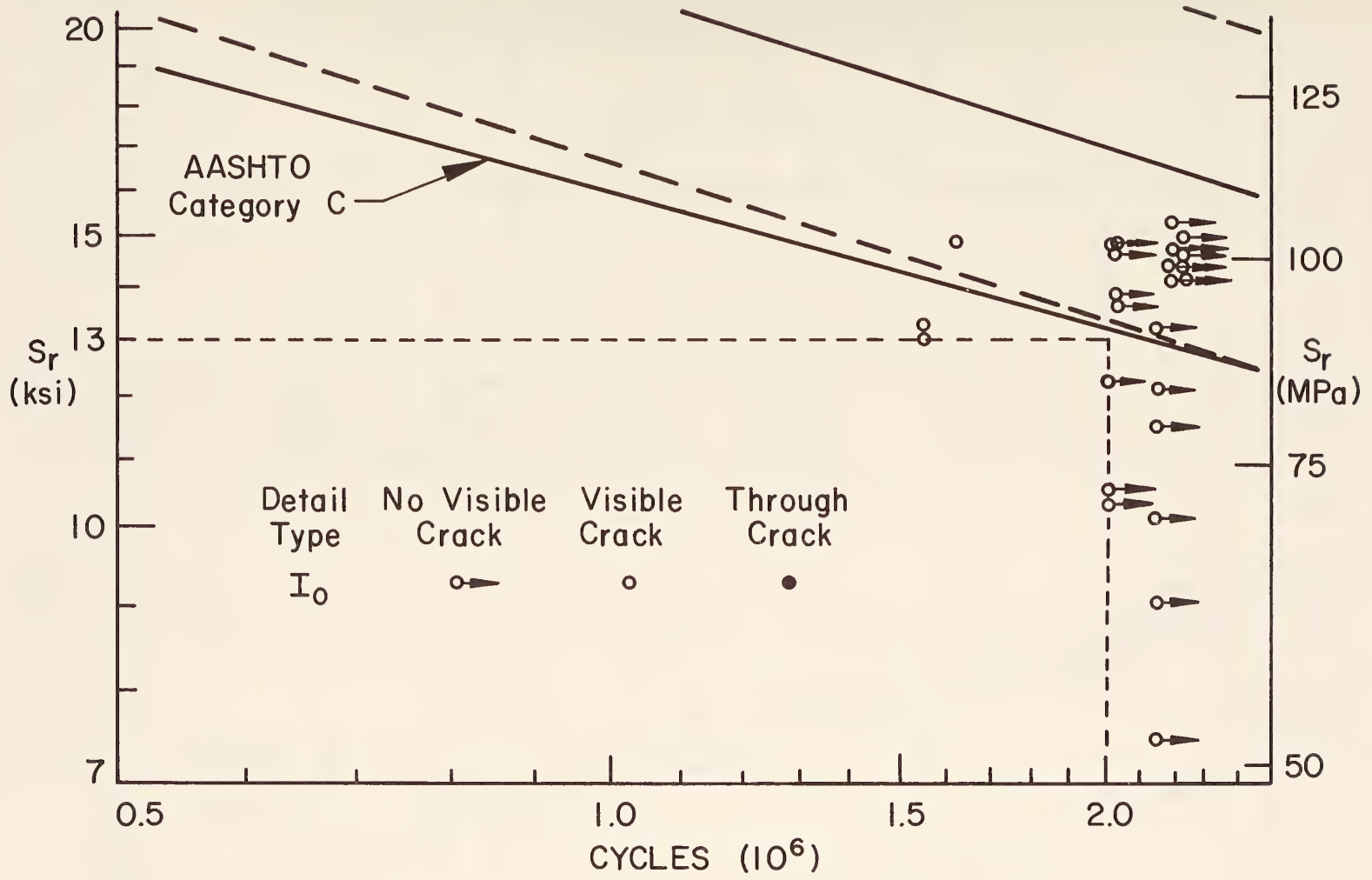

Fig. 75 Fatigue Results - Type I_o Details

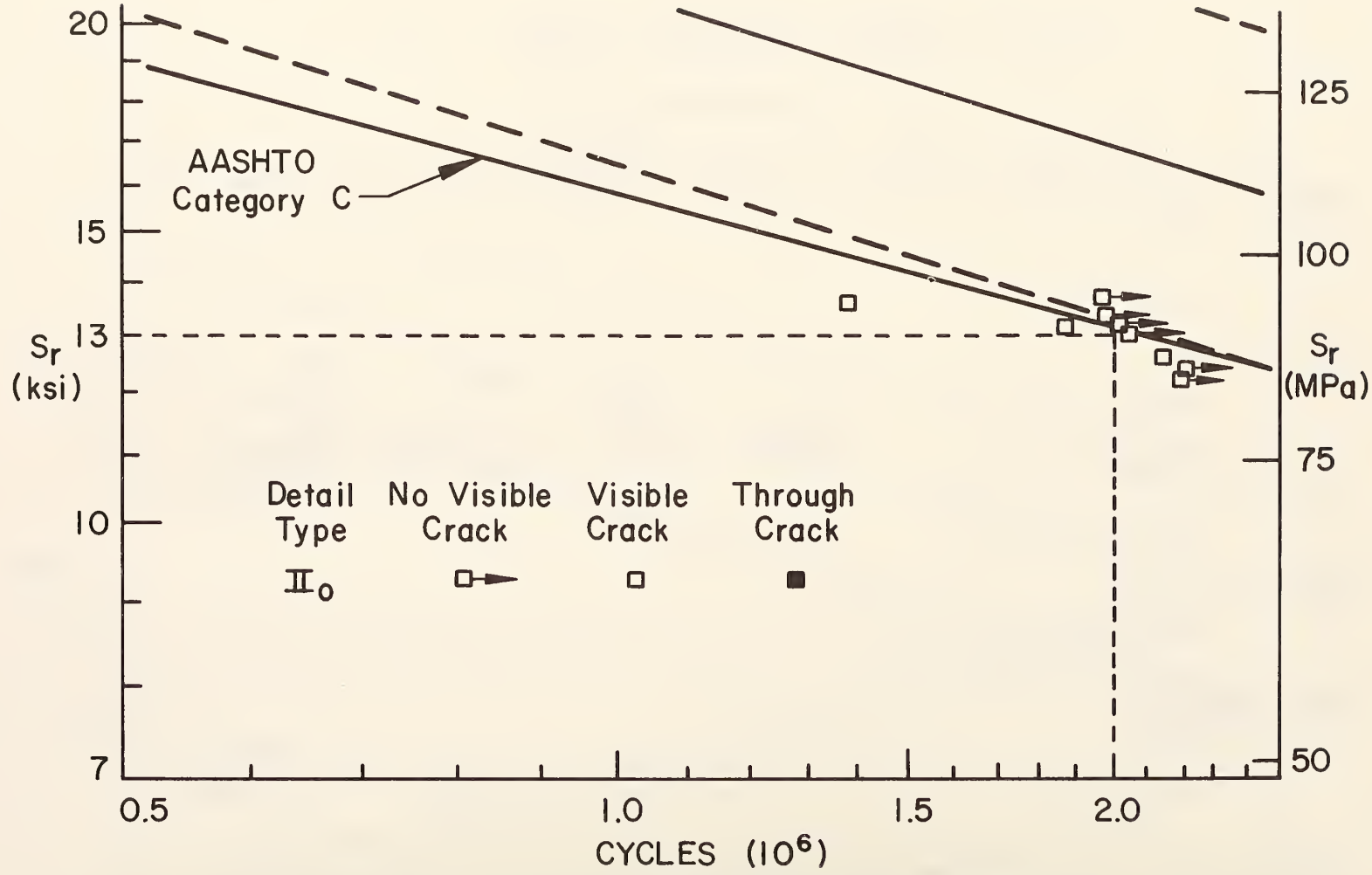

Fig. 76 Fatigue Results - Type II_o Details

The two open symbols at 1.52 million cycles on Fig. 75 represent two visible cracks which formed in the weld metal near the bottom of the web vertical weld on two separate type I_o details. No visible flaws exist at the two locations and the cracks did not grow through the web thickness.

7.2 Detail Type II_o

The fatigue results for type II_o details on all five assemblies are presented in Fig. 76. The type II_o detail is not affected by torsion normal stresses introduced by the curvature when a curved girder is loaded because the detail is welded only to the web. Thus the behavior of a type II_o detail on a curved girder should not differ from its behavior on a straight girder. Fatigue cracks due to out-of-plane bending of the web (Art. 6.2) are not included in the figure.

Six of the type II_o details in Fig. 76 are Group 2 details with no diaphragm members attached to them. Each of these cut-short stiffeners had a 25.4 mm (1 in.) gap between the detail and the bottom flange. Two of these stiffeners had visible fatigue cracks. They did not develop into through-thickness cracks during the two million load cycles.

Three type II_o details in Fig. 76 are Group 1 details with diaphragm members attached. The bottoms of these transverse stiffeners were flush with the top surface of the bottom flange. Only one developed a visible fatigue crack after two million load cycles.

The three Group 1 type II_o details discussed in Art. 6.2 experienced high bending stresses out of the plane of the web. The out-of-plane deformation of the web took place in the 25.4 mm (1 in.) gap between the detail bottom and the top surface of the bottom flange. The diaphragm member forces (Table 4) causing the out-of-plane deformation are higher than would be expected on curved girder assemblies with larger curvature radii or when a concrete slab is present[8]. Nevertheless, the early fatigue cracking on Assemblies 2 and 3, and an analytical study on the cut-short transverse stiffeners on curved box girder assemblies indicate that early fatigue cracking can be expected to occur whenever lateral displacement is allowed to occur between the cut-short stiffener and the flange[14].

In the curved plate girder assembly tests a type II_o detail lacking either the gap or the connection to diaphragm members exhibits a fatigue strength comparable to the straight girder Category C. Thus the AASHTO straight girder Category C is applicable to type II_o details not experiencing secondary fatigue cracking on curved plate girders.

7.3 Detail Types III_{oa} and III_{ob}

Figure 77 presents the III_{oa} and III_{ob} detail test results for all five assemblies. Just as for type II_o, these web details on a curved girder should behave as though they existed on a straight girder. Although the stress ranges varied from 51.7 MPa (7.5 ksi) to 80.7 MPa (11.7 ksi) a majority of the results lie within the 95 percent

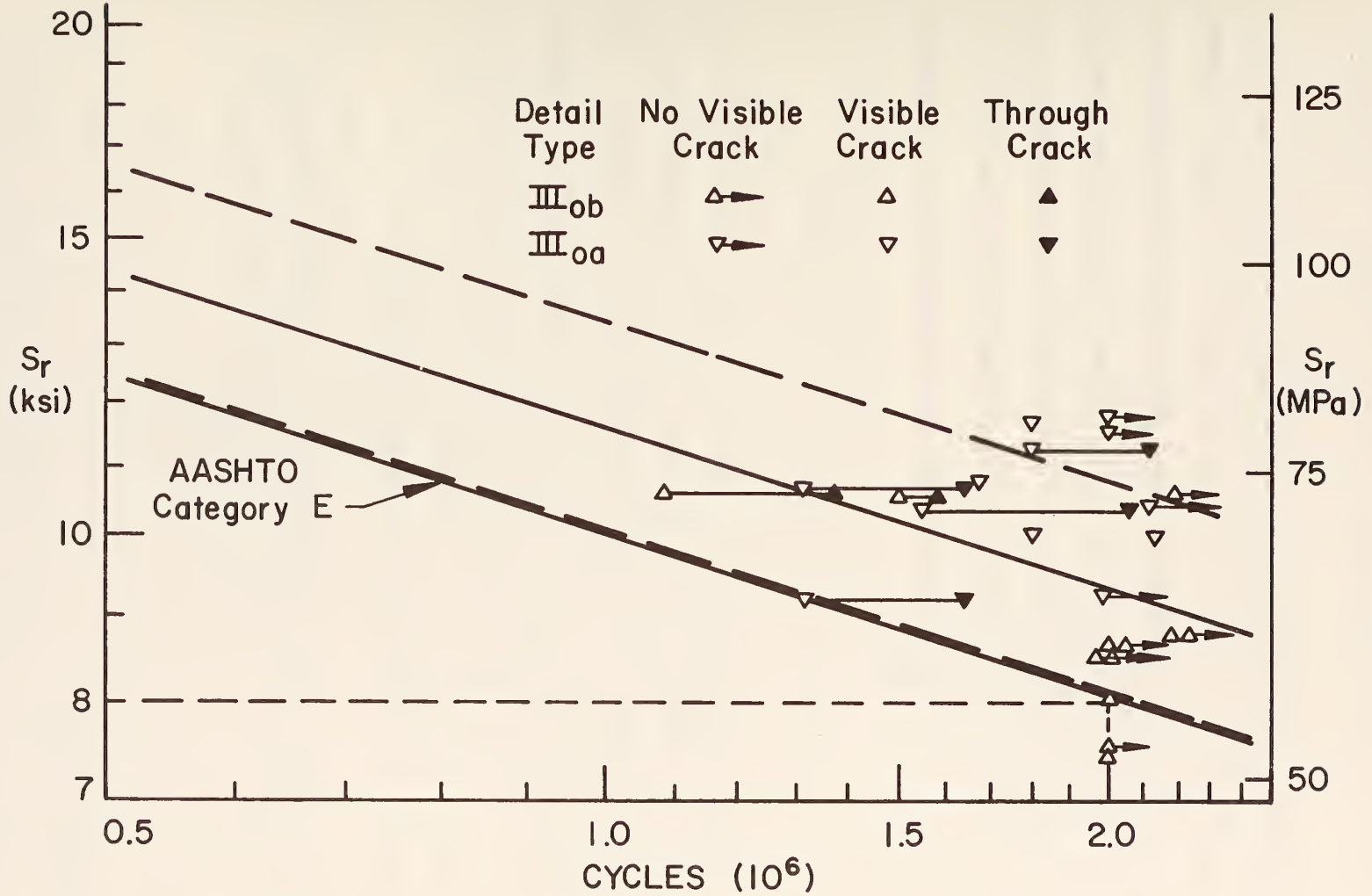

Fig. 77 Fatigue Results - Type III_{oa} and III_{ob} Details

confidence limits in Fig. 77. Only one visible crack at a type III_{ob} detail lies below the AASHTO Category E curve.

The discussion in Art. 6.2 concerning the modified type III_{oa} detail demonstrates the importance of welding the longitudinal gusset plate to the transverse stiffener. Assembly 5 was to have three details similar to type III_{oa} but without the welds joining the gusset plates to the transverse stiffener. Such a detail is labelled III_{ob} in Table 3 of Ref. 8. A fabrication error resulted in those gusset plates being type III_{oa}. It was necessary to modify only the one type III_{oa} detail to note the reduction in fatigue life of the web (Art. 6.2) in the cope area due to out-of-plane web displacement.

All type III_{oa} details on Assemblies 4 and 5 had a bottom lateral bracing member bolted to at least one of the gusset plates. All III_{ob} gusset plates were Group 2 details with no attachments. The distribution of type III_{oa} and III_{ob} fatigue cracks in Fig. 77 demonstrates that apparently the bottom lateral bracing forces (Table 5) have little if any effect on the fatigue life as long as type III_{oa} gusset plates are welded to the transverse stiffener.

The fatigue results plotted in Fig. 77 demonstrate that the AASHTO straight girder Category E is applicable to type III_{oa} and III_{ob} gusset plates on curved plate girders.

7.4 Detail Type IV_o

Fatigue test results for all type IV_o details are plotted in Fig. 78. These groove-welded gusset plates with circular transitions

demonstrate a wide range of ability to achieve the fatigue strength of a Category C detail.

All but three of the visible or through-thickness cracks lie within the 95 percent confidence limits in Fig. 78. The three fatigue cracks falling below the AASHTO Category C allowable stress range curve are at locations a and f on Assembly 4 and location cc on Assembly 5 (Figs. 56 and 57). The fatigue life of two of the three early fatigue cracks is only a small fraction of the expected life. This is cause for further investigation and discussion.

7.4.1 Fatigue Life Prediction

Visible surface flaws were observed at the locations of the three early fatigue cracks. The fatigue test results provide the number of cycles, N, to form a through (edge) crack in the flange. This information coupled with a model of crack shape can be used to estimate the initial crack size causing a through-thickness crack after N number of cycles at a measured stress range, S_r.

The fatigue life calculation requires integration of a crack growth rate equation. Reference 17 provides the crack growth rate equation and the unified stress intensity correction factors required for performing a numerical life integration.

Table 12 contains the calculated estimates of initial crack size, a_i and b_i, for two different crack growth shapes at four type IV_o details. Location ee is included because it falls almost directly on the 95 percent confidence limit curve in Fig. 78. The assumed crack

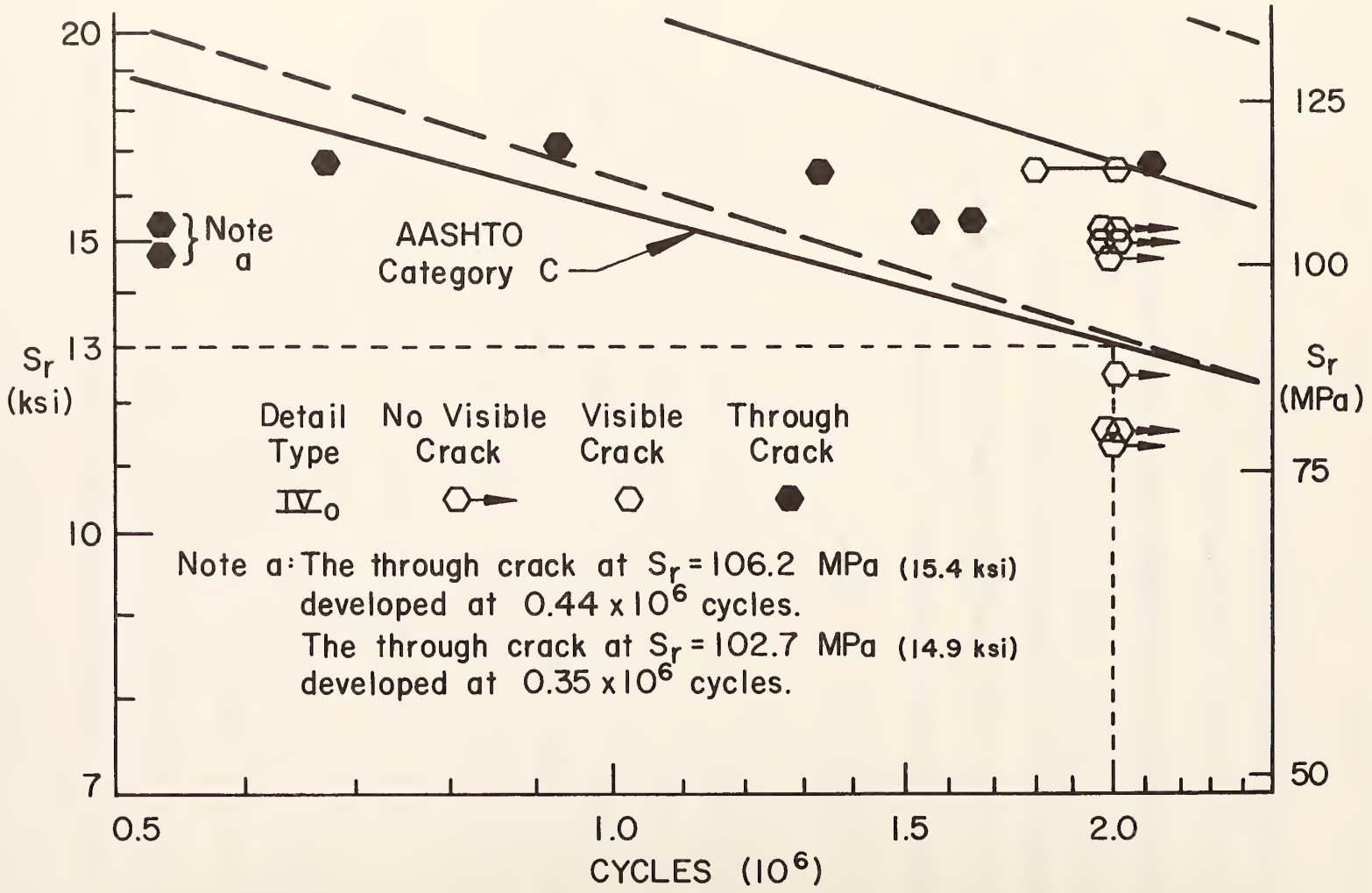

Fig. 78 Fatigue Results - Type IV$_o$ Details

Table 12 Estimated Initial Crack Sizes From Fatigue Life Predictions - Type IV_o Details

Assembly		4	4	5	5
Girder		1	1	2	2
Crack Location		a	f	cc	ee
Measured S_r	MPa (ksi)	114.5 (16.6)	102.7 (14.9)	106.2 (15.4)	117.2 (17.0)
t_f	mm (in.)	12.7 (0.5)	12.7 (0.5)	25.4 (1)	25.4 (1)
N (millions of cycles for through edge crack), actual		0.680	0.350	0.440	0.930
Quarter-Ellipse					
Estimated a_i	mm (in.)	0.13 (0.005)	0.10 (0.004)	1.32 (0.052)	0.33 (0.013)
Estimated b_i		12.55 (0.494)	12.19 (0.480)	20.47 (0.806)	15.47 (0.609)
Semi-Ellipse					
Estimated a_i	mm (in.)	0.53 (0.021)	1.27 (0.050)	3.05 (0.120)	0.81 (0.032)
Estimated $2b_i$		8.08 (0.318)	10.01 (0.394)	14.58 (0.574)	8.81 (0.347)

growth models are either a quarter-elliptical corner crack shape or a semielliptical crack shape. A recent straight girder experimental program including groove-welded gusset plates with circular transitions produced Eq. 1 for quarter-elliptical crack growth[18].

$$b = 19.36\ a^{0.202} \qquad b,a - mm$$
$$(b = 1.465\ a^{0.202}) \qquad (b,a - in.) \tag{1}$$

Since the visible flaws in the circular transitions on Assemblies 4 and 5 were located at about mid-thickness of the flange and did not develop as corner cracks a crack shape equation for semielliptical surface cracks was taken from the work of Maddox[19]. The equation for semielliptical crack growth is as follows:

$$b = 3.355 + 1.29\ a \qquad b,a - mm$$
$$(b = 0.1321 + 1.29\ a) \qquad (b,a - in.) \tag{2}$$

In Eqs. 1 and 2 a is the semi-minor axis (edge crack depth) and b is the semi-major axis (edge crack surface length). The fatigue crack becomes a through-thickness crack when b equals the flange thickness, t_f, for a quarter-elliptical crack or when 2 b equals t_f for a semi-elliptical crack.

The estimated initial crack sizes for each location presented in Table 12 differ for the two assumed crack shapes. However, the visible surface crack length of b and 2 b for the quarter- and semi-elliptical shapes, rèspectively, are about the same order of magnitude.

7.4.2 Actual Flaws

The actual visible flaws at locations a, f, and cc are neither quarter-elliptical nor semielliptical in shape. The Group 1 type IV_o details, groove welded by the fabricator, were ground to a smooth circular transition just prior to testing. The grinding uncovered two visible flaws or pits in the groove welds near the termination of the circular transitions (locations a and f on Assembly 4). The flaws were about 2.54 mm (0.1 in.) deep and between 2.54 (0.1 in.) and 7.62 mm (0.3 in.) in surface length. The sizes of the actual flaws agree fairly well with the estimated initial crack sizes at locations a and f in Table 12.

Location cc on Assembly 5 is one end of a Group 2 type IV_o detail. These details were welded to the flange tip by initially placing a fillet weld on the underside of the gusset plate. This weld held the gusset plate while several weld passes were made to form a full-penetration groove weld. Upon completion of welding the ends of the weld were ground smooth to conform to the circular transition. At location cc the grinding did not penetrate to the small fillet weld on the underside of the gusset plate. Thus a tunnel-like flaw remained in the weld metal near the termination of the circular transition. The flaw was about 2.54 mm (0.1 in.) deep and 5.08 mm (0.2 in.) long.

Location ee on Assembly 5 did not have a visible surface flaw. The estimated initial flaw (Table 12) could actually be just beneath the surface where additional grinding may uncover it. The flaws at locations a and f on Assembly 4 were beneath the surface until the

grinding exposed them. Thus it is conceivable that a substantial hidden flaw exists at location ee as predicted by the fatigue life calculation.

7.4.3 Summary - Type IV_o Detail

Analytical studies of groove-welded gusset plates with circular transition radius r, have shown that the maximum stress concentration occurs a distance of about r/5 from the point-of-tangency[17, 20]. The fatigue cracks in Fig. 78 which are not a result of visible flaws are all located 25.4 mm (1 in.) to 38.1 mm (1.5 in.) from the point-of-tangency for the transition radius of 152.4 mm (6 in.). The visible flaws discussed previously also happened to be located near this region of maximum stress concentration which thus compounded the severity of the flaws.

The fatigue life predictions (Table 12) provide initial crack size estimates whose magnitudes are about the size of the actual surface flaws at the three type IV_o details experiencing early fatigue cracking. The elimination of such large weld flaws would substantially extend the fatigue life of the detail. Only through careful fabrication and inspection techniques can the flaw size be reduced to a size where the circular transition groove-welded gusset plate can be classified an AASHTO Category C detail.

7.5 Detail Type V_{oa}

Fatigue test results for all the type V_{oa} details are plotted in Fig. 79. Only three visible fatigue cracks and one through-

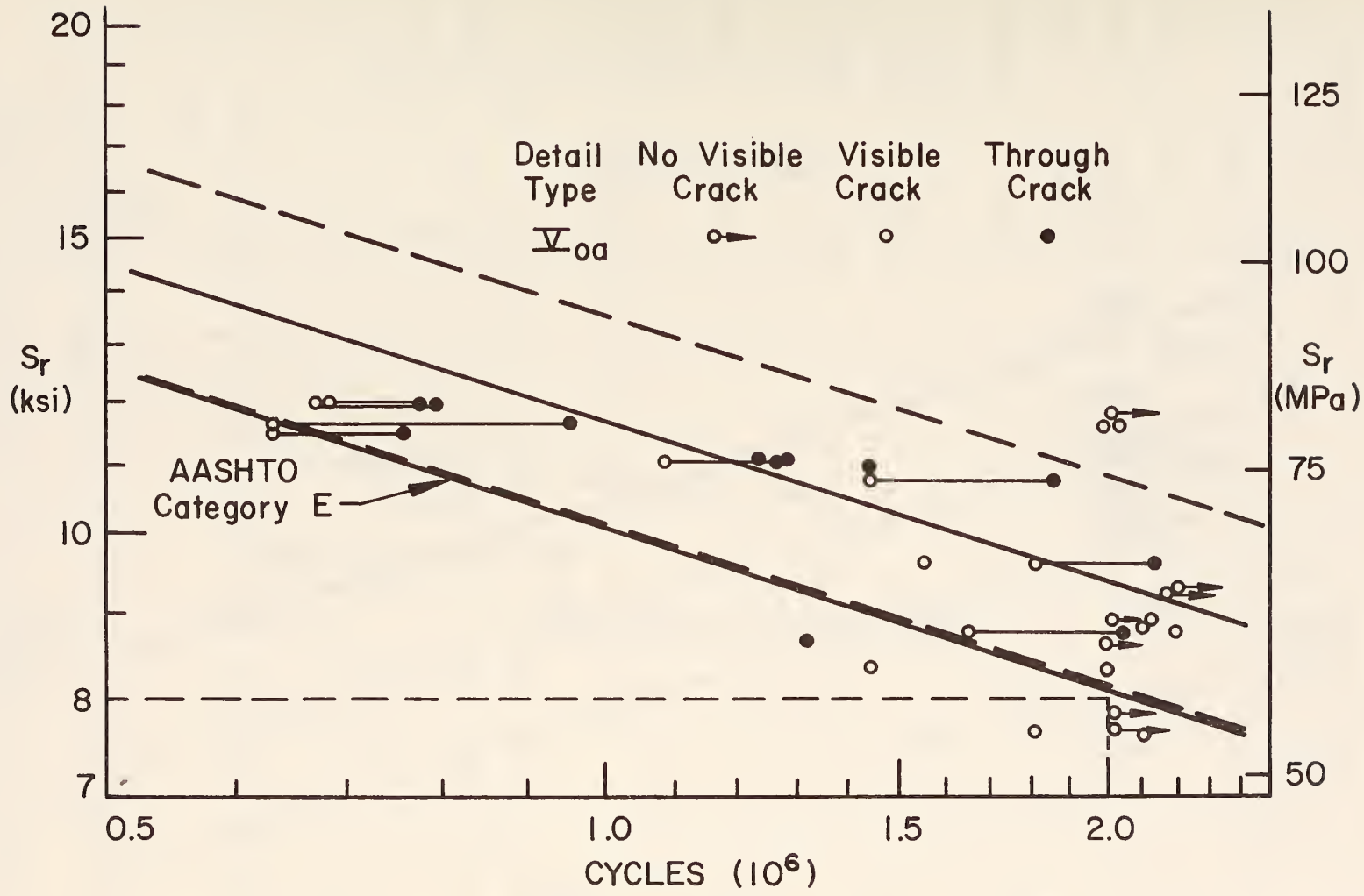

Fig. 79 Fatigue Results - Type V_{oa} Details

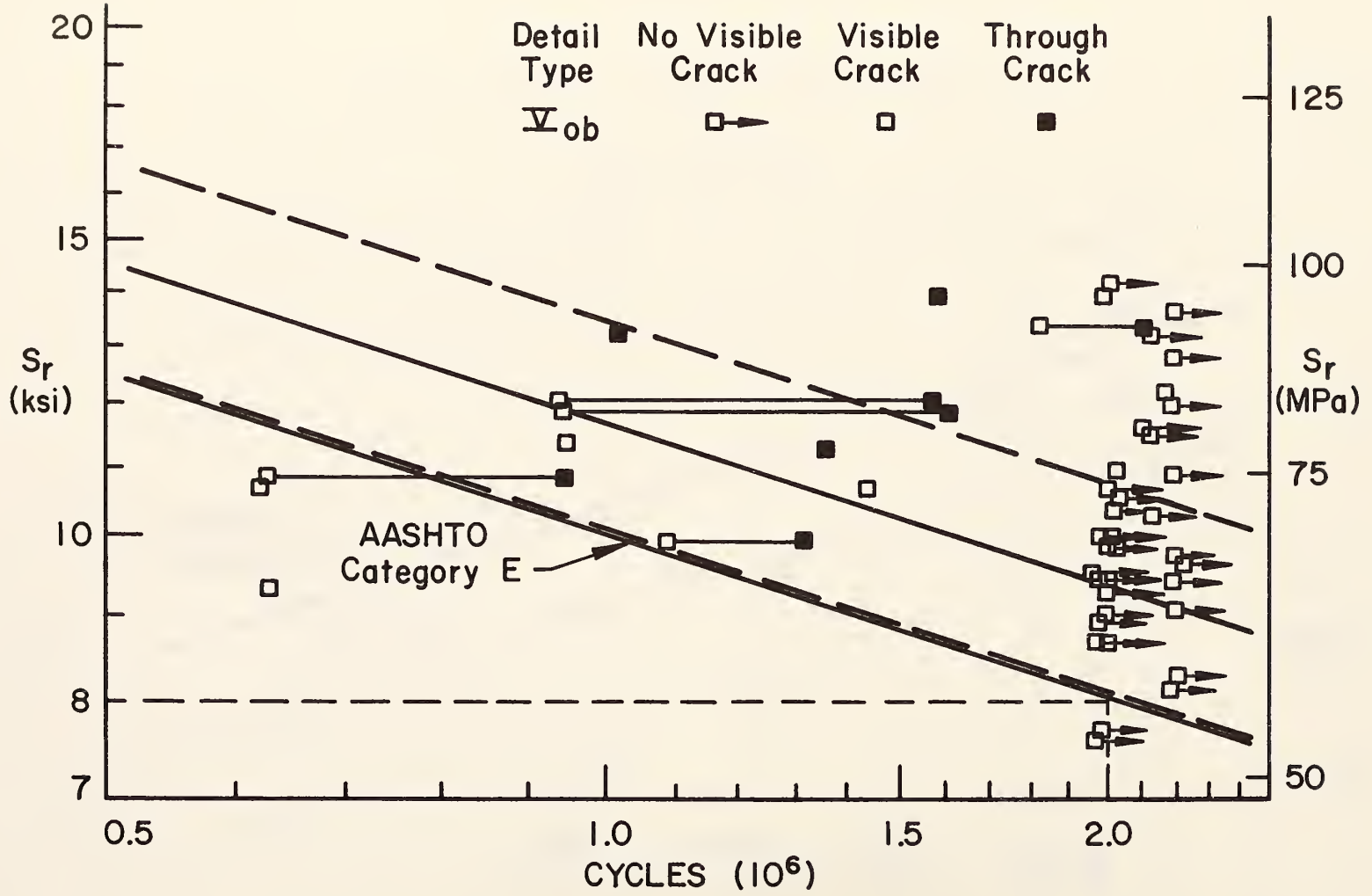

Fig. 80 Fatigue Results - Type V_{ob} Details

thickness crack are below the straight girder AASHTO Category E allowable stress range curve. The through-thickness crack falling below the Category E curve developed at location j on Assembly 4 (Fig. 56). A close visual inspection of the crack location reveals no apparent surface flaw from which the crack grew. No strain gage was mounted adjacent to location j but the symmetric location g on the west end of Assembly 4 was gaged. The measured stress range at g is assigned to location j in plotting the fatigue crack. The actual stress range at j could have been higher than the measured stress range at g. Thus the through-thickness crack at location j could have actually experienced a stress range above the allowable stress range curve or it could be one of the fatigue failures which statistically does not lie above the 95 percent survival line. In either case the AASHTO straight girder Category E is applicable to the type V_{oa} details on the curved plate girder test assemblies.

The type V_{oa} details attached to the flanges by the fabricator (Group 1 details) had the backup bars removed after completing the groove welds. The backup bars on the Group 2 type V_{oa} details remained in place during the fatigue testing. The distribution of fatigue cracks at Group 1 and Group 2 type V_{oa} details is such that the backup bar's presence apparently had no influence on the fatigue strength of the details.

7.6 Detail Type V_{ob}

Fatigue test results for all type V_{ob} details are plotted in Fig. 80. A large percentage of the potential crack locations either

have only a visible crack or have no visible crack after two million load cycles. Eight locations developed through-thickness cracks. Many of the uncracked locations experienced stress ranges far above the Category E allowable stress range curve. Thus the type V_{ob} details on the curved plate girder test assemblies are adequately described by the AASHTO straight girder Category E.

The two visible cracks at 640,000 cycles in Fig. 80 were located in the fillet weld metal and not in the flange metal. Apparently a flaw existed in the weld metal such that its stress concentration overshadowed the usually critical stress concentration at the fillet weld toe. The weld metal cracks did not visibly increase in surface length during the remainder of the fatigue testing.

7.7 Web Fatigue Strength

No web boundary weld cracks were discovered during the fatigue testing of the five curved plate girder assemblies. The web slenderness ratios and transverse stiffener spacings were within prescribed AASHTO and CURT allowable stress design provisions in some instances and exceeded them in others[7,8,9]. The satisfactory performance of the webs without fatigue cracks suggests that the allowable stress range design provisions are adequate with respect to fatigue strength.

The web deflections presented in Table 11 are measured relative to the top and bottom web-flange junctions. The total web movement under load is composed of these deflections superimposed on lateral flange raking. Although extensive web deflections were measured (Art.

6.3), flange raking was only measured by the horizontal deflection dial gages between diaphragms on Assemblies 1, 3, and 4 (Fig. 24). Under 445 kN (100 kip) jack loads, the measured relative lateral displacements between top and bottom flanges range from 2.5 mm (0.10 in.) to 13.7 mm (0.54 in.). The combination of this flange raking and the web deflections introduces plate bending stresses at the web boundaries. Analyses with and without a composite slab show that these displacements and the corresponding plate bending stresses are slightly higher in an assembly when no slab is present[8]. Therefore, the web movements and stresses on the assemblies without a deck are probably more severe than but characteristic of webs on in-service curved plate girder composite highway bridges. Reference 21 contains a theoretical study of web boundary stresses on curved plate girders with and without a deck.

The oil-canning deflections and flange raking have all been measured under static load conditions. The static deflections are representative of web movements during cyclic loading since the assemblies were designed so that inertial forces are minimized and resonance avoided[8]. An analysis could be made of each web panel using the measured static deflections to estimate the plate bending stresses at the web boundaries and then to evaluate the web fatigue strength [22]. More significant is the result that no web boundary weld cracks were discovered even in cases where web slenderness ratios and web aspect ratios are beyond the AASHTO and CURT limits.

8. SUMMARY AND CONCLUSIONS

The primary intent of this phase of the investigation of curved girder fatigue is to evaluate the fatigue performance of welded details on curved plate girders. Five types of AASHTO Category C and Category E welded details have been observed during the testing of five curved plate girder assemblies. Each assembly has been subjected to approximately two million load cycles under one of two loading conditions.

Based on the observation of primary and secondary fatigue cracking the following conclusions are reached:

(1) AASHTO Category C and Category E welded details were evaluated in this fatigue testing program. The fatigue behavior of these welded details, when placed on curved plate girders, is adequately described by the present AASHTO design guidelines for straight girders.

(2) Type II_o detail - When a cut-short transverse stiffener is part of a diaphragm-to-girder connection, displacement induced web stresses in the gap beneath the stiffener can create fatigue problems. Such web stiffeners should be extended to the bottom flange and welded to the flange at least on the side of the lower stressed flange tip.

(3) Type III_o detail - Displacement induced web stresses also create a fatigue problem in the cope of a longitudinal gusset plate when the gusset is located at a diaphragm connection. A gusset plate coped to fit adjacent to a transverse stiffener should be welded to the stiffener to eliminate out-of-plane web bending stresses in the coped region.

(4) Type IV_o detail - Typical fabrication techniques apparently leave relatively large flaws at the termination of circular transitions. Thereby the beneficial effect of a large radius is essentially negated. Strict enforcement of inspection requirements would tend to alleviate the problem and permit such an attachment to be used as a Category C detail.

(5) The fatigue performance of webs with slenderness ratios of 139 to 192 was satisfactory. The present AASHTO allowable stress provisions for web slenderness ratios and transverse stiffener spacings are adequate with respect to fatigue strength of webs. Thus the more conservative CURT web provisions are overly stringent.

9. RECOMMENDATIONS FOR FURTHER WORK

The results of the fatigue testing of five curved plate girder assemblies indicate a need for additional studies in the following areas:

(1) The use of cut-short transverse stiffeners (type II_o detail) where lateral displacement is allowed to occur between the stiffener and the flange can be expected to cause early fatigue cracking. Furthur studies are needed to provide a suitable connection of the cut-short stiffener to the bottom flange in areas where the flange tip stresses prohibit direct attachment to the flange. The $\perp$-type connection shown in Fig. 26 is one possibility.

(2) The existence of relatively large flaws at the termination of circular transitions on several type IV_o groove-welded details indicates a need for further studies on improving fabrication and inspection techniques on such details.

(3) Fatigue crack shapes and sizes were not recorded as a part of this fatigue testing program. The applicability of fatigue life predictions to welded details on curved girders cannot be determined until actual initial flaw sizes and crack growth shapes are established. Further studies should include the inspection of existing fatigue cracks on curved girders to determine crack growth behavior in the stress fields present in curved highway bridges.

10. REFERENCES

1. Brennan, P. J.
   ANALYSIS FOR STRESS AND DEFORMATION OF A HORIZONTALLY CURVED GIRDER BRIDGE THROUGH A GEOMETRIC STRUCTURAL MODEL, Syracuse University Report submitted to the New York State Department of Transportation, August 1970.

2. Culver, C.
   DESIGN RECOMMENDATIONS FOR CURVED HIGHWAY BRIDGES, Carnegie-Mellon University Report submitted to the Pennsylvania Department of Transportation, June 1972.

3. Heins, C. P. and Siminou, J.
   PRELIMINARY DESIGN OF CURVED GIRDER BRIDGES, AISC Engineering Journal, Vol. 7, No. 2, April 1970.

4. Heins, C. P.
   DESIGN DATA FOR CURVED BRIDGES, C.E. Report No. 47, University of Maryland, March 1972.

5. U. S. Steel
   ANALYSIS AND DESIGN OF HORIZONTALLY CURVED STEEL BRIDGE GIRDERS, United States Steel Structural Report ADUCO 91063, May 1963.

6. Colville, J.
   SHEAR CONNECTOR STUDIES ON CURVED GIRDERS, C.E. Report No. 45, University of Maryland, February 1972.

7. CURT
   TENTATIVE DESIGN SPECIFICATIONS FOR HORIZONTALLY CURVED HIGHWAY BRIDGES, Part of Final Report, Research Project HPR-2(111) "Horizontally Curved Highway Bridges", CURT, March 1975.

8. Daniels, J. Hartley, Zettlemoyer, N., Abraham, D. and Batcheler, R. P.
   FATIGUE OF CURVED STEEL BRIDGE ELEMENTS - ANALYSIS AND DESIGN OF PLATE GIRDER AND BOX GIRDER TEST ASSEMBLIES, FHWA Report No. DOT-FH-11-8198.1, NTIS, Springfield, Va. 22161, August 1979.

9. AASHTO STANDARD SPECIFICATION FOR HIGHWAY BRIDGES
   American Association of State Highway and Transportation Officials, Washington, D. C., 1977.

10. AASHTO INTERIM SPECIFICATIONS - BRIDGES, 1978 American Association of State Highway and Transportation Officials, Washington, D. C., 1978.

11. Brennan, P. J. and Mandel, J. A.
    USER'S PROGRAM FOR 3-DIMENSIONAL ANALYSIS OF HORIZONTALLY CURVED BRIDGES, Department of Civil Engineering, Syracuse University, Syracuse, N. Y., December 1974.

12. Powell, G. H.
CURVBRG, A COMPUTER PROGRAM FOR ANALYSIS OF CURVED OPEN GIRDER BRIDGES, University of California, Berkeley, presented at Seminar and Workshop on Curved Girder Highway Bridge Design, Boston, Ma., June 12-13, 1973.

13. Thurlimann, B. and Eney, W. J.
MODERN INSTALLATION FOR TESTING OF LARGE ASSEMBLIES UNDER STATIC AND FATIGUE LOADING, Proceeding of the SESA, Vol. 16, No. 2, 1959.

14. Inukai, G. J.
STRESS HISTORY STUDY ON A CURVED BOX BRIDGE, M.S. Thesis, Lehigh University, Bethlehem, Pa., May 1977.

15. Fisher, John W., Albrecht, P. A., Yen, B. T., Klingerman, D. T. and McNamee, B. M.
FATIGUE STRENGTH OF STEEL BEAMS WITH WELDED STIFFENERS AND ATTACHMENTS, NCHRP Report No. 147, Transportation Research Board, National Research Council, Washington, D. C., 1974.

16. Fisher, John W., Frank, K. H., Hirt, M. A. and McNamee, B. M.
EFFECT OF WELDMENTS OF THE FATIGUE STRENGTH OF STEEL BEAMS, NCHRP Report No. 102, Highway Research Board, National Academy of Sciences - National Research Council, Washington, D. C., 1970.

17. Zettlemoyer, N.
STRESS CONCENTRATION AND FATIGUE OF WELDED DETAILS, Ph.D. Dissertation, Lehigh University, Bethlehem, Pa., October 1976.

18. Boyer, K. D., Fisher, John W., Irwin, G. R., Roberts, R., Krishna, G. V., Morf, U., and Slockbower, R. E.
FRACTURE ANALYSES OF FULL SIZE BEAMS WITH WELDED LATERAL ATTACHMENTS, Fritz Engineering Laboratory Report No. 399-2(76), Lehigh University, Bethlehem, Pa., April 1976.

19. Maddox, S. J.
AN ANALYSIS OF FATIGUE CRACKS IN FILLET WELDED JOINTS, International Journal of Fracture Mechanics, Vol. 11, No. 2, April 1975, p. 221.

20. Batcheler, R. P.
STRESS CONCENTRATION AT GUSSET PLATES WITH CURVED TRANSITIONS, CE 103 Report, Lehigh University, Bethlehem, Pa., May 1975.

21. Daniels, J. Hartley and Batcheler, R. P.
FATIUGE OF CURVED STEEL BRIDGE ELEMENTS - EFFECT OF HEAT CURVING ON THE FATIGUE STRENGTH OF PLATE GIRDERS, FHWA Report No. DOT-FH-11-8198.5, NTIS, Springfield, Va. 22161, August 1979

22. Mueller, J. A. and Yen, B. T.
GIRDER WEB BOUNDARY STRESSES AND FATIGUE, Welding Research Council Bulletin No. 127, January 1968.

23. Zettlemoyer, N., Fisher, John W. and Daniels, J. Hartley
FATIGUE OF CURVED STEEL BRIDGE ELEMENTS - STRESS CONCENTRATION, STRESS RANGE GRADIENT AND PRINCIPAL STRESS EFFECTS ON FATIGUE LIFE, FHWA Report No. DOT-FH-11-8198.2, NTIS, Springfield, Va. 22161, August 1979.

APPENDIX A: STATEMENT OF WORK

"Fatigue of Curved Steel Bridge Elements"

OBJECTIVE

The objectives of this investigation are: (1) to establish the fatigue behavior of horizontally curved steel plate and box girder highway bridges, (2) to develop fatigue design guides in the form of simplified equations or charts suitable for inclusion in the AASHTO Bridge Specifications, and (3) to establish the ultimate strength of curved steel plate and box girder highway bridges.

DELINEATION OF TASKS

Task 1 - Analysis and Design of Large Scale Plate Girder and Box Girder Test Assemblies

Horizontally curved steel plate and box girder bridge designs will be classified on the basis of geometry (radius of curvature, span length, number of span, girders per span, diaphragm spacing, types of stiffener details, type of diaphragm, web slenderness ratios and loading conditions). This will be accomplished through available information from existing literature and other sources, as required.

Current research on the fatigue strength of straight girders has identified and classified those welded details susceptible to fatigue crack growth. This classification shall be extended to include critical welded details peculiar to curved open and closed girder bridges. These welded details shall be examined with respect to their susceptibility to fatigue crack growth and analyses shall be made to estimate the conditions for fatigue crack growth.

Based on the analyses described above, a selected number of representative open and closed section curved bridge girders shall be defined for purposes of performing in-depth analyses, designs, and laboratory fatigue tests of large scale test assemblies. These girders shall be typical and will characterize commonly used girders, to include the use of welded details. The assemblies shall be analyzed and designed using currently available design guides, methods, and/or computer programs. Each test assembly shall be designed to incorporate the maximum number of welded details susceptible to fatigue crack growth. Stresses in all components of the cross section shall be examined so that the significance of each stress condition can be evaluated. An assessment of the significance of flexural stress, principal stress, stress range and stress range gradient shall be determined at each welded detail. The significance of curved boundaries on the stresses shall be examined. Stress states in welded details equivalent to those used in straight girders shall be examined.

Curved plate and box girder test assemblies shall be designed so that ultimate strength tests can be carried out following the planned fatigue tests, with a minimum of modification.

Task 2 - Special Studies

In addition to but independent of the analyses and designs described in Task 1, certain other special studies shall be performed. These special studies are specifically directed towards those problems peculiar to curved girder bridges, as follows: (1) the significance

of a fatigue crack growing across the width of a flange in the presence of a stress range gradient shall be studied, (2) the effect of heat curving on the residual stresses and fatigue strength of welded details shall be examined, (3) newly suggested web slenderness ratios for curved girder webs reduce present slenderness ratios of unstiffened webs. These slenderness ratios shall be examined in terms of fatigue performance of curved webs, and (4) the effect of internal diaphragms in box beam structures will be examined with regard to fatigue behavior.

Task 3 - Fatigue Tests of Curved Plate Girder and Box Girder Test Assemblies

The plate and box girder test assemblies designed in Task 1 shall be tested in fatigue. Emphasis shall be placed on simulating full-scale test conditions. The test results shall be correlated with the analyses made in Task 1 and the results of the special studies performed in Task 2.

Task 4 - Ultimate Load Tests of Curved Plate and Box Girder Assemblies

Following the fatigue tests of Task 3, each plate and box girder test assembly shall be tested statically to determine its ultimate strength and mode of behavior. Fatigue cracks shall be repaired, where necessary, prior to the static tests. Consideration shall be given to providing a composite reinforced concrete slab on each test girder prior to the static tests.

Task 5 - Design Recommendations

Design recommendations for fatigue based on the analytical and experimental work shall be formulated in a manner consistent with that for straight girders. Specification provisions shall be formulated for presentation to the AASHTO Bridge Committee.

APPENDIX B: LIST OF REPORTS PRODUCED UNDER DOT-FH-11-8198

"Fatigue of Curved Steel Bridge Elements"

Daniels, J. Hartley, Zettlemoyer, N., Abraham, D. and Batcheler, R. P.
ANALYSIS AND DESIGN OF PLATE GIRDER AND BOX GIRDER TEST ASSEMBLIES, DOT-FH-11-8198.1, August 1979.

Zettlemoyer, N., Fisher, John W. and Daniels, J. Hartley
STRESS CONCENTRATION, STRESS RANGE GRADIENT AND PRINCIPAL STRESS EFFECTS ON FATIGUE LIFE, DOT-FH-11-8198.2, August 1979.

Daniels, J. Hartley and Herbein, W. C.
FATIGUE TESTS OF CURVED PLATE GIRDER ASSEMBLIES, DOT-FH-11-8198.3, August 1979.

Daniels, J. Hartley and Batcheler, R. P.
FATIGUE TESTS OF CURVED BOX GIRDERS, DOT-FH-11-8198.4, August 1979

Daniels, J. Hartley and Batcheler, R. P.
EFFECT OF HEAT CURVING ON THE FATIGUE STRENGTH OF PLATE GIRDERS, DOT-FH-11-8198.5, August 1979.

Daniels, J. Hartley, Abraham, D. and Yen, B. T.
EFFECT OF INTERNAL DIAPHRAGMS ON FATIGUE STRENGTH OF CURVED BOX GIRDERS, DOT-FH-11-8198.6, August 1979.

Daniels, J. Hartley, Fisher, T. A., Batcheler, R. P. and Maurer, J. K.
ULTIMATE STRENGTH TESTS OF HORIZONTALLY CURVED PLATE AND BOX GIRDERS, DOT-FH-11-8198.7, August 1979.

Daniels, J. Hartley, Fisher, John W. and Yen, B. T.
DESIGN RECOMMENDATIONS FOR FATIGUE OF CURVED PLATE GIRDER AND BOX GIRDER BRIDGES, DOT-FH-11-8198.8, August 1979.

APPENDIX C: MATERIAL PROPERTIES

Tensile coupons were cut from the bottom flange and web of each girder on Assemblies 1, 4, and 5. The coupons were obtained upon completion of ultimate strength tests of the assemblies. Ultimate strength tests have not been performed on Assemblies 2 and 3.

Table C1 presents the tensile test results. All steel is ASTM A36 grade.

Assembly	Girder	Location	Coupon	σ_y MPa	σ_y (ksi)	σ_u MPa	σ_u (ksi)	Elongation %
1	1	Web	G2W	295.1	(42.8)	462.0	(67.0)	30.0
		Flange	G2F	247.5	(35.9)	425.4	(61.7)	33.9
	2	Web	G1W	327.5	(47.5)	426.1	(61.8)	24.5
		Flange	G1F	250.3	(36.3)	439.9	(63.8)	32.3
4	1	Web	G8W	279.9	(40.6)	453.0	(65.7)	30.1
		Flange	G8F	295.1	(42.8)	463.3	(67.2)	27.3
	2	Web	G7W	323.4	(46.9)	436.5	(63.3)	28.3
		Flange	G7F	267.5	(38.8)	474.4	(68.8)	30.5
5	1	Web	G10W	304.1	(44.1)	442.7	(64.2)	29.9
		Flange	G10F	294.4	(42.7)	450.9	(65.4)	29.6
	2	Web	G9W	351.0	(50.9)	455.8	(66.1)	27.6
		Flange	G9F	254.4	(36.9)	437.8	(63.5)	33.2

Notes: Flange coupons are from tension flange.
% Elongation measured over 203.2 mm (8 in.) gage length.

Table C1 Tensile Test Results

* U.S.G.P.O. 624-043/1302-1568


ration.
curved steel
DATE
GP O 896.099

FEDERALLY COORDINATED PROGRAM OF HIGHWAY RESEARCH AND DEVELOPMENT (FCP)

The Offices of Research and Development of the Federal Highway Administration are responsible for a broad program of research with resources including its own staff, contract programs, and a Federal-Aid program which is conducted by or through the State highway departments and which also finances the National Cooperative Highway Research Program managed by the Transportation Research Board. The Federally Coordinated Program of Highway Research and Development (FCP) is a carefully selected group of projects aimed at urgent, national problems, which concentrates these resources on these problems to obtain timely solutions. Virtually all of the available funds and staff resources are a part of the FCP. together with as much of the Federal-aid research funds of the States and the NCHRP resources as the States agree to devote to these projects.*

FCP Category Descriptions

1. Improved Highway Design and Operation for Safety

Safety R&D addresses problems connected with the responsibilities of the Federal Highway Administration under the Highway Safety Act and includes investigation of appropriate design standards, roadside hardware, signing. and physical and scientific data for the formulation of improved safety regulations.

2. Reduction of Traffic Congestion and Improved Operational Efficiency

Traffic R&D is concerned with increasing the operational efficiency of existing highways by advancing technology. by improving designs for existing as well as new facilities, and by keeping the demand-capacity relationship in better balance through traffic management techniques such as bus and carpool preferential treatment. motorist information, and rerouting of traffic.

3. Environmental Considerations in Highway Design, Location, Construction, and Operation

Environmental R&D is directed toward identifying and evaluating highway elements which affect the quality* of the human environment. The ultimate goals are reduction of adverse highway and traffic impacts, and protection and enhancement of the environment.

4. Improved Materials Utilization and Durability

Materials R&D is concerned with expanding the knowledge of materials properties and technology to fully utilize available naturally occurring materials. to develop extender or substitute materials for materials in short supply. and to devise procedures for converting industrial and other wastes into useful highway products. These activities are all directed toward the common goals of lowering the cost of highway construction and extending the period of maintenance-free operation.

5. Improved Design to Reduce Costs, Extend Life Expectancy, and Insure Structural Safety

Structural R&D is concerned with furthering the latest technological advances in structural designs, fabrication processes. and construction techniques, to provide safe. efficient highways at reasonable cost.

6. Prototype Development and Implementation of Research

This category is concerned with developing and transferring research and technology into practice, or, as it has been commonly identified. "technology transfer."

7. Improved Technology for Highway Maintenance

Maintenance R&D objectives include the development and application of new technology to improve management, to augment the utilization of resources, and to increase operational efficiency and safety in the maintenance of highway facilities.

---

* The complete 7-volume official statement of the FCP is available from the National Technical Information Service (NTIS), Springfield, Virginia 22161 (Order No. PB 242057, price $45 postpaid). Single copies of the introductory volume are obtainable without charge from Program Analysis (HRD-2), Offices of Research and Development, Federal Highway Administration, Washington, D.C. 20590.